WCAP-14684

R. E. Ginna
Heatup and Cooldown Limit Curves For Normal Operation

Ed Terek
John D. Perock

June 1996

Work Performed Under Shop Order RBXP-139

Prepared by the Westinghouse Electric Corporation
for the Rochester Gas and Electric Corporation

Approved: D. E. Boyle
D. E. Boyle, Manager
Reactor Equipment & Materials Engineering

WESTINGHOUSE ELECTRIC CORPORATION
Systems and Major Projects Division
P.O. Box 355
Pittsburgh, Pennsylvania 15230-0355

PREFACE

This report has been technically reviewed and verified by:

P. A. Grendys P. A. Grendys Sections 1, 2, 4, 5, 6, and 7

T. M. Lloyd Section 3

TABLE OF CONTENTS

LIST OF TABLES

LIST OF TABLES (Continued)

LIST OF TABLES (Continued)

LIST OF FIGURES

1 INTRODUCTION

Heatup and cooldown limit curves are calculated using the adjusted RT_{NDT} (reference nil-ductility temperature) corresponding to the limiting beltline region material of the reactor vessel. The adjusted RT_{NDT} of the limiting material in the core region of the reactor vessel is determined by using the unirradiated reactor vessel material fracture toughness properties, estimating the radiation-induced ΔRT_{NDT}, and adding a margin. The unirradiated RT_{NDT} is designated as the higher of either the drop weight nil-ductility transition temperature (NDTT) or the temperature at which the material exhibits at least 50 ft-lb of impact energy and 35-mil lateral expansion (normal to the major working direction) minus 60°F.

RT_{NDT} increases as the material is exposed to fast-neutron radiation. Therefore, to find the most limiting RT_{NDT} at any time period in the reactor's life, ΔRT_{NDT} due to the radiation exposure associated with that time period must be added to the unirradiated RT_{NDT} (IRT_{NDT}). The extent of the shift in RT_{NDT} is enhanced by certain chemical elements (such as copper and nickel) present in reactor vessel steels. The Nuclear Regulatory Commission (NRC) has published a method for predicting radiation embrittlement in Regulatory Guide 1.99, Revision 2, "Radiation Embrittlement of Reactor Vessel Materials"[1]. Regulatory Guide 1.99, Revision 2, is used for the calculation of Adjusted Reference Temperature (ART) values (IRT_{NDT} + ΔRT_{NDT} + margins for uncertainties) at the 1/4T and 3/4T locations, where T is the thickness of the vessel at the beltline region measured from the clad/base metal interface. The most limiting ART values are used in the generation of heatup and cooldown pressure-temperature limit curves.

2 PURPOSE

The Rochester Gas and Electric Corporation contracted Westinghouse to re-analyze the vessel fluences using the latest approved methodology contained in WCAP-14040-NP-A, Revision 2[2],and to generate new heatup and cooldown curves for 24, 28, 32 and 40 EFPY. The heatup and cooldown curves were generated without margins for instrumentation errors. The curves include a hydrostatic leak test limit curve from 2485 psig to 1500 psig and include pressure-temperature limits for the vessel flange regions per the requirements of 10 CFR Part 50, Appendix G[3].

The purpose of this report is to present the calculations and the development of the R. E. Ginna heatup and cooldown curves for 24, 28, 32 and 40 EFPY. This report documents the neutron fluence evaluation, the calculated adjusted reference temperature (ART) values following the methods of Regulatory Guide 1.99, Revision 2,[1] for all beltline materials and the development of the heatup and cooldown pressure-temperature limit curves for normal operation.

3 RADIATION ANALYSIS AND NEUTRON DOSIMETRY

3.1 Introduction

Knowledge of the neutron environment within the reactor vessel and surveillance capsule geometry is required as an integral part of LWR reactor vessel surveillance programs for two reasons. First, in order to interpret the neutron radiation induced material property changes observed in the test specimens, the neutron environment (energy spectrum, flux, fluence) to which the test specimens were exposed must be known. Second, in order to relate the changes observed in the test specimens to the present and future condition of the reactor vessel, a relationship must be established between the neutron environment at various positions within the reactor vessel and that experienced by the test specimens. The former requirement is normally met by employing a combination of rigorous analytical techniques and measurements obtained with passive neutron flux monitors contained in each of the surveillance capsules. The latter information is generally derived solely from analysis.

The use of fast neutron fluence (E > 1.0 MeV) to correlate measured material property changes to the neutron exposure of the material has traditionally been accepted for development of damage trend curves as well as for the implementation of trend curve data to assess vessel condition. In recent years, however, it has been suggested that an exposure model that accounts for differences in neutron energy spectra between surveillance capsule locations and positions within the vessel wall could lead to an improvement in the uncertainties associated with damage trend curves as well as to a more accurate evaluation of damage gradients through the reactor vessel wall.

Because of this potential shift away from a threshold fluence toward an energy dependent damage function for data correlation, ASTM Standard Practice E853, "Analysis and Interpretation of Light Water Reactor Surveillance Results," recommends reporting displacements per iron atom (dpa) along with fluence (E > 1.0 MeV) to provide a data base for future reference. The energy dependent dpa function to be used for this evaluation is specified in ASTM Standard Practice E693, "Characterizing Neutron Exposures in Ferritic Steels in Terms of Displacements per Atom." The application of the dpa parameter to the assessment of embrittlement gradients through the thickness of the reactor vessel wall has already been promulgated in Revision 2 to Regulatory Guide 1.99, "Radiation Embrittlement of Reactor Vessel Materials."

This section provides the results of the neutron dosimetry evaluations performed in conjunction with the analysis of test specimens contained in surveillance Capsules V, R, T, and S, withdrawn at the end of the first, third, ninth, and twenty-second fuel cycles, respectively. This update is based on current state-of-the-art methodology and nuclear data including recently released neutron transport and dosimetry cross-section libraries derived from the ENDF/B-VI data base. This report provides a consistent up-to-date neutron exposure data base for use in evaluating the material properties of the Ginna reactor vessel.

In each of the capsule dosimetry evaluations, fast neutron exposure parameters in terms of neutron fluence (E > 1.0 MeV), neutron fluence (E > 0.1 MeV), and iron atom displacements (dpa) are established for the capsule irradiation history. The analytical formalism relating the measured capsule exposure to the exposure of the vessel wall is described and used to project the integrated exposure of the vessel wall. Also, uncertainties associated with the derived exposure parameters at the surveillance capsules and with the projected exposure of the reactor vessel are provided.

3.2 Discrete Ordinates Analysis

A plan view of the reactor geometry at the core midplane is shown in Figure 3-1. Six irradiation capsules attached to the thermal shield are included in the reactor design to constitute the reactor vessel surveillance program. The capsules are located at azimuthal angles of 57°, 67°, 77°, 237°, 247°, and 257° relative to the core cardinal axis as shown in Figure 3-1. A plan view of a surveillance capsule holder attached to the thermal shield is shown in Figure 3-2. The stainless steel specimen containers are approximately 1-inch square and approximately 38 inches in height. The containers are positioned axially such that the test specimens are centered on the core midplane, thus spanning the central three feet of the 12 foot (141.4 in) high reactor core.

From a neutronic standpoint, the surveillance capsules and associated support structures are significant. The presence of these materials has a marked effect on both the spatial distribution of neutron flux and the neutron energy spectrum in the water annulus between the thermal shield and the reactor vessel. In order to determine the neutron environment at the test specimen location, the capsules themselves must be included in the analytical model.

In performing the fast neutron exposure evaluations for the surveillance capsules and reactor vessel, two distinct sets of transport calculations were carried out. The first, a single computation in the conventional forward mode, was used primarily to obtain relative neutron energy distributions throughout the reactor geometry as well as to establish relative radial distributions of exposure parameters {ϕ(E > 1.0 MeV), ϕ(E > 0.1 MeV), and dpa/sec} through the vessel wall. The neutron spectral information was required for the interpretation of neutron dosimetry withdrawn from the surveillance capsules as well as for the determination of exposure parameter ratios; i.e., [dpa/sec]/[ϕ(E > 1.0 MeV)], within the reactor vessel geometry. The relative radial gradient information was required to permit the projection of measured exposure parameters to locations interior to the reactor vessel wall, i.e., the ¼T and ¾T locations.

The second set of calculations consisted of a series of adjoint analyses relating the fast neutron flux, ϕ(E > 1.0 MeV), at surveillance capsule positions and at several azimuthal locations on the reactor vessel inner radius to neutron source distributions within the reactor core. The source importance functions generated from these adjoint analyses provided the basis for all absolute exposure calculations and comparison with measurement. These

importance functions, when combined with fuel cycle specific neutron source distributions, yielded absolute predictions of neutron exposure at the locations of interest for each cycle of irradiation. They also established the means to perform similar predictions and dosimetry evaluations for all subsequent fuel cycles. It is important to note that the cycle specific neutron source distributions utilized in these analyses included not only spatial variations of fission rates within the reactor core but also accounted for the effects of varying neutron yield per fission and fission spectrum introduced by the build-up of plutonium as the burnup of individual fuel assemblies increased.

The absolute cycle specific data from the adjoint evaluations together with the relative neutron energy spectra and radial distribution information from the reference forward calculation provided the means to:

1 - Evaluate neutron dosimetry obtained from surveillance capsules,
2 - Relate dosimetry results to key locations at the inner radius and through the thickness of the reactor vessel wall,
3 - Enable a direct comparison of analytical prediction with measurement, and
4 - Establish a mechanism for projection of reactor vessel exposure as the design of each new fuel cycle evolves.

The forward transport calculation for the reactor model summarized in Figures 3-1 and 3-2 was carried out in R,θ geometry using the DORT two-dimensional discrete ordinates code Version 2.7.3[4] and the BUGLE-93 cross-section library[5]. The BUGLE-93 library is a 47 energy group ENDF/B-VI based data set produced specifically for light water reactor applications. In these analyses anisotropic scattering was treated with a P_3 expansion of the scattering cross-sections and the angular discretization was modeled with an S_8 order of angular quadrature.

The core power distribution utilized in the reference forward transport calculation was derived from statistical studies of long-term operation of Westinghouse 2-loop plants. Inherent in the development of this reference core power distribution is the use of an out-in fuel management strategy; i.e., fresh fuel on the core periphery. Furthermore, for the peripheral fuel assemblies, the neutron source was increased by a 2σ margin derived from the statistical evaluation of plant to plant and cycle to cycle variations in peripheral power. Since it is unlikely that any single reactor would exhibit power levels on the core periphery at the nominal + 2σ value for a large number of fuel cycles, the use of this reference distribution is expected to yield somewhat conservative results.

All adjoint calculations were also carried out using an S_8 order of angular quadrature and the P_3 cross-section approximation from the BUGLE-93 library. Adjoint source locations were chosen at several azimuthal locations along the reactor vessel inner radius as well as at the geometric center of each surveillance capsule. Again, these calculations were run in R,θ

geometry to provide neutron source distribution importance functions for the exposure parameter of interest, in this case $\phi(E > 1.0\ MeV)$.

Having the importance functions and appropriate core source distributions, the response of interest could be calculated as:

$$R(r,\theta) = \int_r \int_\theta \int_E I(r,\theta,E)\ S(r,\theta,E)\ r\ dr\ d\theta\ dE$$

where:
- $R(r,\theta)$ = $\phi(E > 1.0\ MeV)$ at radius r and azimuthal angle θ.
- $I(r,\theta,E)$= Adjoint source importance function at radius r, azimuthal angle θ, and neutron source energy E.
- $S(r,\theta;E)$= Neutron source strength at core location r,θ and energy E.

Although the adjoint importance functions used in this analysis were based on a response function defined by the threshold neutron flux $\phi(E > 1.0\ MeV)$, prior calculations[6] have shown that, while the implementation of low leakage loading patterns significantly impacts both the magnitude and spatial distribution of the neutron field, changes in the relative neutron energy spectrum are of second order. Thus, for a given location the ratio of [dpa/sec]/[$\phi(E > 1.0$ MeV)] is insensitive to changing core source distributions. In the application of these adjoint importance functions to the Ginna reactor, therefore, the iron atom displacement rates (dpa/sec) and the neutron flux $\phi(E > 0.1\ MeV)$ were computed on a cycle specific basis by using [dpa/sec]/[$\phi(E > 1.0$ MeV)] and [$\phi(E > 0.1$ MeV)]/[$\phi(E > 1.0$ MeV)] ratios from the forward analysis in conjunction with the cycle specific $\phi(E > 1.0\ MeV)$ solutions from the individual adjoint evaluations.

The reactor core power distributions used in the plant specific adjoint calculations were taken from the fuel cycle design reports for the first twenty-five operating cycles and the upcoming twenty-sixth cycle of Ginna [7 through 29].

Selected results from the neutron transport analyses are provided in Tables 3-1 through 3-5. The data listed in these tables establish the means for absolute comparisons of analysis and measurement for the capsule irradiation periods and provide the means to correlate dosimetry results with the corresponding exposure of the reactor vessel wall.

In Table 3-1, the calculated exposure parameters [$\phi(E > 1.0$ MeV), $\phi(E > 0.1$ MeV), and dpa/sec] are given at the geometric center of the three azimuthally symmetric surveillance capsule positions (13°, 23°, and 33°) for both the reference and the plant specific core power distributions. The plant specific data, based on the adjoint transport analysis, are meant to establish the absolute comparison of measurement with analysis. The reference data derived from the forward calculation are provided as a conservative exposure evaluation against which plant specific fluence calculations can be compared. Similar data are given in Table 3-2 for the reactor vessel inner radius. Again, the three pertinent exposure parameters are listed for the reference and Cycles 1 through 25 plant specific power distributions.

It is important to note that the data for the vessel inner radius were taken at the clad/base metal interface, and thus, represent the maximum predicted exposure levels of the vessel plates and welds.

Radial gradient information applicable to $\phi(E > 1.0\ MeV)$, $\phi(E > 0.1\ MeV)$, and dpa/sec is given in Tables 3-3, 3-4, and 3-5, respectively. The data, obtained from the reference forward neutron transport calculation, are presented on a relative basis for each exposure parameter at several azimuthal locations. Exposure distributions through the vessel wall may be obtained by normalizing the calculated or projected exposure at the vessel inner radius to the gradient data listed in Tables 3-3 through 3-5.

For example, the neutron flux $\phi(E > 1.0\ MeV)$ at the ¼T depth in the reactor vessel wall along the 0° azimuth is given by:

$$\phi_{1/4T}(0°) = \phi(168.04,\ 0°)\ F(172.25,\ 0°)$$

where:

$\phi_{¼T}(0°) =$	Projected neutron flux at the ¼T position on the 0° azimuth.
$\phi(168.04,0°) =$	Projected or calculated neutron flux at the vessel inner radius on the 0° azimuth.
$F(172.25,0°) =$	Ratio of the neutron flux at the ¼T position to the flux at the vessel inner radius for the 0° azimuth. This data is obtained from Table 3-3.

Similar expressions apply for exposure parameters expressed in terms of $\phi(E > 0.1\ MeV)$ and dpa/sec where the attenuation function F is obtained from Tables 3-4 and 3-5, respectively.

3.3 Neutron Dosimetry

The passive neutron sensors included in the Ginna surveillance program are listed in Table 3-6. Also given in Table 3-6 are the primary nuclear reactions and associated nuclear constants that were used in the evaluation of the neutron energy spectrum within the surveillance capsules and in the subsequent determination of the various exposure parameters of interest [$\phi(E > 1.0\ MeV)$, $\phi(E > 0.1\ MeV)$, dpa/sec]. The relative locations of the neutron sensors within the capsules are shown in WCAP-13902[51]. The iron, nickel, copper, and cobalt-aluminum monitors, in wire form, were placed in holes drilled in spacers at several axial levels within the capsules. The cadmium shielded uranium and neptunium fission monitors were accommodated within the dosimeter block located near the center of the capsule.

The use of passive monitors such as those listed in Table 3-6 does not yield a direct measure of the energy dependent neutron flux at the point of interest. Rather, the activation or fission process is a measure of the integrated effect that the time and energy dependent neutron flux has on the target material over the course of the irradiation period. An accurate assessment of the average neutron flux level incident on the various monitors may be derived from the

activation measurements only if the irradiation parameters are well known. In particular, the following variables are of interest:

- The measured specific activity of each monitor,
- The physical characteristics of each monitor,
- The operating history of the reactor,
- The energy response of each monitor, and
- The neutron energy spectrum at the monitor location.

The specific activity of each of the neutron monitors was determined using established ASTM procedures[30 through 43]. Following sample preparation and weighing, the activity of each monitor was determined by means of a lithium-drifted germanium, Ge(Li), gamma spectrometer. The irradiation history of the Ginna reactor was obtained from NUREG-0020, "Licensed Operating Reactors Status Summary Report," and plant personnel for the cycles 1 through 25 operating period. The irradiation history applicable to the exposure of Capsules V, R, T, and S is given in Table 3-7.

Having the measured specific activities, the physical characteristics of the sensors, and the operating history of the reactor, reaction rates referenced to full power operation were determined from the following equation:

$$R = \frac{A}{N_0 F Y \sum \frac{P_j}{P_{ref}} C_j [1-e^{-\lambda t_j}] [e^{-\lambda t_d}]}$$

where:

R	=	Reaction rate averaged over the irradiation period and referenced to operation at a core power level of P_{ref} (rps/nucleus).
A	=	Measured specific activity (dps/gm).
N_0	=	Number of target element atoms per gram of sensor.
F	=	Weight fraction of the target isotope in the sensor material.
Y	=	Number of product atoms produced per reaction.
P_j	=	Average core power level during irradiation period j (MW).
P_{ref}	=	Maximum or reference power level of the reactor (MW).
C_j	=	Calculated ratio of $\phi(E > 1.0$ MeV) during irradiation period j to the time weighted average $\phi(E > 1.0$ MeV) over the entire irradiation period.
λ	=	Decay constant of the product isotope (1/sec).
t_j	=	Length of irradiation period j (sec).
t_d	=	Decay time following irradiation period j (sec).

and the summation is carried out over the total number of monthly intervals comprising the irradiation period.

In the equation describing the reaction rate calculation, the ratio $[P_j]/[P_{ref}]$ accounts for month by month variation of reactor core power level within any given fuel cycle as well as over multiple fuel cycles. The ratio C_j, which can be calculated for each fuel cycle using the adjoint transport technology discussed in Section 3.2, accounts for the change in sensor reaction rates caused by variations in flux level induced by changes in core spatial power distributions from fuel cycle to fuel cycle. For a single cycle irradiation C_j is normally taken to be 1.0. However, for multiple cycle irradiations, particularly those employing low leakage fuel management, the additional C_j term should be employed. The impact of changing flux levels for constant power operation can be quite significant for sensor sets that have been irradiated for many cycles in a reactor that has transitioned from non-low leakage to low leakage fuel management or for sensor sets contained in surveillance capsules that have been moved from one capsule location to another.

For the irradiation history of Capsules V, R, T, and S, the flux level term in the reaction rate calculations was developed from the plant specific analysis provided in Table 3-1. Measured and saturated reaction product specific activities as well as the derived full power reaction rates are listed in Table 3-8. The specific activities and reaction rates of the ^{238}U sensors provided in Table 3-8 include corrections for ^{235}U impurities, plutonium build-in, and gamma ray induced fissions. Corrections for gamma ray induced fissions were also included in the specific activities and reaction rates for the ^{237}Np sensors as well.

Values of key fast neutron exposure parameters were derived from the measured reaction rates using the FERRET least squares adjustment code[44]. The FERRET approach used the measured reaction rate data, sensor reaction cross-sections, and a calculated trial spectrum as input and proceeded to adjust the group fluxes from the trial spectrum to produce a best fit (in a least squares sense) to the measured reaction rate data. The "measured" exposure parameters along with the associated uncertainties were then obtained from the adjusted spectrum.

In the FERRET evaluations, a log-normal least squares algorithm weights both the a priori values and the measured data in accordance with the assigned uncertainties and correlations. In general, the measured values f are linearly related to the flux ϕ by some response matrix A:

$$f_i^{(s,\alpha)} = \sum_g A_{ig}^{(s)} \phi_g^{(\alpha)}$$

where i indexes the measured values belonging to a single data set s, g designates the energy group, and α delineates spectra that may be simultaneously adjusted. For example,

$$R_i = \sum_g \sigma_{ig} \phi_g$$

relates a set of measured reaction rates R_i to a single spectrum ϕ_g by the multigroup reaction cross-section σ_{ig}. The log-normal approach automatically accounts for the physical constraint of positive fluxes, even with large assigned uncertainties.

In the least squares adjustment, the continuous quantities (i.e., neutron spectra and cross-sections) were approximated in a multi-group format consisting of 53 energy groups. The trial input spectrum was converted to the FERRET 53 group structure using the SAND-II code[45]. This procedure was carried out by first expanding the 47 group calculated spectrum into the SAND-II 620 group structure using a SPLINE interpolation procedure in regions where group boundaries do not coincide. The 620 point spectrum was then re-collapsed into the group structure used in FERRET.

The sensor set reaction cross-sections, obtained from the ENDF/B-VI dosimetry file[46], were also collapsed into the 53 energy group structure using the SAND-II code. In this instance, the trial spectrum, as expanded to 620 groups, was employed as a weighting function in the cross-section collapsing procedure. Reaction cross-section uncertainties in the form of a 53 × 53 covariance matrix for each sensor reaction were also constructed from the information contained on the ENDF/B-VI data files. These matrices included energy group to energy group uncertainty correlations for each of the individual reactions. However, correlations between cross-sections for different sensor reactions were not included. The omission of this additional uncertainty information does not significantly impact the results of the adjustment.

Due to the importance of providing a trial spectrum that exhibits a relative energy distribution close to the actual spectrum at the sensor set locations, the neutron spectrum input to the FERRET evaluation was taken from the center of the surveillance capsule modeled in the reference forward transport calculation. While the 53 × 53 group covariance matrices applicable to the sensor reaction cross-sections were developed from the ENDF/B-VI data files, the covariance matrix for the input trial spectrum was constructed from the following relation:

$$M_{gg'} = R_n^2 + R_g R_{g'} P_{gg'}$$

where R_n specifies an overall fractional normalization uncertainty (i.e., complete correlation) for the set of values. The fractional uncertainties R_g specify additional random uncertainties for group g that are correlated with a correlation matrix given by:

$$P_{gg'} = [1-\theta]\ \delta_{gg'} + \theta\ e^{-H}$$

where:

$$H = \frac{(g-g')^2}{2\ \gamma^2}$$

The first term in the correlation matrix equation specifies purely random uncertainties, while the second term describes short range correlations over a group range γ (θ specifies the strength of the latter term). The value of δ is 1 when g = g' and 0 otherwise. For the trial spectrum used in the current evaluations, a short range correlation of γ = 6 groups was used. This choice implies that neighboring groups are strongly correlated when θ is close to 1. Strong long range correlations (or anti-correlations) were justified based on information presented by R. E. Maerker[47]. The uncertainties associated with the measured reaction rates included both statistical (counting) and systematic components. The systematic component of the overall uncertainty accounts for counter efficiency, counter calibrations, irradiation history corrections, and corrections for competing reactions in the individual sensors.

Results of the FERRET evaluations of the Capsules V, R, T, and S dosimetry are given in Table 3-9. The data summarized in this table include fast neutron exposure evaluations in terms of Φ(E > 1.0 MeV), Φ(E > 0.1 MeV), and dpa. In general, excellent results were achieved in the fits of the adjusted spectra to the individual measured reaction rates. The measured and FERRET adjusted reaction rates for each reaction are given in Table 3-10. An examination of Table 3-10 shows that, in all cases, reaction rates calculated with the adjusted spectra match the measured reaction rates to better than 8%. The adjusted spectra from the least squares evaluation is given in Table 3-11 in the FERRET 53 energy group structure.

In Table 3-12, absolute comparisons of the measured and calculated fluence at the center of each capsule are presented. The results for the Capsules V, R, T, and S dosimetry evaluations (M/C ratios of 1.03 for Φ(E > 1.0 MeV)) are consistent with results obtained from similar evaluations of dosimetry from other reactors using methodologies based on ENDF/B-VI cross-sections.

3.4 Projections of Reactor Vessel Exposure

The best estimate exposure of the Ginna reactor vessel was developed using a combination of absolute plant specific transport calculations and all available plant specific measurement data. In the case of Ginna, the measurement data base consists of the four surveillance capsules discussed in this report.

Combining this measurement data base with the plant specific calculations, the best estimate vessel exposure is obtained from the following relationship:

$$\Phi_{Best\ Est.} = K\,\Phi_{Calc.}$$

where: $\Phi_{Best.\ Est.}$ = The best estimate fast neutron exposure at the location of interest.

K = The plant specific measurement/calculation (M/C) bias factor derived from the surveillance capsule dosimetry data.

$\Phi_{Calc.}$ = The absolute calculated fast neutron exposure at the location of interest.

The approach defined in the above equation is based on the premise that the measurement data represent the most accurate plant specific information available at the locations of the dosimetry; and, further that the use of the measurement data on a plant specific basis essentially removes biases present in the analytical approach and mitigates the uncertainties that would result from the use of analysis alone.

That is, at the measurement points the uncertainty in the best estimate exposure is dominated by the uncertainties in the measurement process. At locations within the reactor vessel wall, additional uncertainty is incurred due to the analytically determined relative ratios among the various measurement points and locations within the reactor vessel wall.

For Ginna, the derived plant specific bias factors were 1.03, 1.13, and 1.08 for $\Phi(E > 1.0$ MeV), $\Phi(E > 0.1$ MeV), and dpa, respectively. Bias factors of this magnitude are fully consistent with experience using the BUGLE-93 cross-section library.

The use of the bias factors derived from the measurement data base acts to remove plant specific biases associated with the definition of the core source, actual vs. assumed reactor dimensions, and operational variations in water density within the reactor. As a result, the overall uncertainty in the best estimate exposure projections within the vessel wall depends on the individual uncertainties in the measurement process, the uncertainty in the dosimetry location, and, in the uncertainty in the calculated ratio of the neutron exposure at the point of interest to that at the measurement location.

The uncertainty in the derived neutron flux for an individual measurement is obtained directly from the results of a least squares evaluation of dosimetry data. The least squares approach combines individual uncertainty in the calculated neutron energy spectrum, the uncertainties in dosimetry cross-sections, and the uncertainties in measured foil specific activities to produce a net uncertainty in the derived neutron flux at the measurement point. The associated uncertainty in the plant specific bias factor, K, derived from the M/C data base, in turn, depends on the total number of available measurements as well as on the uncertainty of each measurement.

In developing the overall uncertainty associated with the reactor vessel exposure, the positioning uncertainties for dosimetry are taken from parametric studies of sensor position performed as part a series of analytical sensitivity studies included in the qualification of the methodology. The uncertainties in the exposure ratios relating dosimetry results to positions within the vessel wall are again based on the analytical sensitivity studies of the vessel thickness tolerance, downcomer water density variations and vessel inner radius tolerance. Thus, this portion of the overall uncertainty is controlled entirely by dimensional tolerances associated with the reactor design and by the operational characteristics of the reactor.

The net uncertainty in the bias factor, K, is combined with the uncertainty from the analytical sensitivity study to define the overall fluence uncertainty at the reactor vessel wall. In the case of Ginna, the derived uncertainties in the bias factor, K, and the additional uncertainty from the analytical sensitivity studies combine to yield a net uncertainty of ±12.9%.

Based on this best estimate approach, neutron exposure projections at key locations on the reactor vessel inner radius are given in Table 3-13. Along with the current (19.51 EFPY) exposure, projections are also provided for exposure periods of 28 EFPY, 32 EFPY, 42 EFPY, and 48 EFPY. Projections for future operation were based on the assumption that the average exposure rates during the upcoming cycle 26 (18 month fuel cycle operation) irradiation period would continue to be applicable throughout plant life.

In the calculation of exposure gradients within the reactor vessel wall for the Ginna reactor vessel, exposure projections to 28, 32, 42 and 48 EFPY were also employed. Data based on both a $\Phi(E > 1.0\ MeV)$ slope and a plant specific dpa slope through the vessel wall are provided in Table 3-14.

In order to access RT_{NDT} vs fluence curves, dpa equivalent fast neutron fluence levels for the ¼T and ¾T positions were defined by the relations:

$$\phi(1/4T) = \phi(0T)\ \frac{dpa(1/4T)}{dpa(0T)}$$

and

$$\phi(3/4T) = \phi(0T)\ \frac{dpa(3/4T)}{dpa(0T)}$$

Using this approach results in the dpa equivalent fluence values listed in Table 3-14. In Table 3-15 updated lead factors are listed for each of the Ginna surveillance capsules. Lead factor data based on the accumulated fluence through the Cycle 26 projection are provided for each remaining capsule.

FIGURE 3-1

ARRANGEMENT OF SURVEILLANCE CAPSULES IN THE R. E. GINNA REACTOR VESSEL

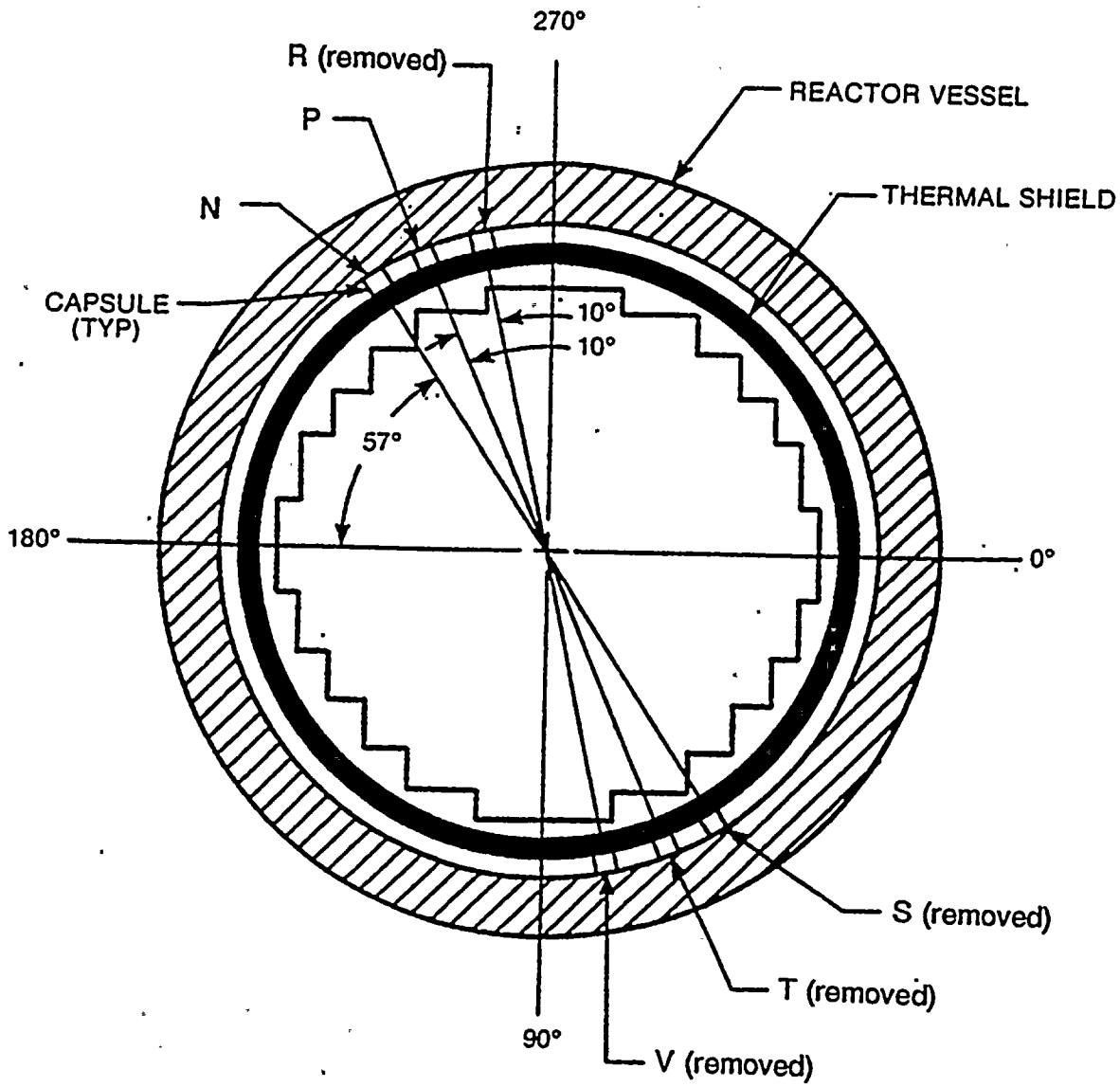

FIGURE 3-2

PLAN VIEW OF A REACTOR VESSEL SURVEILLANCE CAPSULE

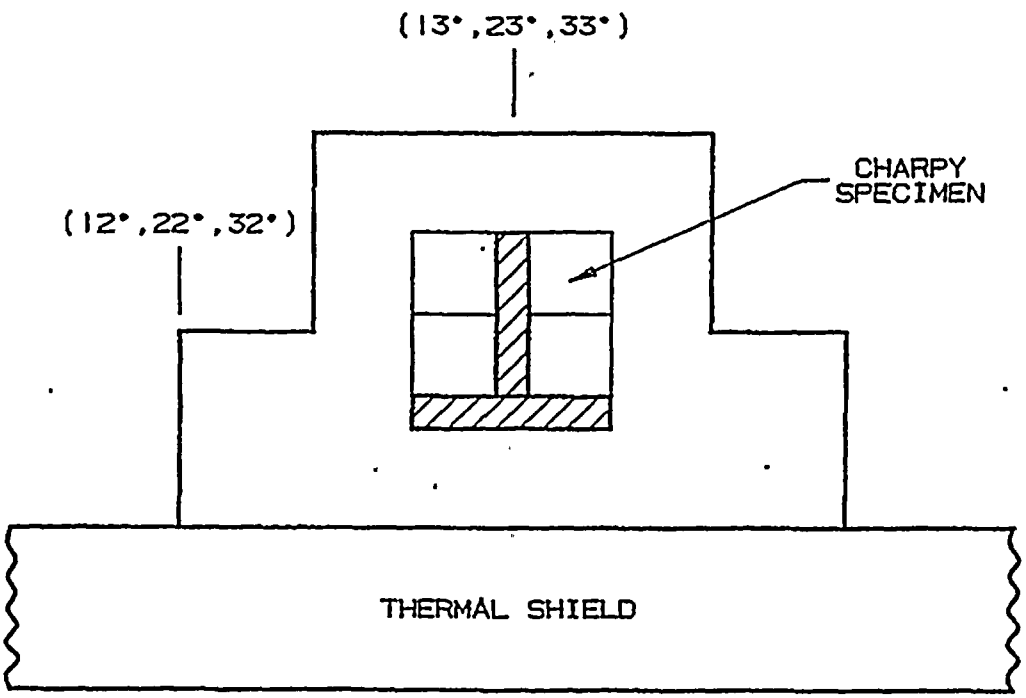

TABLE 3-1

CALCULATED FAST NEUTRON EXPOSURE RATES AND IRON ATOM DISPLACEMENT RATES AT THE SURVEILLANCE CAPSULE CENTER

$\phi(E > 1.0\ MeV)$ $(n/cm^2\text{-}sec)$

Cycle No.	13°	23°	33°
Reference	1.59e+11	9.35e+10	8.83e+10
1A	1.195e+11	7.051e+10	6.684e+10
1B	1.424e+11	8.009e+10	7.141e+10
2	1.369e+11	8.096e+10	7.682e+10
3	1.144e+11	6.661e+10	6.263e+10
4	1.083e+11	7.266e+10	7.217e+10
5	1.326e+11	7.714e+10	7.069e+10
6	1.375e+11	8.240e+10	7.397e+10
7	1.193e+11	7.520e+10	7.026e+10
8	1.434e+11	8.433e+10	8.033e+10
9	1.359e+11	8.455e+10	8.303e+10
10	1.242e+11	7.865e+10	7.751e+10
11	1.250e+11	7.127e+10	6.474e+10
12	1.377e+11	7.241e+10	6.357e+10
13	1.063e+11	6.870e+10	6.252e+10
14	1.027e+11	7.053e+10	6.926e+10
15	9.149e+10	6.622e+10	6.567e+10
16	9.652e+10	6.054e+10	5.953e+10
17	1.030e+11	6.362e+10	5.936e+10
18	9.259e+10	6.261e+10	5.835e+10
19	9.133e+10	6.065e+10	5.883e+10
20	9.723e+10	6.228e+10	5.762e+10
21	9.691e+10	6.476e+10	5.982e+10
22	1.038e+11	6.575e+10	6.057e+10
23	9.322e+10	6.167e+10	6.004e+10
24	9.072e+10	5.884e+10	5.497e+10
25	8.436e+10	5.510e+10	5.293e+10
26	8.418e+10	5.299e+10	5.016e+10

TABLE 3-1 cont'd

CALCULATED FAST NEUTRON EXPOSURE RATES AND IRON ATOM DISPLACEMENT RATES AT THE SURVEILLANCE CAPSULE CENTER

ϕ(E > 0.1 MeV) (n/cm^2-sec)

Cycle No.	13°	23°	33°
Reference	6.02e+11	3.22e+11	3.11e+11
1A	4.529e+11	2.426e+11	2.353e+11
1B	5.398e+11	2.755e+11	2.513e+11
2	5.189e+11	2.785e+11	2.704e+11
3	4.337e+11	2.291e+11	2.205e+11
4	4.105e+11	2.500e+11	2.541e+11
5	5.025e+11	2.654e+11	2.488e+11
6	5.211e+11	2.835e+11	2.604e+11
7	4.520e+11	2.587e+11	2.473e+11
8	5.435e+11	2.901e+11	2.828e+11
9	5.149e+11	2.909e+11	2.923e+11
10	4.706e+11	2.706e+11	2.728e+11
11	4.737e+11	2.452e+11	2.279e+11
12	5.220e+11	2.491e+11	2.238e+11
13	4.030e+11	2.363e+11	2.201e+11
14	3.893e+11	2.426e+11	2.438e+11
15	3.468e+11	2.278e+11	2.311e+11
16	3.658e+11	2.082e+11	2.095e+11
17	3.904e+11	2.189e+11	2.089e+11
18	3.509e+11	2.154e+11	2.054e+11
19	3.462e+11	2.086e+11	2.071e+11
20	3.685e+11	2.142e+11	2.028e+11
21	3.673e+11	2.228e+11	2.106e+11
22	3.933e+11	2.262e+11	2.132e+11
23	3.533e+11	2.121e+11	2.114e+11
24	3.438e+11	2.024e+11	1.935e+11
25	3.197e+11	1.896e+11	1.863e+11
26	3.191e+11	1.823e+11	1.766e+11

TABLE 3-1 cont'd

CALCULATED FAST NEUTRON EXPOSURE RATES AND IRON ATOM DISPLACEMENT RATES AT THE SURVEILLANCE CAPSULE CENTER

	Displacement Rate (dpa/sec)		
Cycle No.	13°	23°	33°
Reference	2.83e-10	1.59e-10	1.52e-10
1A	2.127e-10	1.199e-10	1.150e-10
1B	2.535e-10	1.362e-10	1.228e-10
2	2.437e-10	1.376e-10	1.321e-10
3	2.037e-10	1.132e-10	1.077e-10
4	1.928e-10	1.235e-10	1.241e-10
5	2.360e-10	1.311e-10	1.216e-10
6	2.448e-10	1.401e-10	1.272e-10
7	2.123e-10	1.278e-10	1.208e-10
8	2.553e-10	1.434e-10	1.382e-10
9	2.418e-10	1.437e-10	1.428e-10
10	2.210e-10	1.337e-10	1.333e-10
11	2.225e-10	1.212e-10	1.113e-10
12	2.452e-10	1.231e-10	1.093e-10
13	1.893e-10	1.168e-10	1.075e-10
14	1.829e-10	1.199e-10	1.191e-10
15	1.629e-10	1.126e-10	1.129e-10
16	1.718e-10	1.029e-10	1.024e-10
17	1.833e-10	1.082e-10	1.021e-10
18	1.648e-10	1.064e-10	1.004e-10
19	1.626e-10	1.031e-10	1.012e-10
20	1.731e-10	1.059e-10	9.910e-11
21	1.725e-10	1.101e-10	1.029e-10
22	1.847e-10	1.118e-10	1.042e-10
23	1.659e-10	1.048e-10	1.033e-10
24	1.615e-10	1.000e-10	9.454e-11
25	1.502e-10	9.368e-11	9.103e-11
26	1.498e-10	9.009e-11	8.627e-11

TABLE 3-2

CALCULATED AZIMUTHAL VARIATION OF FAST NEUTRON EXPOSURE RATES AND IRON ATOM DISPLACEMENT RATES AT THE REACTOR VESSEL CLAD/BASE METAL INTERFACE

$\phi(E > 1.0\ MeV)\ (n/cm^2\text{-}sec)$

Cycle No.	0°	15°	30°	45°
Reference	4.14e+09	3.20e+09	2.19e+09	1.83e+09
1A	4.022e+10	2.452e+10	1.680e+10	1.420e+10
1B	4.784e+10	2.909e+10	1.831e+10	1.517e+10
2	4.590e+10	2.811e+10	1.926e+10	1.688e+10
3	3.792e+10	2.348e+10	1.576e+10	1.374e+10
4	3.488e+10	2.290e+10	1.796e+10	1.581e+10
5	4.441e+10	2.720e+10	1.799e+10	1.501e+10
6	4.505e+10	2.836e+10	1.901e+10	1.475e+10
7	3.835e+10	2.488e+10	1.784e+10	1.459e+10
8	4.828e+10	2.938e+10	2.014e+10	1.735e+10
9	4.484e+10	2.816e+10	2.066e+10	1.820e+10
10	4.092e+10	2.582e+10	1.930e+10	1.683e+10
11	4.076e+10	2.570e+10	1.650e+10	1.543e+10
12	4.746e+10	2.787e+10	1.635e+10	1.500e+10
13	3.616e+10	2.258e+10	1.615e+10	1.355e+10
14	3.404e+10	2.213e+10	1.735e+10	1.690e+10
15	2.800e+10	2.003e+10	1.640e+10	1.664e+10
16	3.078e+10	2.043e+10	1.482e+10	1.546e+10
17	3.633e+10	2.170e+10	1.514e+10	1.380e+10
18	3.008e+10	1.995e+10	1.496e+10	1.300e+10
19	3.003e+10	1.956e+10	1.483e+10	1.366e+10
20	3.127e+10	2.068e+10	1.475e+10	1.315e+10
21	3.007e+10	2.080e+10	1.537e+10	1.338e+10
22	3.510e+10	2.203e+10	1.553e+10	1.380e+10
23	3.039e+10	1.995e+10	1.511e+10	1.408e+10
24	3.000e+10	1.938e+10	1.406e+10	1.249e+10
25	2.794e+10	1.803e+10	1.340e+10	1.226e+10
26	2.885e+10	1.788e+10	1.275e+10	1.181e+10

TABLE 3-2 cont'd

CALCULATED AZIMUTHAL VARIATION OF FAST NEUTRON EXPOSURE RATES AND IRON ATOM DISPLACEMENT RATES AT THE REACTOR VESSEL CLAD/BASE METAL INTERFACE

$\phi(E > 0.1\ MeV)$ (n/cm^2-sec)

Cycle No.	0°	15°	30°	45°
Reference	3.25e+10	2.76e+10	1.90e+10	1.50e+10
1A	3.121e+11	2.116e+11	1.465e+11	1.164e+11
1B	3.712e+11	2.511e+11	1.597e+11	1.244e+11
2	3.562e+11	2.426e+11	1.680e+11	1.384e+11
3	2.942e+11	2.026e+11	1.374e+11	1.126e+11
4	2.706e+11	1.976e+11	1.566e+11	1.297e+11
5	3.446e+11	2.348e+11	1.568e+11	1.230e+11
6	3.496e+11	2.447e+11	1.658e+11	1.210e+11
7	2.976e+11	2.147e+11	1.556e+11	1.197e+11
8	3.746e+11	2.536e+11	1.757e+11	1.422e+11
9	3.480e+11	2.430e+11	1.802e+11	1.492e+11
10	3.176e+11	2.228e+11	1.683e+11	1.380e+11
11	3.163e+11	2.218e+11	1.438e+11	1.266e+11
12	3.683e+11	2.406e+11	1.425e+11	1.230e+11
13	2.806e+11	1.948e+11	1.408e+11	1.111e+11
14	2.641e+11	1.910e+11	1.513e+11	1.386e+11
15	2.173e+11	1.729e+11	1.430e+11	1.364e+11
16	2.389e+11	1.764e+11	1.292e+11	1.268e+11
17	2.819e+11	1.872e+11	1.320e+11	1.131e+11
18	2.334e+11	1.722e+11	1.304e+11	1.066e+11
19	2.330e+11	1.688e+11	1.293e+11	1.120e+11
20	2.427e+11	1.785e+11	1.286e+11	1.079e+11
21	2.333e+11	1.795e+11	1.340e+11	1.097e+11
22	2.724e+11	1.901e+11	1.354e+11	1.132e+11
23	2.358e+11	1.721e+11	1.318e+11	1.155e+11
24	2.328e+11	1.672e+11	1.226e+11	1.024e+11
25	2.168e+11	1.556e+11	1.169e+11	1.005e+11
26	2.239e+11	1.543e+11	1.112e+11	9.687e+10

TABLE 3-2 cont'd

CALCULATED AZIMUTHAL VARIATION OF FAST NEUTRON EXPOSURE RATES AND IRON ATOM DISPLACEMENT RATES AT THE REACTOR VESSEL CLAD/BASE METAL INTERFACE

	Displacement Rate (dpa/sec)			
Cycle No.	0°	15°	30°	45°
Reference	1.17e-11	9.70e-12	6.70e-12	5.36e-12
1A	1.138e-10	7.430e-11	5.141e-11	4.160e-11
1B	1.354e-10	8.815e-11	5.604e-11	4.446e-11
2	1.299e-10	8.517e-11	5.894e-11	4.946e-11
3	1.073e-10	7.113e-11	4.823e-11	4.025e-11
4	9.870e-11	6.938e-11	5.496e-11	4.633e-11
5	1.257e-10	8.242e-11	5.503e-11	4.397e-11
6	1.275e-10	8.593e-11	5.818e-11	4.322e-11
7	1.085e-10	7.538e-11	5.460e-11	4.276e-11
8	1.366e-10	8.903e-11	6.164e-11	5.082e-11
9	1.269e-10	8.531e-11	6.322e-11	5.331e-11
10	1.158e-10	7.823e-11	5.904e-11	4.930e-11
11	1.154e-10	7.787e-11	5.048e-11	4.522e-11
12	1.343e-10	8.446e-11	5.002e-11	4.395e-11
13	1.023e-10	6.841e-11	4.941e-11	3.971e-11
14	9.633e-11	6.706e-11	5.308e-11	4.952e-11
15	7.924e-11	6.070e-11	5.019e-11	4.875e-11
16	8.712e-11	6.192e-11	4.534e-11	4.530e-11
17	1.028e-10	6.574e-11	4.632e-11	4.042e-11
18	8.513e-11	6.046e-11	4.577e-11	3.809e-11
19	8.498e-11	5.927e-11	4.538e-11	4.002e-11
20	8.850e-11	6.267e-11	4.514e-11	3.854e-11
21	8.510e-11	6.301e-11	4.702e-11	3.920e-11
22	9.933e-11	6.674e-11	4.752e-11	4.045e-11
23	8.599e-11	6.044e-11	4.624e-11	4.127e-11
24	8.491e-11	5.871e-11	4.301e-11	3.660e-11
25	7.906e-11	5.463e-11	4.101e-11	3.592e-11
26	8.164e-11	5.418e-11	3.901e-11	3.461e-11

TABLE 3-3

RELATIVE RADIAL DISTRIBUTION OF ϕ(E > 1.0 MeV)
WITHIN THE REACTOR VESSEL WALL

RADIUS	AZIMUTHAL ANGLE			
(cm)	0°	15°	30°	45°
168.04	1.000	1.000	1.000	1.000
168.27	0.987	0.987	0.985	0.987
168.88	0.940	0.942	0.937	0.942
169.75	0.862	0.865	0.857	0.866
170.93	0.754	0.757	0.749	0.760
172.25	0.639	0.644	0.636	0.647
173.53	0.540	0.546	0.539	0.550
174.98	0.444	0.451	0.444	0.454
176.46	0.362	0.370	0.363	0.372
177.58	0.308	0.317	0.311	0.318
179.03	0.250	0.259	0.253	0.260
180.66	0.196	0.206	0.201	0.206
181.63	0.169	0.179	0.175	0.178
182.60	0.144	0.154	0.151	0.154
184.06	0.110	0.122	0.120	0.122
184.87	0.101	0.113	0.112	0.113

Note: Base Metal Inner Radius = 168.04 cm.
Base Metal ¼T = 172.25 cm.
Base Metal ½T = 176.46 cm.
Base Metal ¾T = 180.66 cm.
Base Metal Outer Radius = 184.87 cm.

TABLE 3-4

RELATIVE RADIAL DISTRIBUTION OF ϕ(E > 0.1 MeV)
WITHIN THE REACTOR VESSEL WALL

RADIUS	AZIMUTHAL ANGLE			
(cm)	0°	15°	30°	45°
168.04	1.000	1.000	1.000	1.000
168.27	1.005	1.007	1.005	1.007
168.88	1.002	1.007	1.004	1.008
169.75	0.980	0.990	0.985	0.992
170.93	0.934	0.948	0.945	0.953
172.25	0.873	0.891	0.889	0.899
173.53	0.809	0.831	0.831	0.841
174.98	0.736	0.763	0.763	0.773
176.46	0.662	0.693	0.694	0.703
177.58	0.606	0.640	0.642	0.650
179.03	0.536	0.573	0.577	0.582
180.66	0.461	0.502	0.507	0.509
181.63	0.416	0.458	0.466	0.465
182.60	0.369	0.415	0.423	0.421
184.06	0.298	0.348	0.361	0.357
184.87	0.276	0.327	0.343	0.339

Note: Base Metal Inner Radius = 168.04 cm.
Base Metal ¼T = 172.25 cm.
Base Metal ½T = 176.46 cm.
Base Metal ¾T = 180.66 cm.
Base Metal Outer Radius = 184.87 cm.

TABLE 3-5

RELATIVE RADIAL DISTRIBUTION OF dpa/sec
WITHIN THE REACTOR VESSEL WALL

RADIUS	AZIMUTHAL ANGLE			
(cm)	0°	15°	30°	45°
168.04	1.000	1.000	1.000	1.000
168.27	0.988	0.990	0.988	0.989
168.88	0.951	0.955	0.950	0.954
169.75	0.889	0.896	0.889	0.857
170.93	0.804	0.814	0.805	0.812
172.25	0.712	0.726	0.716	0.723
173.53	0.630	0.648	0.638	0.644
174.98	0.547	0.568	0.558	0.563
176.46	0.472	0.495	0.486	0.490
177.58	0.420	0.445	0.436	0.439
179.03	0.360	0.386	0.379	0.380
180.66	0.301	0.328	0.322	0.322
181.63	0.267	0.296	0.291	0.289
182.60	0.234	0.264	0.261	0.258
184.06	0.187	0.219	0.220	0.216
184.87	0.173	0.206	0.208	0.205

Note: Base Metal Inner Radius = 168.04 cm.
Base Metal ¼T = 172.25 cm.
Base Metal ½T = 176.46 cm.
Base Metal ¾T = 180.66 cm.
Base Metal Outer Radius = 184.87 cm.

TABLE 3-6

NUCLEAR PARAMETERS USED IN THE EVALUATION OF NEUTRON SENSORS

Monitor Material	Reaction of Interest	Target Atom Fraction	Response Range	Product Half-life	Fission Yield (%)
Copper	^{63}Cu (n,α)	0.6917	E > 4.7 MeV	5.271 y	
Iron	^{54}Fe (n,p)	0.0580	E > 1.0 MeV	312.5 d	
Nickel	^{58}Ni (n,p)	0.6827	E > 1.0 MeV	70.78 d	
Uranium-238	^{238}U (n,f)	0.9996	E > 0.4 MeV	30.17 y	6.00
Neptunium-237	^{237}Np (n,f)	1.0000	E > 0.08 MeV	30.17 y	6.27
Cobalt-Al	^{59}Co (n,γ)	0.0015	E > 0.015 MeV	5.271 y	

Note: ^{238}U and ^{237}Np monitors are cadmium shielded.

TABLE 3-7

MONTHLY THERMAL GENERATION DURING THE FIRST TWENTY-FIVE FUEL CYCLES OF THE GINNA REACTOR

Cycle 1A		Cycle 1B		Cycle 2		Cycle 3	
Month	Thermal Gen. MWt-hr	Month	Thermal Gen. MWt-hr	Month	Thermal Gen. MWt-hr	Month	Thermal Gen. MWt-hr
Nov-69	0					Nov-72	381843
Dec-69	0					Dec-72	1053950
Jan-70	435541	Apr-71	0			Jan-73	886067
Feb-70	435541	May-71	330899			Feb-73	852420
Mar-70	435541	Jun-71	831633			Mar-73	942682
Apr-70	435541	Jul-71	835525			Apr-73	914688
May-70	435541	Aug-71	922141	May-72	0	May-73	947502
Jun-70	435541	Sep-71	913338	Jun-72	7722	Jun-73	906810
Jul-70	435541	Oct-71	957036	Jul-72	818270	Jul-73	678681
Aug-70	930964	Nov-71	956391	Aug-72	897991	Aug-73	945755
Sep-70	860611	Dec-71	941632	Sep-72	910771	Sep-73	951662
Oct-70	481017	Jan-72	956804	Oct-72	329771	Oct-73	818471
Nov-70	830385	Feb-72	955012			Nov-73	980073
Dec-70	840563	Mar-72	740009			Dec-73	923316
Jan-71	831856	Apr-72	655096			Jan-74	2908
Feb-71	956228					Feb-74	0
Mar-71	27388					Mar-74	0

TABLE 3-7 cont'd

MONTHLY THERMAL GENERATION DURING THE FIRST TWENTY-FIVE FUEL CYCLES OF THE GINNA REACTOR

Cycle 4		Cycle 5		Cycle 6		Cycle 7	
Month	Thermal Gen. MWt-hr	Month	Thermal Gen. MWt-hr	Month	Thermal Gen. MWt-hr	Month	Thermal Gen. MWt-hr
Apr-74	89688			Apr-76	262656		
May-74	739986	May-75	154344	May-76	667032	May-77	195504
Jun-74	582048	Jun-75	624696	Jun-76	1069992	Jun-77	1081512
Jul-74	710424	Jul-75	1088160	Jul-76	1079064	Jul-77	810480
Aug-74	895176	Aug-75	1115328	Aug-76	151512	Aug-77	973440
Sep-74	992088	Sep-75	1086864	Sep-76	747336	Sep-77	1083960
Oct-74	1034808	Oct-75	1047312	Oct-76	331608	Oct-77	1116840
Nov-74	562206	Nov-75	1085784	Nov-76	1087128	Nov-77	948096
Dec-74	1102170	Dec-75	1036296	Dec-76	1055472	Dec-77	1088328
Jan-75	1123848	Jan-76	532560	Jan-77	1108248	Jan-78	872256
Feb-75	1018003	Feb-76	0	Feb-77	1013808	Feb-78	888480
Mar-75	325920	Mar-76	0	Mar-77	1119720	Mar-78	870024
Apr-75	0			Apr-77	541872	Apr-78	0

TABLE 3-7 cont'd

MONTHLY THERMAL GENERATION DURING THE FIRST TWENTY-FIVE FUEL CYCLES OF THE GINNA REACTOR

Cycle 8		Cycle 9		Cycle 10		Cycle 11	
Month	Thermal Gen. MWt-hr	Month	Thermal Gen. MWt-hr	Month	Thermal Gen. MWt-hr	Month	Thermal Gen. MWt-hr
May-78	245784	Mar-79	312	May-80	238944		
Jun-78	1082184	Apr-79	856560	Jun-80	1084200	Jun-81	335016
Jul-78	1107864	May-79	1111296	Jul-80	1120680	Jul-81	1110480
Aug-78	1081872	Jun-79	1085088	Aug-80	1119528	Aug-81	1112424
Sep-78	1079232	Jul-79	212952	Sep-80	1084296	Sep-81	1087728
Oct-78	1120344	Aug-79	952248	Oct-80	1124472	Oct-81	1122552
Nov-78	1078368	Sep-79	1084848	Nov-80	72	Nov-81	1028280
Dec-78	1066896	Oct-79	1089960	Dec-80	1035552	Dec-81	1121904
Jan-79	1116480	Nov-79	1059936	Jan-81	1043136	Jan-82	881568
Feb-79	290064	Dec-79	486144	Feb-81	1018488	Feb-82	0
		Jan-80	1127568	Mar-81	1118424	Mar-82	0
		Feb-80	1055352	Apr-81	604920	Apr-82	0
		Mar-80	935736	May-81	0		
		Apr-80	0				

TABLE 3-7 cont'd

MONTHLY THERMAL GENERATION DURING THE FIRST TWENTY-FIVE FUEL CYCLES OF THE GINNA REACTOR

Cycle 12		Cycle 13		Cycle 14		Cycle 15	
Month	Thermal Gen. MWt-hr	Month	Thermal Gen. MWt-hr	Month	Thermal Gen. MWt-hr	Month	Thermal Gen. MWt-hr
May-82	87336						
Jun-82	1078152	Jun-83	153007	May-84	160440	Apr-85	614232
Jul-82	1118424	Jul-83	1114224	Jun-84	1002072	May-85	1126704
Aug-82	1087944	Aug-83	1126776	Jul-84	1123896	Jun-85	1034760
Sep-82	866400	Sep-83	1025808	Aug-84	1106304	Jul-85	1126464
Oct-82	352944	Oct-83	1123392	Sep-84	1089792	Aug-85	1126776
Nov-82	1082784	Nov-83	1088808	Oct-84	1127040	Sep-85	1010352
Dec-82	1121448	Dec-83	1121328	Nov-84	1084032	Oct-85	1116312
Jan-83	996120	Jan-84	1114992	Dec-84	1126992	Nov-85	1042512
Feb-83	1018944	Feb-84	1027536	Jan-85	1127616	Dec-85	1119144
Mar-83	906408	Mar-84	64896	Feb-85	964344	Jan-86	1056672
Apr-83	0	Apr-84	0	Mar-85	27648	Feb-86	198456
May-83	0						

TABLE 3-7 cont'd

MONTHLY THERMAL GENERATION DURING THE FIRST TWENTY-FIVE FUEL CYCLES OF THE GINNA REACTOR

Cycle 16		Cycle 17		Cycle 18		Cycle 19	
Month	Thermal Gen. MWt-hr	Month	Thermal Gen. MWt-hr	Month	Thermal Gen. MWt-hr	Month	Thermal Gen. MWt-hr
Mar-86	280056			Mar-88	223258		
Apr-86	1091832	Mar-87	708461	Apr-88	1072037	May-89	13848
May-86	1129992	Apr-87	1088688	May-88	1108301	Jun-89	878174
Jun-86	1080912	May-87	1088112	Jun-88	939036	Jul-89	1040174
Jul-86	1035216	Jun-87	1089638	Jul-88	1044756	Aug-89	710578
Aug-86	1123488	Jul-87	1126248	Aug-88	1113811	Sep-89	1080422
Sep-86	1093752	Aug-87	1125559	Sep-88	1068655	Oct-89	1122288
Oct-86	1075584	Sep-87	1057654	Oct-88	1125024	Nov-89	1074098
Nov-86	1040304	Oct-87	1128811	Nov-88	1088028	Dec-89	1107108
Dec-86	1121160	Nov-87	1091532	Dec-88	1104055	Jan-90	1105469
Jan-87	1088064	Dec-87	1113677	Jan-89	1061697	Feb-90	1012205
Feb-87	171240	Jan-88	1029730	Feb-89	1006661	Mar-90	808550
		Feb-88	125990	Mar-89	556975	Apr-90	0
				Apr-89	0		

TABLE 3-7 cont'd

MONTHLY THERMAL GENERATION DURING THE FIRST TWENTY-FIVE FUEL CYCLES OF THE GINNA REACTOR

Cycle 20		Cycle 21		Cycle 22		Cycle 23	
Month	Thermal Gen. MWt-hr	Month	Thermal Gen. MWt-hr	Month	Thermal Gen. MWt-hr	Month	Thermal Gen. MWt-hr
May-90	769318	May-91	599282	May-92	610650	Apr-93	91944
Jun-90	1012320	Jun-91	1065760	Jun-92	948520	May-93	1059620
Jul-90	1098566	Jul-91	1100696	Jul-92	1097720	Jun-93	1068915
Aug-90	1098437	Aug-91	1022214	Aug-92	1101108	Jul-93	1105566
Sep-90	959083	Sep-91	1049792	Sep-92	1059758	Aug-93	1088384
Oct-90	1093051	Oct-91	1103223	Oct-92	1103684	Sep-93	1068747
Nov-90	1056218	Nov-91	1067033	Nov-92	1045291	Oct-93	1106564
Dec-90	715030	Dec-91	1102728	Dec-92	1106157	Nov-93	731946
Jan-91	1096111	Jan-92	1106865	Jan-93	1100087	Dec-93	1099588
Feb-91	988894	Feb-92	780610	Feb-93	1004079	Jan-94	1088034
Mar-91	668083	Mar-92	868877	Mar-93	386820	Feb-94	998757
Apr-91	0	Apr-92	0			Mar-94	116893

TABLE 3-7 cont'd

MONTHLY THERMAL GENERATION DURING THE FIRST TWENTY-FIVE FUEL CYCLES OF THE GINNA REACTOR

Cycle 24		Cycle 25	
Month	Thermal Gen. MWt-hr	Month	Thermal Gen. MWt-hr
Apr-94	283107	Apr-95	9
May-94	1019528	May-95	934804
Jun-94	960449	Jun-95	1040844
Jul-94	1103548	Jul-95	1085722
Aug-94	615679	Aug-95	975736
Sep-94	1060583	Sep-95	1055684
Oct-94	1115487	Oct-95	1093897
Nov-94	1081351	Nov-95	1057617
Dec-94	1115511	Dec-95	1095856
Jan-95	1095892	Jan-96	1096191
Feb-95	1000530	Feb-96	1024993
Mar-95	911453	Mar-96	947615
		Apr-96	30568

TABLE 3-8

MEASURED SENSOR ACTIVITIES AND REACTION RATES
SURVEILLANCE CAPSULE V
SATURATED ACTIVITIES AND REACTION RATES

Reaction	Measured Activity (dps/gm)	Saturated Activity (dps/gm)	Reaction Rate (rps/atom)
^{63}Cu (n,α) ^{60}Co			
Top	7.38e+04	4.64e+05	6.79e-17
Top Middle	6.77e+04	4.25e+05	6.23e-17
Bottom Middle	7.48e+04	4.70e+05	6.88e-17
Bottom	8.13e+04	5.11e+05	7.48e-17
^{54}Fe (n,p) ^{54}Mn			
W 1	2.47e+06	5.00e+06	7.60e-15
R 1	2.57e+06	5.21e+06	7.91e-15
S 6	2.18e+06	4.42e+06	6.71e-15
P 7	2.57e+06	5.21e+06	7.91e-15
W 2	2.04e+06	4.13e+06	7.67e-15
R 3	1.95e+06	3.95e+06	7.33e-15
S 8	2.02e+06	4.09e+06	7.59e-15
P 9	2.10e+06	4.26e+06	7.89e-15
^{58}Ni (n,p) ^{58}Co			
Middle	2.38e+07	6.51e+07	8.83e-15
^{238}U (n,f) ^{137}Cs			
Middle	2.30e+05	7.29e+06	4.81e-14
^{237}Np (n,f) ^{137}Cs			
Middle	1.23e+06	3.90e+07	2.45e-13

TABLE 3-8 cont'd

MEASURED SENSOR ACTIVITIES AND REACTION RATES
SURVEILLANCE CAPSULE R
SATURATED ACTIVITIES AND REACTION RATES

Reaction	Measured Activity (dps/gm)	Saturated Activity (dps/gm)	Reaction Rate (rps/atom)
^{63}Cu (n,α) ^{60}Co			
Top	1.08e+05	4.42e+05	6.47e-17
Top Middle	9.68e+04	3.96e+05	5.80e-17
Bottom Middle	1.15e+05	4.70e+05	6.89e-17
Bottom	1.15e+05	4.70e+05	6.89e-17
^{54}Fe (n,p) ^{54}Mn			
W 13	2.08e+06	5.19e+06	7.88e-15
R 14	1.98e+06	4.94e+06	7.51e-15
P 18	2.06e+06	5.14e+06	7.81e-15
W 14	1.63e+06	4.07e+06	7.54e-15
R 15	1.70e+06	4.24e+06	7.87e-15
P 19	1.85e+06	4.62e+06	8.56e-15
^{58}Ni (n,p) ^{58}Co			
Middle	5.83e+06	7.38e+07	1.00e-14
^{59}Co (n,γ) ^{60}Co			
Top	3.09e+07	1.26e+08	8.00e-12
Top Middle	3.14e+07	1.28e+08	8.13e-12
Middle	2.96e+07	1.21e+08	7.66e-12
Bottom Middle	2.94e+07	1.20e+08	7.61e-12
Bottom	2.94e+07	1.20e+08	7.61e-12
^{59}Co (n,γ) ^{60}Co (Cd)			
Top	1.19e+07	4.87e+07	3.21e-12
Top Middle	1.18e+07	4.83e+07	3.18e-12
Middle	1.07e+07	4.38e+07	2.88e-12
Bottom Middle	1.24e+07	5.07e+07	3.34e-12
Bottom	1.24e+07	5.07e+07	3.34e-12
^{238}U (n,f) ^{137}Cs			
Middle	4.32e+05	7.81e+06	5.15e-14
^{237}Np (n,f) ^{137}Cs			
Middle	4.25e+06	7.68e+07	4.83e-13

TABLE 3-8 cont'd

MEASURED SENSOR ACTIVITIES AND REACTION RATES
SURVEILLANCE CAPSULE T
SATURATED ACTIVITIES AND REACTION RATES

Reaction	Measured Activity (dps/gm)	Saturated Activity (dps/gm)	Reaction Rate (rps/atom)
^{63}Cu (n,α) ^{60}Co			
Top	1.60e+05	3.52e+05	5.10e-17
Top Middle	1.40e+05	3.08e+05	4.47e-17
Bottom Middle	1.66e+05	3.65e+05	5.29e-17
Bottom	1.74e+05	3.83e+05	5.55e-17
^{54}Fe (n,p) ^{54}Mn			
S 22	1.14e+06	3.38e+06	5.13e-15
P 28	1.27e+06	3.76e+06	5.71e-15
W 21	1.30e+06	3.85e+06	5.85e-15
S 23	1.01e+06	2.99e+06	5.50e-15
P 29	1.03e+06	3.05e+06	5.61e-15
W 22	1.10e+06	3.26e+06	5.99e-15
^{58}Ni (n,p) ^{58}Co			
Middle	8.62e+05	5.30e+07	7.19e-15
^{59}Co (n,γ) ^{60}Co			
Top	3.17e+07	6.98e+07	4.32e-12
Top Middle	3.06e+07	6.73e+07	4.17e-12
Middle	3.03e+07	6.67e+07	4.13e-12
Bottom Middle	3.27e+07	7.20e+07	4.46e-12
Bottom	3.07e+07	6.76e+07	4.19e-12
^{59}Co (n,γ) ^{60}Co (Cd)			
Top	1.21e+07	2.66e+07	1.68e-12
Top Middle	1.13e+07	2.49e+07	1.57e-12
Middle	1.16e+07	2.55e+07	1.62e-12
Bottom Middle	1.26e+07	2.77e+07	1.76e-12
Bottom	1.20e+07	2.64e+07	1.67e-12
^{238}U (n,f) ^{137}Cs			
Middle	7.41e+05	5.36e+06	3.53e-14
^{237}Np (n,f) ^{137}Cs			
Middle	6.09e+06	4.40e+07	2.76e-13

TABLE 3-8 cont'd

MEASURED SENSOR ACTIVITIES AND REACTION RATES
SURVEILLANCE CAPSULE S
SATURATED ACTIVITIES AND REACTION RATES

Reaction	Measured Activity (dps/gm)	Saturated Activity (dps/gm)	Reaction Rate (rps/atom)
^{63}Cu (n,α) ^{60}Co			
Top	2.06e+05	3.07e+05	4.44e-17
Top Middle	1.82e+05	2.71e+05	3.93e-17
Bottom Middle	1.98e+05	2.95e+05	4.27e-17
Bottom	2.18e+05	3.24e+05	4.70e-17
^{54}Fe (n,p) ^{54}Mn			
P 31	1.62e+06	2.94e+06	4.46e-15
^{58}Ni (n,p) ^{58}Co			
Middle	8.51e+06	4.29e+07	5.82e-15
^{59}Co (n,γ) ^{60}Co			
Top	3.55e+07	5.28e+07	3.31e-12
Top Middle	3.71e+07	5.52e+07	3.46e-12
Middle	3.39e+07	5.05e+07	3.16e-12
Bottom Middle	3.60e+07	5.36e+07	3.36e-12
Bottom	3.45e+07	5.14e+07	3.22e-12
^{59}Co (n,γ) ^{60}Co (Cd)			
Top	1.43e+07	2.13e+07	1.38e-12
Top Middle	1.37e+07	2.04e+07	1.32e-12
Middle	1.31e+07	1.95e+07	1.26e-12
Bottom Middle	1.45e+07	2.16e+07	1.39e-12
Bottom	1.35e+07	2.01e+07	1.30e-12
^{238}U (n,f) ^{137}Cs			
Middle	1.40e+06	4.64e+06	3.06e-14
^{237}Np (n,f) ^{137}Cs			
Middle	1.11e+07	3.68e+07	2.31e-13

TABLE 3-9

SUMMARY OF NEUTRON DOSIMETRY RESULTS
SURVEILLANCE CAPSULES V, R, T AND S

Measured Flux and Fluence for Capsule V

Quantity	Flux	Quantity	Fluence	Uncertainty
	[n/cm^2-sec]		[n/cm^2]	
ϕ (E > 1.0 MeV)	1.129e+11	Φ (E > 1.0 MeV)	5.028e+18	10%
ϕ (E > 0.1 MeV)	4.426e+11	Φ (E > 0.1 MeV)	1.971e+19	21%
ϕ (E < 0.414 eV)	2.314e+11	Φ (E < 0.414 eV)	1.031e+19	83%
dpa/sec	2.062e-10	dpa	9.183e-03	15%

Measured Flux and Fluence for Capsule R

Quantity	Flux	Quantity	Fluence	Uncertainty
	[n/cm^2-sec]		[n/cm^2]	
ϕ (E > 1.0 MeV)	1.374e+11	Φ (E > 1.0 MeV)	1.105e+19	8%
ϕ (E > 0.1 MeV)	5.892e+11	Φ (E > 0.1 MeV)	4.738e+19	15%
ϕ (E < 0.414 eV)	1.964e+11	Φ (E < 0.414 eV)	1.579e+19	20%
dpa/sec	2.606e-10	dpa	2.096e-02	11%

Measured Flux and Fluence for Capsule T

Quantity	Flux	Quantity	Fluence	Uncertainty
	[n/cm^2-sec]		[n/cm^2]	
ϕ (E > 1.0 MeV)	8.611e+10	Φ (E > 1.0 MeV)	1.864e+19	8%
ϕ (E > 0.1 MeV)	3.250e+11	Φ (E > 0.1 MeV)	7.035e+19	15%
ϕ (E < 0.414 eV)	1.080e+11	Φ (E < 0.414 eV)	2.338e+19	19%
dpa/sec	1.528e-10	dpa	3.307e-02	10%

Measured Flux and Fluence for Capsule S

Quantity	Flux	Quantity	Fluence	Uncertainty
	[n/cm^2-sec]		[n/cm^2]	
ϕ (E > 1.0 MeV)	6.982e+10	Φ (E > 1.0 MeV)	3.746e+19	8%
ϕ (E > 0.1 MeV)	2.743e+11	Φ (E > 0.1 MeV)	1.472e+20	15%
ϕ (E < 0.414 eV)	8.341e+10	Φ (E < 0.414 eV)	4.475e+19	19%
dpa/sec	1.268e-10	dpa	6.803e-02	11%

TABLE 3-10

COMPARISON OF MEASURED AND FERRET CALCULATED REACTION RATES AT THE SURVEILLANCE CAPSULE CENTER

Surveillance Capsule V

Reaction Rate (rps/nucleus)

	Measured	Adjusted Calc.	M/C Adjusted
^{63}Cu (n,α)	6.84e-17	6.73e-17	1.02
^{54}Fe (n,p)	7.58e-15	7.41e-15	1.02
^{58}Ni (n,p)	8.84e-15	9.36e-15	0.94
^{238}U (n,f) (Cd)	3.94e-14	3.71e-14	1.06

Surveillance Capsule R

Reaction Rate (rps/nucleus)

	Measured	Adjusted Calc.	M/C Adjusted
^{63}Cu (n,α)	6.51e-17	6.44e-17	1.01
^{54}Fe (n,p)	7.86e-15	7.77e-15	1.01
^{58}Ni (n,p)	1.00e-14	1.04e-14	0.96
^{238}U (n,f) (Cd)	4.14e-14	4.23e-14	0.98
^{237}Np (n,f) (Cd)	4.75e-13	4.38e-13	1.08
^{59}Co (n,γ)	7.80e-12	7.81e-12	1.00
^{59}Co (n,γ) (Cd)	3.19e-12	3.19e-12	1.00

TABLE 3-10 cont'd

COMPARISON OF MEASURED AND FERRET CALCULATED
REACTION RATES AT THE SURVEILLANCE CAPSULE CENTER

Surveillance Capsule T

Reaction Rate (rps/nucleus)

	Measured	Adjusted Calc.	M/C Adjusted
^{63}Cu (n,α)	5.10e-17	5.06e-17	1.01
^{54}Fe (n,p)	5.63e-15	5.58e-15	1.01
^{58}Ni (n,p)	7.19e-15	7.40e-15	0.97
^{238}U (n,f) (Cd)	2.77e-14	2.79e-14	0.99
^{237}Np (n,f) (Cd)	2.72e-13	2.54e-13	1.07
^{59}Co (n,γ)	4.26e-12	4.26e-12	1.00
^{59}Co (n,γ) (Cd)	1.66e-12	1.66e-12	1.00

Surveillance Capsule S

Reaction Rate (rps/nucleus)

	Measured	Adjusted Calc.	M/C Adjusted
^{63}Cu (n,α)	4.34e-17	4.26e-17	1.02
^{54}Fe (n,p)	4.46e-15	4.47e-15	1.00
^{58}Ni (n,p)	5.82e-15	5.98e-15	0.97
^{238}U (n,f) (Cd)	2.21e-14	2.25e-14	0.98
^{237}Np (n,f) (Cd)	2.27e-13	2.11e-13	1.08
^{59}Co (n,γ)	3.30e-12	3.31e-12	1.00
^{59}Co (n,γ) (Cd)	1.33e-12	1.33e-12	1.00

TABLE 3-11

ADJUSTED NEUTRON ENERGY SPECTRUM AT THE CENTER OF SURVEILLANCE CAPSULES

Capsule V

Group #	Energy (MeV)	Flux (n/cm^2-sec)	Group #	Energy (MeV)	Flux (n/cm^2-sec)
1	1.73e+01	7.97e+06	28	9.12e-03	2.52e+10
2	1.49e+01	1.73e+07	29	5.53e-03	2.71e+10
3	1.35e+01	6.54e+07	30	3.35e-03	8.57e+09
4	1.16e+01	1.82e+08	31	2.84e-03	8.32e+09
5	1.00e+01	4.16e+08	32	2.40e-03	8.29e+09
6	8.61e+00	7.40e+08	33	2.03e-03	2.50e+10
7	7.41e+00	1.80e+09	34	1.23e-03	2.50e+10
8	6.07e+00	2.81e+09	35	7.49e-04	2.44e+10
9	4.97e+00	5.99e+09	36	4.54e-04	2.25e+10
10	3.68e+00	7.14e+09	37	2.75e-04	2.41e+10
11	2.87e+00	1.35e+10	38	1.67e-04	2.52e+10
12	2.23e+00	1.76e+10	39	1.01e-04	2.49e+10
13	1.74e+00	2.34e+10	40	6.14e-05	2.47e+10
14	1.35e+00	2.48e+10	41	3.73e-05	2.45e+10
15	1,11e+00	4.23e+10	42	2.26e-05	2.40e+10
16	8.21e-01	4.70e+10	43	1.37e-05	2.32e+10
17	6.39e-01	5.04e+10	44	8.31e-06	2.28e+10
18	4.98e-01	3.43e+10	45	5.04e-06	2.27e+10
19	3.88e-01	4.79e+10	46	3.06e-06	2.26e+10
20	3.02e-01	5.89e+10	47	1.86e-06	2.24e+10
21	1.83e-01	5.45e+10	48	1.13e-06	1.99e+10
22	1.11e-01	4.22e+10	49	6.83e-07	1.85e+10
23	6.74e-02	3.52e+10	50	4.14e-07	3.40e+10
24	4.09e-02	2.19e+10	51	2.51e-07	3.70e+10
25	2.55e-02	2.09e+10	52	1.52e-07	4.03e+10
26	1.99e-02	1.40e+10	53	9.24e-08	1.20e+11
27	1.50e-02	2.32e+10			

Note: Tabulated energy levels represent the upper energy in each group.

TABLE 3-11 cont'd

ADJUSTED NEUTRON ENERGY SPECTRUM AT THE CENTER OF SURVEILLANCE CAPSULES

Capsule R

Group #	Energy (MeV)	Flux (n/cm^2-sec)	Group #	Energy (MeV)	Flux (n/cm^2-sec)
1	1.73e+01	7.58e+06	28	9.12e-03	2.78e+10
2	1.49e+01	1.63e+07	29	5.53e-03	2.94e+10
3	1.35e+01	6.14e+07	30	3.35e-03	9.14e+09
4	1.16e+01	1.70e+08	31	2.84e-03	8.74e+09
5	1.00e+01	3.93e+08	32	2.40e-03	8.58e+09
6	8.61e+00	7.08e+08	33	2.03e-03	2.54e+10
7	7.41e+00	1.76e+09	34	1.23e-03	2.50e+10
8	6.07e+00	2.84e+09	35	7.49e-04	2.40e+10
9	4.97e+00	6.29e+09	36	4.54e-04	2.17e+10
10	3.68e+00	7.80e+09	37	2.75e-04	2.30e+10
11	2.87e+00	1.54e+10	38	1.67e-04	2.23e+10
12	2.23e+00	2.08e+10	39	1.01e-04	2.36e+10
13	1.74e+00	2.91e+10	40	6.14e-05	2.38e+10
14	1.35e+00	3.24e+10	41	3.73e-05	2.38e+10
15	1.11e+00	5.75e+10	42	2.26e-05	2.35e+10
16	8.21e-01	6.52e+10	43	1.37e-05	2.29e+10
17	6.39e-01	7.06e+10	44	8.31e-06	2.27e+10
18	4.98e-01	4.78e+10	45	5.04e-06	2.26e+10
19	3.88e-01	6.62e+10	46	3.06e-06	2.26e+10
20	3.02e-01	8.01e+10	47	1.86e-06	2.25e+10
21	1.83e-01	7.24e+10	48	1.13e-06	1.99e+10
22	1.11e-01	5.47e+10	49	6.83e-07	1.76e+10
23	6.74e-02	4.42e+10	50	4.14e-07	3.15e+10
24	4.09e-02	2.67e+10	51	2.51e-07	3.31e+10
25	2.55e-02	2.48e+10	52	1.52e-07	3.51e+10
26	1.99e-02	1.62e+10	53	9.24e-08	9.66e+10
27	1.50e-02	2.61e+10			

Note: Tabulated energy levels represent the upper energy in each group.

TABLE 3-11 cont'd

ADJUSTED NEUTRON ENERGY SPECTRUM AT THE CENTER OF SURVEILLANCE CAPSULES

Capsule T

Group #	Energy (MeV)	Flux (n/cm^2-sec)	Group #	Energy (MeV)	Flux (n/cm^2-sec)
1	1.73e+01	6.40e+06	28	9.12e-03	1.44e+10
2	1.49e+01	1.37e+07	29	5.53e-03	1.52e+10
3	1.35e+01	5.05e+07	30	3.35e-03	4.69e+09
4	1.16e+01	1.39e+08	31	2.84e-03	4.50e+09
5	1.00e+01	3.17e+08	32	2.40e-03	4.43e+09
6	8.61e+00	5.59e+08	33	2.03e-03	1.32e+10
7	7.41e+00	1.39e+09	34	1.23e-03	1.30e+10
8	6.07e+00	2.16e+09	35	7.49e-04	1.24e+10
9	4.97e+00	4.52e+09	36	4.54e-04	1.13e+10
10	3.68e+00	5.27e+09	37	2.75e-04	1.19e+10
11	2.87e+00	1.02e+10	38	1.67e-04	1.16e+10
12	2.23e+00	1.33e+10	39	1.01e-04	1.22e+10
13	1.74e+00	1.79e+10	40	6.14e-05	1.22e+10
14	1.35e+00	1.92e+10	41	3.73e-05	1.22e+10
15	1.11e+00	3.26e+10	42	2.26e-05	1.20e+10
16	8.21e-01	3.57e+10	43	1.37e-05	1.17e+10
17	6.39e-01	3.77e+10	44	8.31e-06	1.16e+10
18	4.98e-01	2.53e+10	45	5.04e-06	1.16e+10
19	3.88e-01	3.44e+10	46	3.06e-06	1.16e+10
20	3.02e-01	4.15e+10	47	1.86e-06	1.16e+10
21	1.83e-01	3.70e+10	48	1.13e-06	1.04e+10
22	1.11e-01	2.78e+10	49	6.83e-07	9.06e+09
23	6.74e-02	2.25e+10	50	4.14e-07	1.55e+10
24	4.09e-02	1.35e+10	51	2.51e-07	1.72e+10
25	2.55e-02	1.26e+10	52	1.52e-07	1.91e+10
26	1.99e-02	8.29e+09	53	9.24e-08	5.62e+10
27	1.50e-02	1.35e+10			

Note: Tabulated energy levels represent the upper energy in each group.

TABLE 3-11 cont'd

ADJUSTED NEUTRON ENERGY SPECTRUM AT THE CENTER OF SURVEILLANCE CAPSULES

Capsule S

Group #	Energy (MeV)	Flux (n/cm^2-sec)	Group #	Energy (MeV)	Flux (n/cm^2-sec)
1	1.73e+01	5.49e+06	28	9.12e-03	1.27e+10
2	1.49e+01	1.17e+07	29	5.53e-03	1.34e+10
3	1.35e+01	4.31e+07	30	3.35e-03	4.15e+09
4	1.16e+01	1.17e+08	31	2.84e-03	3.95e+09
5	1.00e+01	2.66e+08	32	2.40e-03	3.85e+09
6	8.61e+00	4.64e+08	33	2.03e-03	1.13e+10
7	7.41e+00	1.13e+09	34	1.23e-03	1.11e+10
8	6.07e+00	1.73e+09	35	7.49e-04	1.04e+10
9	4.97e+00	3.62e+09	36	4.54e-04	9.36e+09
10	3.68e+00	4.24e+09	37	2.75e-04	9.82e+09
11	2.87e+00	8.14e+09	38	1.67e-04	9.16e+09
12	2.23e+00	1.07e+10	39	1.01e-04	1.00e+10
13	1.74e+00	1.45e+10	40	6.14e-05	1.01e+10
14	1.35e+00	1.57e+10	41	3.73e-05	1.02e+10
15	1.11e+00	2.69e+10	42	2.26e-05	1.02e+10
16	8.21e-01	2.99e+10	43	1.37e-05	9.92e+09
17	6.39e-01	3.19e+10	44	8.31e-06	9.89e+09
18	4.98e-01	2.16e+10	45	5.04e-06	9.93e+09
19	3.88e-01	2.96e+10	46	3.06e-06	9.94e+09
20	3.02e-01	3.61e+10	47	1.86e-06	9.91e+09
21	1.83e-01	3.25e+10	48	1.13e-06	8.80e+09
22	1.11e-01	2.46e+10	49	6.83e-07	7.60e+09
23	6.74e-02	1.99e+10	50	4.14e-07	1.30e+10
24	4.09e-02	1.20e+10	51	2.51e-07	1.39e+10
25	2.55e-02	1.12e+10	52	1.52e-07	1.50e+10
26	1.99e-02	7.35e+09	53	9.24e-08	4.16e+10
27	1.50e-02	1.19e+10			

Note: Tabulated energy levels represent the upper energy in each group.

TABLE 3-12

COMPARISON OF CALCULATED AND MEASURED INTEGRATED NEUTRON EXPOSURE OF GINNA SURVEILLANCE CAPSULES V, R, T, AND S

CAPSULE V

		Calculated	Measured	M/C
$\Phi(E > 1.0$ MeV)	[n/cm^2]	5.864e+18	5.028e+18	0.86
$\Phi(E > 0.1$ MeV)	[n/cm^2]	2.223e+19	1.971e+19	0.89
dpa		1.044e-02	9.183e-03	0.88

CAPSULE R

		Calculated	Measured	M/C
$\Phi(E > 1.0$ MeV)	[n/cm^2]	1.013e+19	1.105e+19	1.09
$\Phi(E > 0.1$ MeV)	[n/cm^2]	3.839e+19	4.738e+19	1.23
dpa		1.803e-02	2.096e-02	1.16

CAPSULE T

		Calculated	Measured	M/C
$\Phi(E > 1.0$ MeV)	[n/cm^2]	1.669e+19	1.864e+19	1.12
$\Phi(E > 0.1$ MeV)	[n/cm^2]	5.741e+19	7.035e+19	1.23
dpa		2.837e-02	3.307e-02	1.17

CAPSULE S

		Calculated	Measured	M/C
$\Phi(E > 1.0$ MeV)	[n/cm^2]	3.575e+19	3.746e+19	1.05
$\Phi(E > 0.1$ MeV)	[n/cm^2]	1.259e+20	1.472e+20	1.17
dpa		6.150e-02	6.803e-02	1.11

TABLE 3-13

NEUTRON EXPOSURE PROJECTIONS AT KEY LOCATIONS
ON THE REACTOR VESSEL CLAD/BASE METAL INTERFACE

Best Estimate Exposure (19.51 EFPY) at the Reactor Vessel Inner Radius

	0°	15°	30°	45°
Φ (E > 1.0 MeV)	2.32e+19	1.47e+19	1.05e+19	9.69e+18
Φ (E > 0.1 MeV)	1.97e+20	1.39e+20	1.00e+20	8.38e+19
dpa	6.88e-02	4.68e-02	3.36e-02	2.86e-02

Best Estimate Exposure (28 EFPY) at the Reactor Vessel Inner Radius

	0°	15°	30°	45°
Φ (E > 1.0 MeV)	3.11e+19	1.96e+19	1.40e+19	1.29e+19
Φ (E > 0.1 MeV)	2.65e+20	1.86e+20	1.34e+20	1.13e+20
dpa	9.24e-02	6.24e-02	4.49e-02	3.86e-02

Best Estimate Exposure (32 EFPY) at the Reactor Vessel Inner Radius

	0°	15°	30°	45°
Φ (E > 1.0 MeV)	3.49e+19	2.20e+19	1.56e+19	1.45e+19
Φ (E > 0.1 MeV)	2.97e+20	2.08e+20	1.50e+20	1.27e+20
dpa	1.03e-01	6.98e-02	5.02e-02	4.33e-02

Best Estimate Exposure (42 EFPY) at the Reactor Vessel Inner Radius

	0°	15°	30°	45°
Φ (E > 1.0 MeV)	4.42e+19	2.78e+19	1.98e+19	1.83e+19
Φ (E > 0.1 MeV)	3.77e+20	2.63e+20	1.89e+20	1.61e+20
dpa	1.31e-01	8.83e-02	6.34e-02	5.51e-02

Best Estimate Exposure (48 EFPY) at the Reactor Vessel Inner Radius

	0°	15°	30°	45°
Φ (E > 1.0 MeV)	4.98e+19	3.13e+19	2.22e+19	2.06e+19
Φ (E > 0.1 MeV)	4.25e+20	2.96e+20	2.13e+20	1.82e+20
dpa	1.48e-01	9.93e-02	7.14e-02	6.22e-02

TABLE 3-14

NEUTRON EXPOSURE VALUES WITHIN THE GINNA REACTOR VESSEL

FLUENCE BASED ON E > 1.0 MeV SLOPE

28 EFPY Φ (E > 1.0 MeV) [n/cm^2]

	0°	15°	30°	45°
Surface	3.11e+19	1.96e+19	1.40e+19	1.29e+19
¼ T	1.99e+19	1.27e+19	8.89e+18	8.38e+18
¾ T	6.10e+18	4.05e+18	2.81e+18	2.67e+18

32 EFPY Φ (E > 1.0 MeV) [n/cm^2]

	0°	15°	30°	45°
Surface	3.49e+19	2.20e+19	1.56e+19	1.45e+19
¼ T	2.23e+19	1.41e+19	9.94e+18	9.37e+18
¾ T	6.83e+18	4.53e+18	3.14e+18	2.98e+18

42 EFPY Φ (E > 1.0 MeV) [n/cm^2]

	0°	15°	30°	45°
Surface	4.42e+19	2.78e+19	1.98e+19	1.83e+19
¼ T	2.83e+19	1.79e+19	1.26e+19	1.18e+19
¾ T	8.67e+18	5.72e+18	3.97e+18	3.77e+18

48 EFPY Φ (E > 1.0 MeV) [n/cm^2]

	0°	15°	30°	45°
Surface	4.98e+19	3.13e+19	2.22e+19	2.06e+19
¼ T	3.18e+19	2.01e+19	1.41e+19	1.33e+19
¾ T	9.77e+18	6.44e+18	4.47e+18	4.25e+18

TABLE 3-14 cont'd

NEUTRON EXPOSURE VALUES WITHIN THE
GINNA REACTOR VESSEL

FLUENCE BASED ON dpa SLOPE

28 EFPY Φ (E > 1.0 MeV) [n/cm^2]

	0°	15°	30°	45°
Surface	3.11e+19	1.96e+19	1.40e+19	1.29e+19
¼ T	2.22e+19	1.43e+19	1.00e+19	9.36e+18
¾ T	9.37e+18	6.44e+18	4.50e+18	4.17e+18

32 EFPY Φ (E > 1.0 MeV) [n/cm^2]

	0°	15°	30°	45°
Surface	3.49e+19	2.20e+19	1.56e+19	1.45e+19
¼ T	2.48e+19	1.59e+19	1.12e+19	1.05e+19
¾ T	1.05e+19	7.21e+18	5.03e+18	4.66e+18

42 EFPY Φ (E > 1.0 MeV) [n/cm^2]

	0°	15°	30°	45°
Surface	4.42e+19	2.78e+19	1.98e+19	1.83e+19
¼ T	3.15e+19	2.02e+19	1.42e+19	1.32e+19
¾ T	1.33e+19	9.11e+18	6.36e+18	5.90e+18

48 EFPY Φ (E > 1.0 MeV) [n/cm^2]

	0°	15°	30°	45°
Surface	4.98e+19	3.13e+19	2.22e+19	2.06e+19
¼ T	3.55e+19	2.27e+19	1.59e+19	1.49e+19
¾ T	1.50e+19	1.03e+19	7.16e+18	6.64e+18

TABLE 3-15

UPDATED LEAD FACTORS FOR GINNA
SURVEILLANCE CAPSULES

Capsule	Lead Factor
V[a]	2.97
T[b]	2.99
R[c]	1.82
S[d]	1.77
N[e]	1.78
P[e]	1.89

[a] - Withdrawn at the end of Cycle 1B.
[b] - Withdrawn at the end of Cycle 3.
[c] - Withdrawn at the end of Cycle 9.
[d] - Withdrawn at the end of Cycle 22.
[e] - Capsules remaining in the reactor.

4 CRITERIA FOR ALLOWABLE PRESSURE-TEMPERATURE RELATIONSHIPS

Appendix G to 10 CFR Part 50, "Fracture Toughness Requirements"[3] specifies fracture toughness requirements for ferritic materials of pressure-retaining components of the reactor coolant pressure boundary of light water nuclear power reactors to provide adequate margins of safety during any condition of normal operation, including anticipated operational occurrences and system hydrostatic tests, to which the pressure boundary may be subjected over its service lifetime. The ASME Boiler and Pressure Vessel Code forms the basis for these requirements. Section XI, Division 1, "Rules for Inservice Inspection of Nuclear Power Plant Components", Appendix G[48], contains the conservative methods of analysis.

The ASME approach for calculating the allowable limit curves for various heatup and cooldown rates specifies that the total stress intensity factor, K_I, for the combined thermal and pressure stresses at any time during heatup or cooldown cannot be greater than the reference stress intensity factor, K_{Ia}, for the metal temperature at that time. K_{Ia} is obtained from the reference fracture toughness curve, defined in Appendix G of Section XI of the ASME Code. The K_{Ia} curve is given by the following equation:

$$K_{Ia}=26.78+1.233*e^{[0.0145(T-RT_{NDT}+160)]} \quad (1)$$

where,

K_{Ia} = reference stress intensity factor as a function of the metal temperature T and the metal reference nil-ductility temperature RT_{NDT}

Therefore, the governing equation for the heatup-cooldown analysis is defined in Appendix G of the ASME Code as follows:

$$C*K_{Im}+K_{It}<K_{Ia} \quad (2)$$

where,

K_{Im} = stress intensity factor caused by membrane (pressure) stress
K_{It} = stress intensity factor caused by the thermal gradients
K_{Ia} = function of temperature relative to the RT_{NDT} of the material
C = 2.0 for Level A and Level B service limits
C = 1.5 for hydrostatic and leak test conditions during which the reactor core is not critical

At any time during the heatup or cooldown transient, K_{Ia} is determined by the metal temperature at the tip of a postulated flaw at the 1/4T and 3/4T location, the appropriate value for RT_{NDT}, and the reference fracture toughness curve. The thermal stresses resulting from the temperature gradients through the vessel wall are calculated and then the corresponding (thermal) stress intensity factors, K_{It}, for the reference flaw are computed. From Equation 2, the pressure stress intensity factors are obtained and, from these, the allowable pressures are calculated.

For the calculation of the allowable pressure versus coolant temperature during cooldown, the reference flaw of Appendix G to the ASME Code is assumed to exist at the inside of the vessel wall. During cooldown, the controlling location of the flaw is always at the inside of the wall because the thermal gradients produce tensile stresses at the inside, which increase with increasing cooldown rates. Allowable pressure-temperature relations are generated for both steady-state and finite cooldown rate situations. From these relations, composite limit curves are constructed for each cooldown rate of interest.

The use of the composite curve in the cooldown analysis is necessary because control of the cooldown procedure is based on the measurement of reactor coolant temperature, whereas the limiting pressure is actually dependent on the material temperature at the tip of the assumed flaw. During cooldown, the 1/4T vessel location is at a higher temperature than the fluid adjacent to the vessel inner diameter. This condition, of course, is not true for the steady-state situation. It follows that, at any given reactor coolant temperature, the ΔT (temperature) developed during cooldown results in a higher value of K_{Ia} at the 1/4T location for finite cooldown rates than for steady-state operation. Furthermore, if conditions exist so that the increase in K_{Ia} exceeds K_{It}, the calculated allowable pressure during cooldown will be greater than the steady-state value.

The above procedures are needed because there is no direct control on temperature at the 1/4T location and, therefore, allowable pressures may unknowingly be violated if the rate of cooling is decreased at various intervals along a cooldown ramp. The use of the composite curve eliminates this problem and ensures conservative operation of the system for the entire cooldown period.

Three separate calculations are required to determine the limit curves for finite heatup rates. As is done in the cooldown analysis, allowable pressure-temperature relationships are developed for steady-state conditions as well as finite heatup rate conditions assuming the presence of a 1/4T defect at the inside of the wall. The heatup results in compressive stresses at the inside surface that alleviate the tensile stresses produced by internal pressure. The metal temperature at the crack tip lags the coolant temperature; therefore, the K_{Ia} for the 1/4T crack during heatup is lower than the K_{Ia} for the 1/4T crack during steady-state conditions at the same coolant temperature. During heatup, especially at the end of the transient, conditions may exist so that the effects of compressive thermal stresses and lower K_{Ia} values do not offset each other, and the pressure-temperature curve based on steady-state

conditions no longer represents a lower bound of all similar curves for finite heatup rates when the 1/4T flaw is considered. Therefore, both cases have to be analyzed in order to ensure that at any coolant temperature the lower value of the allowable pressure calculated for steady-state and finite heatup rates is obtained.

The second portion of the heatup analysis concerns the calculation of the pressure-temperature limitations for the case in which a 1/4T flaw located at the 1/4T location from the outside surface is assumed. Unlike the situation at the vessel inside surface, the thermal gradients established at the outside surface during heatup produce stresses which are tensile in nature and therefore tend to reinforce any pressure stresses present. These thermal stresses are dependent on both the rate of heatup and the time (or coolant temperature) along the heatup ramp. Since the thermal stresses at the outside are tensile and increase with increasing heatup rates, each heatup rate must be analyzed on an individual basis.

Following the generation of pressure-temperature curves for both the steady state and finite heatup rate situations, the final limit curves are produced by constructing a composite curve based on a point-by-point comparison of the steady-state and finite heatup rate data. At any given temperature, the allowable pressure is taken to be the lesser of the three values taken from the curves under consideration. The use of the composite curve is necessary to set conservative heatup limitations because it is possible for conditions to exist wherein, over the course of the heatup ramp, the controlling condition switches from the inside to the outside, and the pressure limit must at all times be based on analysis of the most critical criterion.

10 CFR Part 50, Appendix G addresses the metal temperature of the closure head flange and vessel flange regions. This rule states that the metal temperature of the closure flange regions must exceed the material unirradiated RT_{NDT} by at least 120°F for normal operation when the pressure exceeds 20 percent of the preservice hydrostatic test pressure (3106 psig[49]), which is 621 psig for R. E. Ginna.

The limiting unirradiated RT_{NDT} of -52°F[49] occurs in the vessel flange of the R. E. Ginna reactor vessel, so the minimum allowable temperature of this region is 68°F at pressures greater than 621 psig. However, this limit does not impact the curves presented in Figures 6-1 through 6-8.

5 CALCULATION OF ADJUSTED REFERENCE TEMPERATURE

From Regulatory Guide 1.99, Revision 2, the adjusted reference temperature (ART) for each material in the beltline region is given by the following expression:

$$ART = InitialRT_{NDT} + \Delta RT_{NDT} + Margin \quad (3)$$

Initial RT_{NDT} is the reference temperature for the unirradiated material as defined in paragraph NB-2331 of Section III of the ASME Boiler and Pressure Vessel Code[50]. If measured values of initial RT_{NDT} for the material in question are not available, generic mean values for that class of material may be used if there are sufficient test results to establish a mean and standard deviation for the class of material.

ΔRT_{NDT} is the mean value of the adjustment in reference temperature caused by irradiation and should be calculated as follows:

$$\Delta RT_{NDT} = CF * f^{(0.28 - 0.10 \log f)} \quad (4)$$

To calculate ΔRT_{NDT} at any depth (e.g., at 1/4T or 3/4T), the following formula must first be used to attenuate the fluence at the specific depth.

$$f_{(depth\,x)} = f_{surface} * e^{(-0.24x)} \quad (5)$$

where x inches (vessel beltline thickness is 6.5 inches[49]) is the depth into the vessel wall measured from the vessel clad/base metal interface. The resultant fluence is then placed in Equation 4 to calculate the ΔRT_{NDT} at the specific depth.

The Westinghouse Radiation Engineering and Analysis group evaluated the vessel fluence projections and the results are presented in Section 3 of this report. The evaluation used the ENDF/B-VI scattering cross-section data set. This is consistent with the methods presented in WCAP-14040-NP-A, "Methodology Used to Develop Cold Overpressure Mitigating System Setpoints and RCS Heatup and Cooldown Limit Curves"[2]. Table 5-1 contains the reevaluated fluence values used to calculate the ART values for all beltline materials in the Ginna reactor vessel. Additionally, the surveillance capsule fluence values are presented in Table 5-2.

TABLE 5-1
Summary of the Peak Pressure Vessel Neutron Fluence Values
used for the Calculation of ART Values
(E > 1.0 MeV, n/cm^2)

EFPY	Surface	1/4 T	3/4 T
24	2.74×10^{19}	1.85×10^{19}	8.50×10^{18}
28	3.11×10^{19}	2.11×10^{19}	9.65×10^{18}
32	3.49×10^{19}	2.36×10^{19}	1.08×10^{19}
40	4.23×10^{19}	2.87×10^{19}	1.31×10^{19}

TABLE 5-2
Measured Integrated Neutron Exposure of the R. E. Ginna Surveillance Capsules

Capsule	Fluence
V	5.028×10^{18} n/cm^2 (E > 1.0 MeV)
R	1.105×10^{19} n/cm^2 (E > 1.0 MeV)
T	1.864×10^{19} n/cm^2 (E > 1.0 MeV)
S	3.746×10^{19} n/cm^2 (E > 1.0 MeV)

Margin is calculated as, $M = 2 * (\sigma_i^2 + \sigma_\Delta^2)^{1/2}$. The standard deviation for the initial RT_{NDT} margin term, σ_i, is 0°F when the initial RT_{NDT} is a measured value, and 17°F when a generic value is used. The standard deviation for the ΔRT_{NDT} margin term, σ_Δ, is 17°F for plates or forgings when surveillance capsule data is not used and 8.5°F for plates or forgings when surveillance capsule data is used. For welds, σ_Δ is 28 °F when surveillance capsule data is not used and 14°F when surveillance capsule data is used. σ_Δ need not exceed one-half the mean value of ΔRT_{NDT}. Per the request of the Rochester Gas and Electric Corporation[52], the margin term to be used for the circumferential weld Seam SA-847 when using surveillance capsule data is 48.3°F.

Contained in Table 5-3 is a summary of the Measured 30 ft-lb transition temperature shifts of the beltline materials contained in the surveillance program[51].

TABLE 5-3
Measured 30 ft-lb Transition Temperature Shifts of the Beltline Materials Contained in the Surveillance Program

Material	Capsule	Measured 30 ft-lb Transition Temperature Shift
Lower Shell Forging 125P666	V	25°F
	R	25°F
	T	30°F
	S	42°F
Intermediate Shell Forging 125S255	V	0°F
	R	0°F
	T	0°F
	S	60°F
Surveillance Weld Metal	V	140°F
	R	165°F
	T	150°F
	S	205°F

Table 5-4 Contains a summary of the weight percent of copper, the weight percent of nickel and the initial RT_{NDT} of the beltline materials, vessel flanges and the surveillance program weld metal. The weight percent values of Cu and Ni given in Table 5-4 were used to generate the calculated chemistry factor (CF) values based on Tables 1 and 2 of Regulatory Guide 1.99, Revision 2, and presented in Table 5-6. Table 5-5 provides the calculation of the CF values based on surveillance capsule data, Regulatory Guide 1.99, Revision 2, Position 2.1.

TABLE 5-4
Reactor Vessel Beltline Material Unirradiated Toughness Properties

Material Description	Cu (%)	Ni (%)	Initial RT_{NDT} (°F)
Closure Head Flange	- -	- -	- 75
Vessel Flange	- -	- -	- 52
Intermediate Shell Forging 125S255	0.07	0.69	20
Lower Shell Forging 125P666	0.05	0.69	40
Circumferential Weld Seam SA	0.25	0.56	-4.8

TABLE 5-4A
Compilation of Copper and Nickel Weight Percent Values for the Ginna Surveillance Program Weld Metal

Reference	Weight % Cu	Weight % Ni
51	0.23	0.56
51	0.22	0.50
54	0.25	0.57
54	0.25	0.52
54	0.27	0.58
54	0.22	0.45
54	0.23	0.50
54	0.23	0.50
54	0.21	0.46
54	0.25	0.53
Average	0.236	0.517

TABLE 5-5
Calculation of Chemistry Factors using Ginna Surveillance Capsule Data

Material	Capsule	Fluence[a]	FF	ΔRT_{NDT}	FF * ΔRT_{NDT}	FF^2
Lower Shell Forging 125P666 (Tangential)	V	5.028×10^{18}	0.8081	25°F	20.2°F	0.6530
	R	1.105×10^{19}	1.0279	25°F	25.7°F	1.0566
	T	1.864×10^{19}	1.1706	30°F	35.1°F	1.3703
	S	3.746×10^{19}	1.3418	42°F	56.4°F	1.8004
				SUM:	137.4°F	4.8803
	Chemistry Factor = 137.4 ÷ 4.8803 = 28.2°F					
Intermediate Shell Forging 125S255 (Tangential)	V	5.028×10^{18}	0.8081	0°F	0°F	0.6530
	R	1.105×10^{19}	1.0279	0°F	0°F	1.0566
	T	1.864×10^{19}	1.1706	0°F	0°F	1.3703
	S	3.746×10^{19}	1.3418	60°F	80.5°F	1.8004
				SUM:	80.5°F	4.8803
	Chemistry Factor = 80.5 ÷ 4.8803 = 16.5°F					
Circ. Weld Seam SA-847[b]	V	5.028×10^{18}	0.8081	149.7°F	121.0°F	0.6530
	R	1.105×10^{19}	1.0279	176.4°F	181.3°F	1.0566
	T	1.864×10^{19}	1.1706	160.4°F	187.8°F	1.3703
	S	3.746×10^{19}	1.3418	219.1°F	294.0°F	1.8004
				SUM:	784.1°F	4.8803
	Chemistry Factor = 784.1 ÷ 4.8803 = 160.7°F					

(a) Fluence values are in units of n/cm^2, E > 1.0 MeV.

(b) The ΔRT_{NDT} values given in this Table have been multiplied by a ratio factor of 1.069. The ratio factor was calculated per Regulatory Guide 1.99, Revision 2 as follows:

Ratio Factor = $CF_{vessel\ weld} \div CF_{surveillance\ weld}$ = 170.4°F ÷ 159.4°F = 1.069

TABLE 5-6
Summary of the Ginna Reactor Vessel Beltline Material Chemistry Factors

Material	Reg. Guide 1.99 , Rev. 2, Position 1.1 CFs	Reg. Guide 1.99 , Rev. 2, Position 2.1 CFs
Inter. Shell Forging 125P666	44°F	16.5°F
Lower Shell Forging 125S255	31°F	28.2°F
Circ. Weld Seam SA-847	170.4°F	160.7°F

Contained in Table 5-7 is a summary of the fluence factors (FF) used in the calculation of adjusted reference temperatures for the Ginna reactor vessel beltline materials.

TABLE 5-7
Summary of the Calculated Fluence Factors Used for the Generation of the 24, 28, 32 and 40 EFPY Heatup and Cooldown Curves

EFPY	1/4 T FF	3/4 T FF
24	1.17	0.95
28	1.20	1.00
32	1.23	1.02
40	1.28	1.08

The adjusted reference temperature (ART) must be calculated for 24, 28, 32 and 40 EFPY for each beltline material at the 1/4T and 3/4T locations. In addition, ART values must be calculated per Regulatory Guide 1.99, Revision 2, Position 1.1 (RG 1.99, R2, P1.1) and Regulatory Guide 1.99, Revision 2, Position 2.1 (RG 1.99, R2, P2.1).

Contained in Tables 5-8 through 5-15 is the calculation of the ART values used for the generation of the heatup and cooldown curves.

TABLE 5-8
Calculation of the ART Values for the 1/4T Location and 24 EFPY

Material	Method	CF	FF	ΔRT_{NDT}	Margin	IRT_{NDT}	ART
Inter. Shell Forging 125S255	RG 1.99, R2, P1.1	44°F	1.17	51.5°F	34°F	20°F	106°F
	RG 1.99, R2, P2.1	16.5°F	1.17	19.3°F	17°F	20°F	56°F
Lower Shell Forging 125P666	RG 1.99, R2, P1.1	31°F	1.17	36.3°F	34°F	40°F	110°F
	RG 1.99, R2, P2.1	28.2°F	1.17	33.0°F	17°F	40°F	90°F
Circ. Weld Seam SA-847	RG 1.99, R2, P1.1	170.4°F	1.17	199.4°F	56°F	-4.8°F	251°F
	RG 1.99, R2, P2.1	160.7°F	1.17	188.0°F	48.3°F	-4.8°F	232°F

TABLE 5-9
Calculation of the ART Values for the 3/4T Location and 24 EFPY

Material	Method	CF	FF	ΔRT_{NDT}	Margin	IRT_{NDT}	ART
Inter. Shell Forging 125S255	RG 1.99, R2, P1.1	44°F	0.95	41.8°F	34°F	20°F	96°F
	RG 1.99, R2, P2.1	16.5°F	0.95	15.7°F	15.7°F	20°F	51°F
Lower Shell Forging 125P666	RG 1.99, R2, P1.1	31°F	0.95	29.5°F	29.5°F	40°F	99°F
	RG 1.99, R2, P2.1	28.2°F	0.95	26.8°F	17°F	40°F	84°F
Circ. Weld Seam SA-847	RG 1.99, R2, P1.1	170.4°F	0.95	161.9°F	56°F	-4.8°F	213°F
	RG 1.99, R2, P2.1	160.7°F	0.95	152.7°F	48.3°F	-4.8°F	196°F

TABLE 5-10
Calculation of the ART Values for the 1/4T Location and 28 EFPY

Material	Method	CF	FF	ΔRT_{NDT}	Margin	IRT_{NDT}	ART
Inter. Shell Forging 125S255	RG 1.99, R2, P1.1	44°F	1.20	52.8°F	34°F	20°F	107°F
	RG 1.99, R2, P2.1	16.5°F	1.20	19.8°F	17°F	20°F	57°F
Lower Shell Forging 125P666	RG 1.99, R2, P1.1	31°F	1.20	37.2°F	34°F	40°F	111°F
	RG 1.99, R2, P2.1	28.2°F	1.20	33.8°F	17°F	40°F	91°F
Circ. Weld Seam SA-847	RG 1.99, R2, P1.1	170.4°F	1.20	204.5°F	56°F	-4.8°F	256°F
	RG 1.99, R2, P2.1	160.7°F	1.20	192.8°F	48.3°F	-4.8°F	236°F

TABLE 5-11
Calculation of the ART Values for the 3/4T Location and 28 EFPY

Material	Method	CF	FF	ΔRT_{NDT}	Margin	IRT_{NDT}	ART
Inter. Shell Forging 125S255	RG 1.99, R2, P1.1	44°F	1.00	44.0°F	34°F	20°F	98°F
	RG 1.99, R2, P2.1	16.5°F	1.00	16.5°F	16.5°F	20°F	53°F
Lower Shell Forging 125P666	RG 1.99, R2, P1.1	31°F	1.00	31.0°F	31.0°F	40°F	102°F
	RG 1.99, R2, P2.1	28.2°F	1.00	28.2°F	17°F	40°F	85°F
Circ. Weld Seam SA-847	RG 1.99, R2, P1.1	170.4°F	1.00	170.4°F	56°F	-4.8°F	222°F
	RG 1.99, R2, P2.1	160.7°F	1.00	160.7°F	48.3°F	-4.8°F	204°F

TABLE 5-12
Calculation of the ART Values for the 1/4T Location and 32 EFPY

Material	Method	CF	FF	ΔRT_{NDT}	Margin	IRT_{NDT}	ART
Inter. Shell Forging 125S255	RG 1.99, R2, P1.1	44°F	1.23	54.1°F	34°F	20°F	108°F
	RG 1.99, R2, P2.1	16.5°F	1.23	20.3°F	17°F	20°F	57°F
Lower Shell Forging 125P666	RG 1.99, R2, P1.1	31°F	1.23	38.1°F	34°F	40°F	112°F
	RG 1.99, R2, P2.1	28.2°F	1.23	34.7°F	17°F	40°F	92°F
Circ. Weld Seam SA-847	RG 1.99, R2, P1.1	170.4°F	1.23	209.6°F	56°F	-4.8°F	261°F
	RG 1.99, R2, P2.1	160.7°F	1.23	197.7°F	48.3°F	-4.8°F	241°F

TABLE 5-13
Calculation of the ART Values for the 3/4T Location and 32 EFPY

Material	Method	CF	FF	ΔRT_{NDT}	Margin	IRT_{NDT}	ART
Inter. Shell Forging 125S255	RG 1.99, R2, P1.1	44°F	1.02	44.9°F	34°F	20°F	99°F
	RG 1.99, R2, P2.1	16.5°F	1.02	16.8°F	16.8°F	20°F	54°F
Lower Shell Forging 125P666	RG 1.99, R2, P1.1	31°F	1.02	31.6°F	31.6°F	40°F	103°F
	RG 1.99, R2, P2.1	28.2°F	1.02	28.8°F	17°F	40°F	86°F
Circ. Weld Seam SA-847	RG 1.99, R2, P1.1	170.4°F	1.02	173.8°F	56°F	-4.8°F	225°F
	RG 1.99, R2, P2.1	160.7°F	1.02	163.9°F	48.3°F	-4.8°F	207°F

TABLE 5-14
Calculation of the ART Values for the 1/4T Location and 40 EFPY

Material	Method	CF	FF	ΔRT_{NDT}	Margin	IRT_{NDT}	ART
Inter. Shell Forging 125S255	RG 1.99, R2, P1.1	44°F	1.28	56.3°F	34°F	20°F	110°F
	RG 1.99, R2, P2.1	16.5°F	1.28	21.1°F	17°F	20°F	58°F
Lower Shell Forging 125P666	RG 1.99, R2, P1.1	31°F	1.28	39.7°F	34°F	40°F	114°F
	RG 1.99, R2, P2.1	28.2°F	1.28	36.1°F	17°F	40°F	93°F
Circ. Weld Seam SA-847	RG 1.99, R2, P1.1	170.4°F	1.28	218.1°F	56°F	-4.8°F	269°F
	RG 1.99, R2, P2.1	160.7°F	1.28	205.7°F	48.3°F	-4.8°F	249°F

TABLE 5-15
Calculation of the ART Values for the 3/4T Location and 40 EFPY

Material	Method	CF	FF	ΔRT_{NDT}	Margin	IRT_{NDT}	ART
Inter. Shell Forging 125S255	RG 1.99, R2, P1.1	44°F	1.08	47.5°F	34°F	20°F	102°F
	RG 1.99, R2, P2.1	16.5°F	1.08	17.8°F	17°F	20°F	55°F
Lower Shell Forging 125P666	RG 1.99, R2, P1.1	31°F	1.08	33.5°F	33.5°F	40°F	107°F
	RG 1.99, R2, P2.1	28.2°F	1.08	30.5°F	17°F	40°F	88°F
Circ. Weld Seam SA-847	RG 1.99, R2, P1.1	170.4°F	1.08	184.0°F	56°F	-4.8°F	235°F
	RG 1.99, R2, P2.1	160.7°F	1.08	173.6°F	48.3°F	-4.8°F	217°F

The circumferential weld seam SA-847 is the limiting beltline material for all heatup and cooldown curves to be generated. Contained in Table 5-16 is a summary of the limiting ARTs to be used in the generation of the Ginna reactor vessel heatup and cooldown curves.

TABLE 5-16
Summary of the Limiting ART Values Used in the
Generation of the Ginna Heatup/Cooldown Curves

EFPY	1/4 T Limiting ART	3/4 Limiting ART
24	232°F	196°F
28	236°F	204°F
32	241°F	207°F
40	249°F	217°F

6 HEATUP AND COOLDOWN PRESSURE-TEMPERATURE LIMIT CURVES

Pressure-temperature limit curves for normal heatup and cooldown of the primary reactor coolant system have been calculated for the pressure and temperature in the reactor vessel beltline region using the methods[53] discussed in Section 3.0, 4.0 and 5.0 of this report. This approved methodology is also presented in WCAP-14040-NP-A, dated January 1996[2].

Figures 6-1, 6-3, 6-5 and 6-7 present the heatup curves without margins for possible instrumentation errors using heatup rates of 60 and 100°F/hr. These curves are applicable to 24, 28, 32 and 40 EFPY for the R. E. Ginna reactor vessel. Additionally, Figures 6-2, 6-4, 6-6 and 6-8 present the cooldown curves without margins for possible instrumentation errors using cooldown rates of 0, 20, 40 60 and 100°F/hr. These curves are also applicable to 24, 28, 32 and 40 EFPY for the R. E. Ginna reactor vessel. Allowable combinations of temperature and pressure for specific temperature change rates are below and to the right of the limit lines shown in Figures 6-1 through 6-8. This is in addition to other criteria which must be met before the reactor is made critical, as discussed below in the following paragraphs.

The reactor must not be made critical until pressure-temperature combinations are to the right of the criticality limit line shown in Figures 6-1, 6-3, 6-5 and 6-7. The straight-line portion of the criticality limit is at the minimum permissible temperature for the 2485 psig inservice hydrostatic test as required by Appendix G to 10 CFR Part 50. The governing equation for the hydrostatic test is defined in Appendix G to Section XI of the ASME Code[48] as follows:

$$1.5K_{Im} < K_{Ia} \tag{6}$$

where,
K_{Im} is the stress intensity factor covered by membrane (pressure) stress,
$K_{Ia} = 26.78 + 1.233\, e^{[0.0145\,(T - RTNDT + 160)]}$,
T is the minimum permissible metal temperature, and
RT_{NDT} is the metal reference nil-ductility temperature

The criticality limit curve specifies pressure-temperature limits for core operation to provide additional margin during actual power production as specified in Reference 50. The pressure-temperature limits or core operation (except for low power physics tests) are that the reactor vessel must be at a temperature equal to or higher than the minimum temperature required for the inservice hydrostatic test, and at least 40°F higher than the minimum permissible temperature in the corresponding pressure-temperature curve for heatup and cooldown calculated as described in Section 4.0 of this report. The vertical line drawn from these points on the pressure-temperature curve, intersecting a curve 40°F higher than the pressure-temperature limit curve, constitutes the limit for core operation for the reactor vessel.

Figures 6-1 through 6-8 define all of the above limits for ensuring prevention of nonductile failure for the R. E. Ginna reactor vessel. The data points for the heatup and cooldown pressure-temperature limit curves shown in Figures 6-1 through 6-8 are presented in Tables 6-1 through 6-8.

MATERIAL PROPERTY BASIS

LIMITING MATERIAL: CIRCUMFERENTIAL WELD SA-847
LIMITING ART VALUES AT 24 EFPY: 1/4T, 232°F
3/4T, 196°F

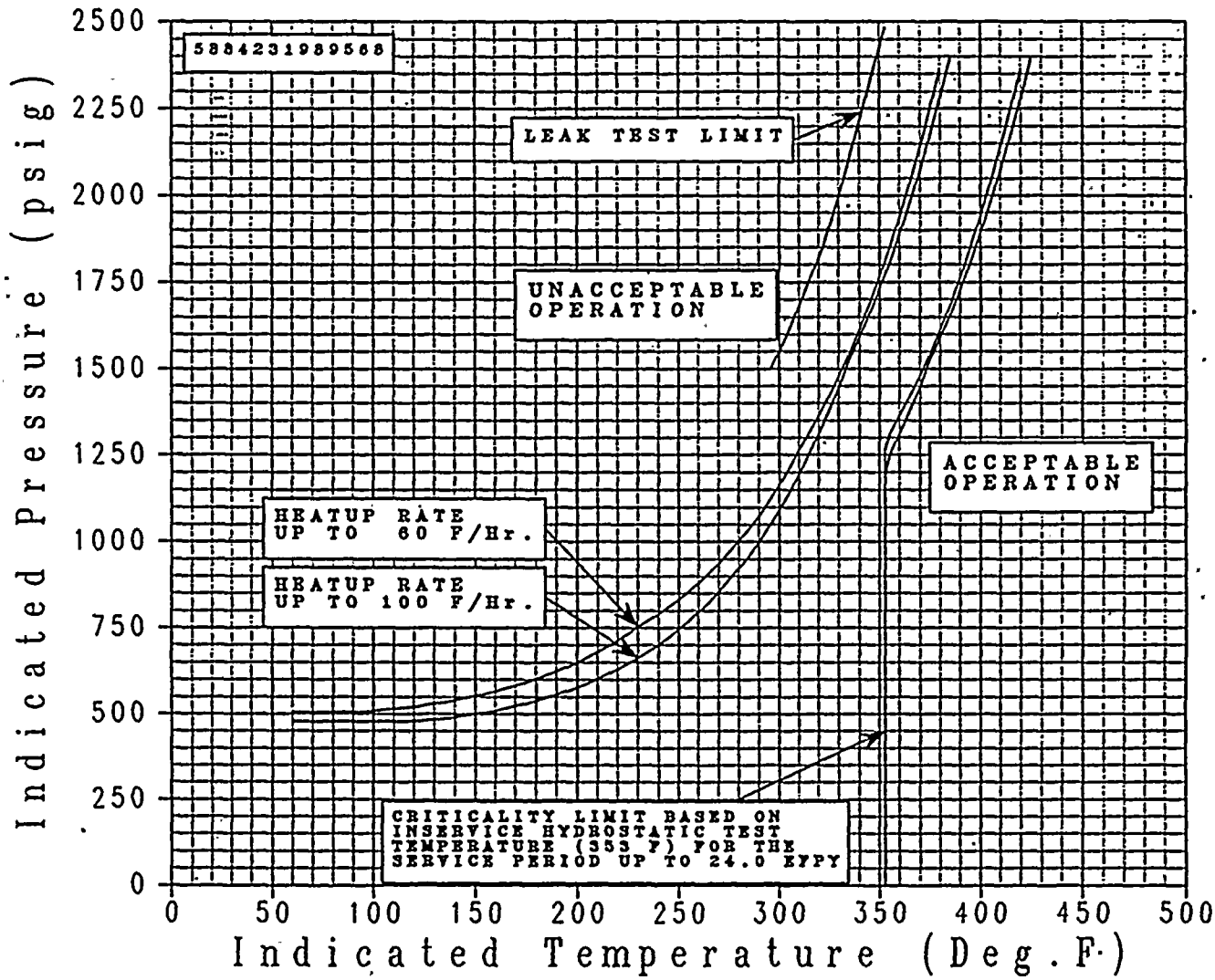

FIGURE 6-1 R. E. Ginna Reactor Coolant System Heatup Limitations (Heatup Rates of 60 and 100°F) Applicable to 24 EFPY (Without Margins for Instrumentation Errors)

MATERIAL PROPERTY BASIS

LIMITING MATERIAL: CIRCUMFERENTIAL WELD SA-847
LIMITING ART VALUES AT 24 EFPY: 1/4T, 232°F
3/4T, 196°F

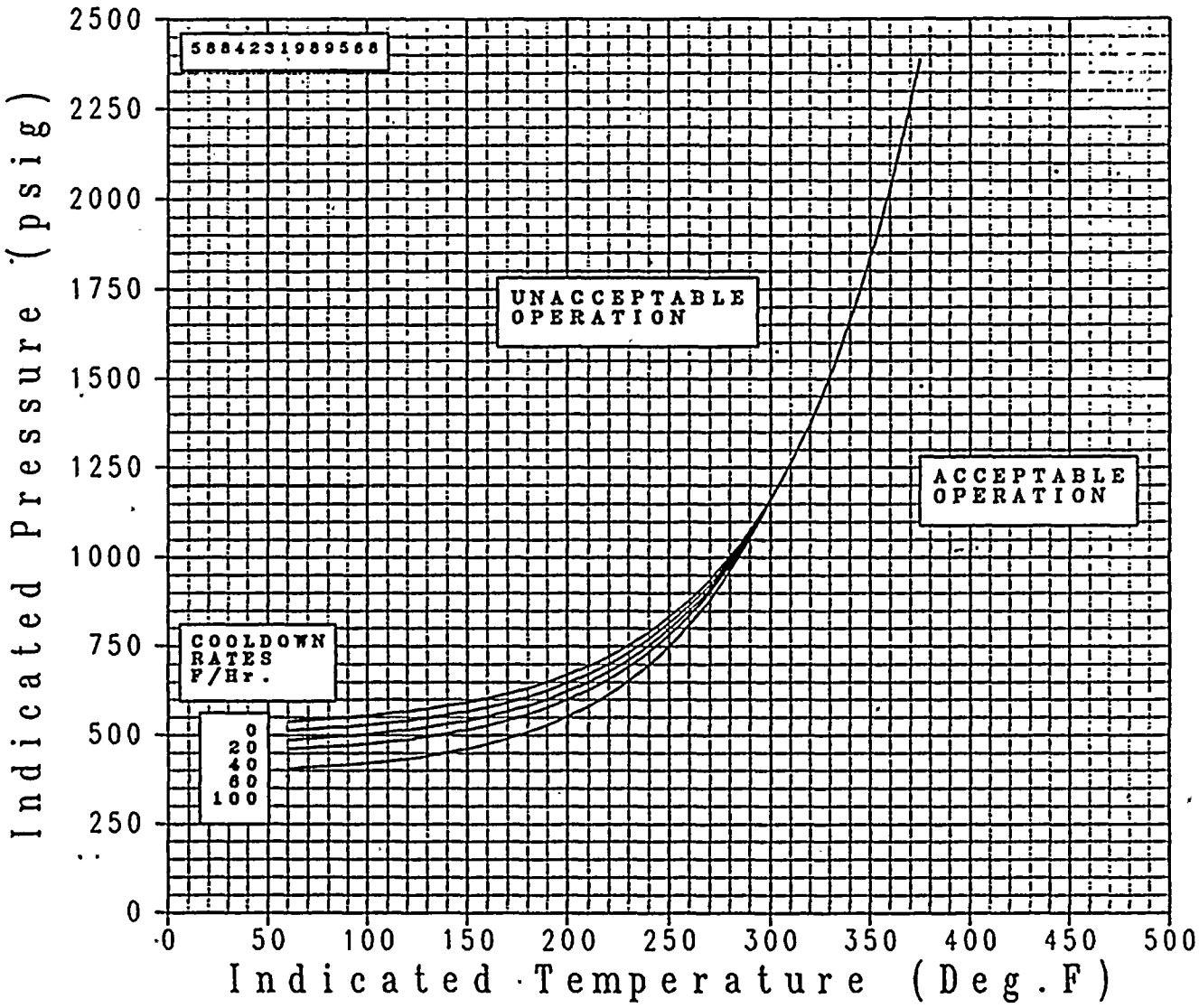

FIGURE 6-2 R. E. Ginna Reactor Coolant System Cooldown Limitations (Cooldown Rates of 0, 20 40 60 and 100°F/hr) Applicable to 24 EFPY (Without Margins for Instrumentation Errors)

MATERIAL PROPERTY BASIS

LIMITING MATERIAL: CIRCUMFERENTIAL WELD SA-847
LIMITING ART VALUES AT 28 EFPY: 1/4T, 236°F
3/4T, 204°F

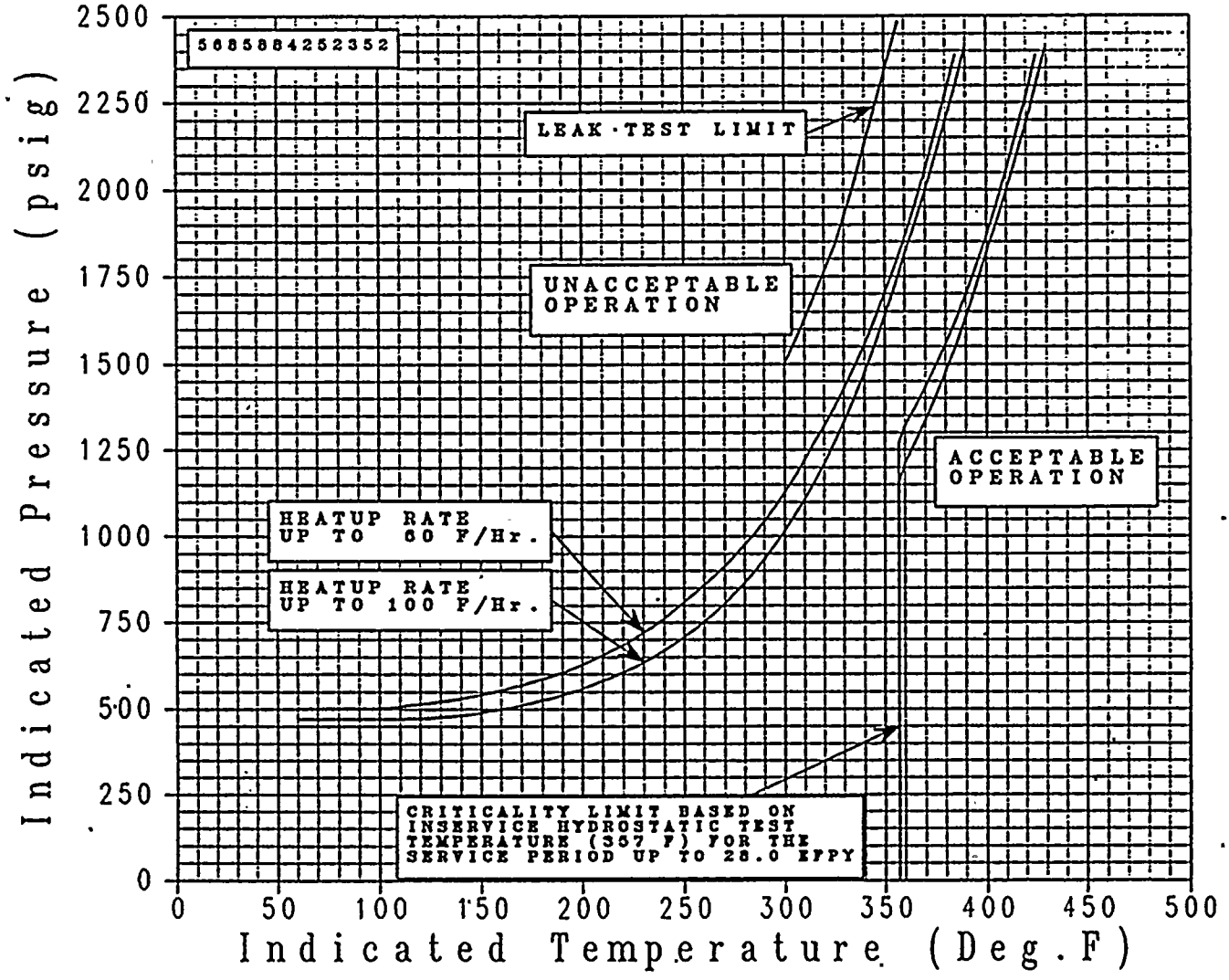

FIGURE 6-3 R. E. Ginna Reactor Coolant System Heatup Limitations (Heatup Rates of 60 and 100°F) Applicable to 28 EFPY (Without Margins for Instrumentation Errors)

MATERIAL PROPERTY BASIS

LIMITING MATERIAL: CIRCUMFERENTIAL WELD SA-847
LIMITING ART VALUES AT 28 EFPY: 1/4T, 236°F
3/4T, 204°F

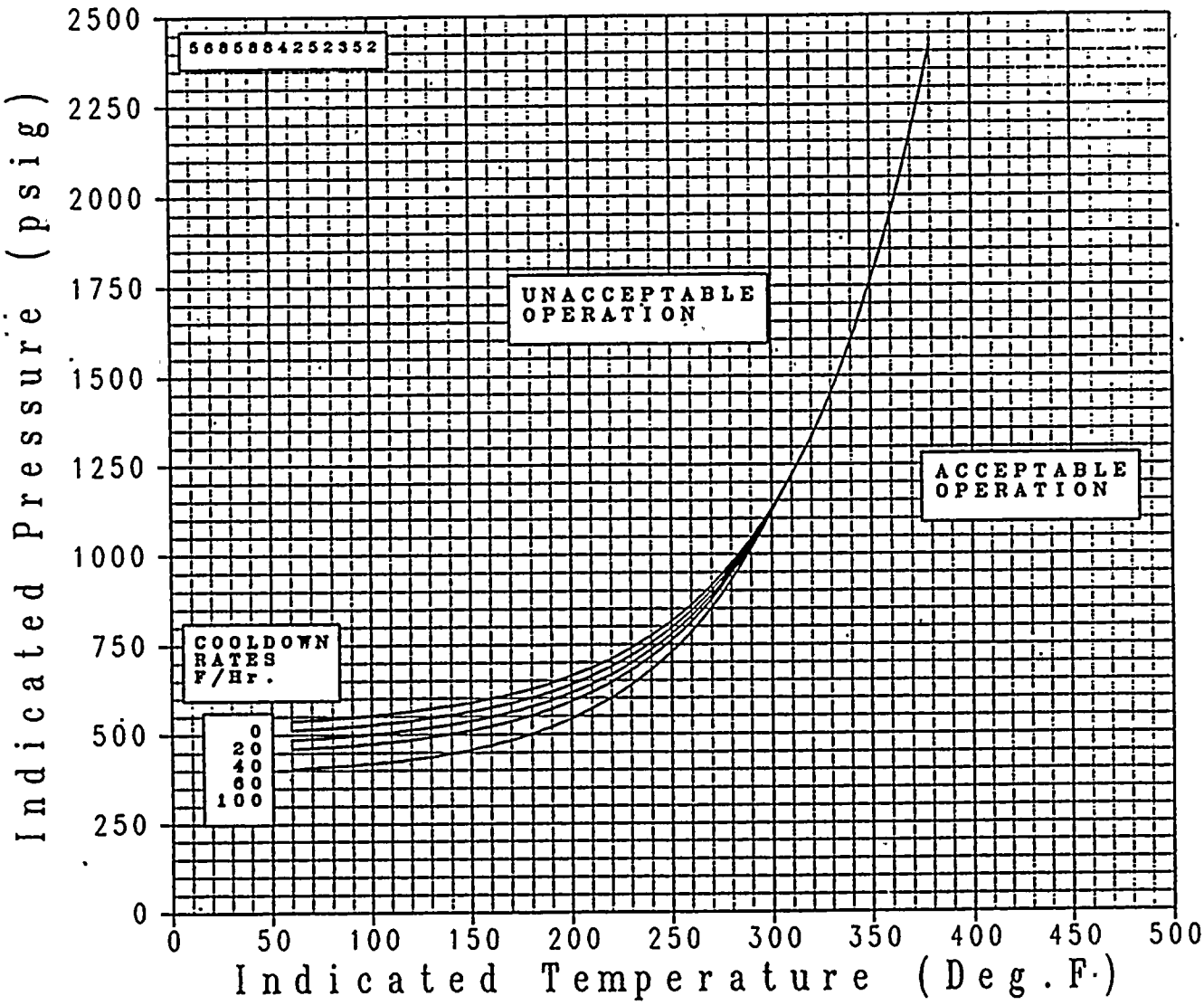

FIGURE 6-4 R. E. Ginna Reactor Coolant System Cooldown Limitations (Cooldown Rates of 0, 20 40 60 and 100°F/hr) Applicable to 28 EFPY (Without Margins for Instrumentation Errors)

MATERIAL PROPERTY BASIS

LIMITING MATERIAL: CIRCUMFERENTIAL WELD SA-847
LIMITING ART VALUES AT 32 EFPY: 1/4T, 241°F
3/4T, 207°F

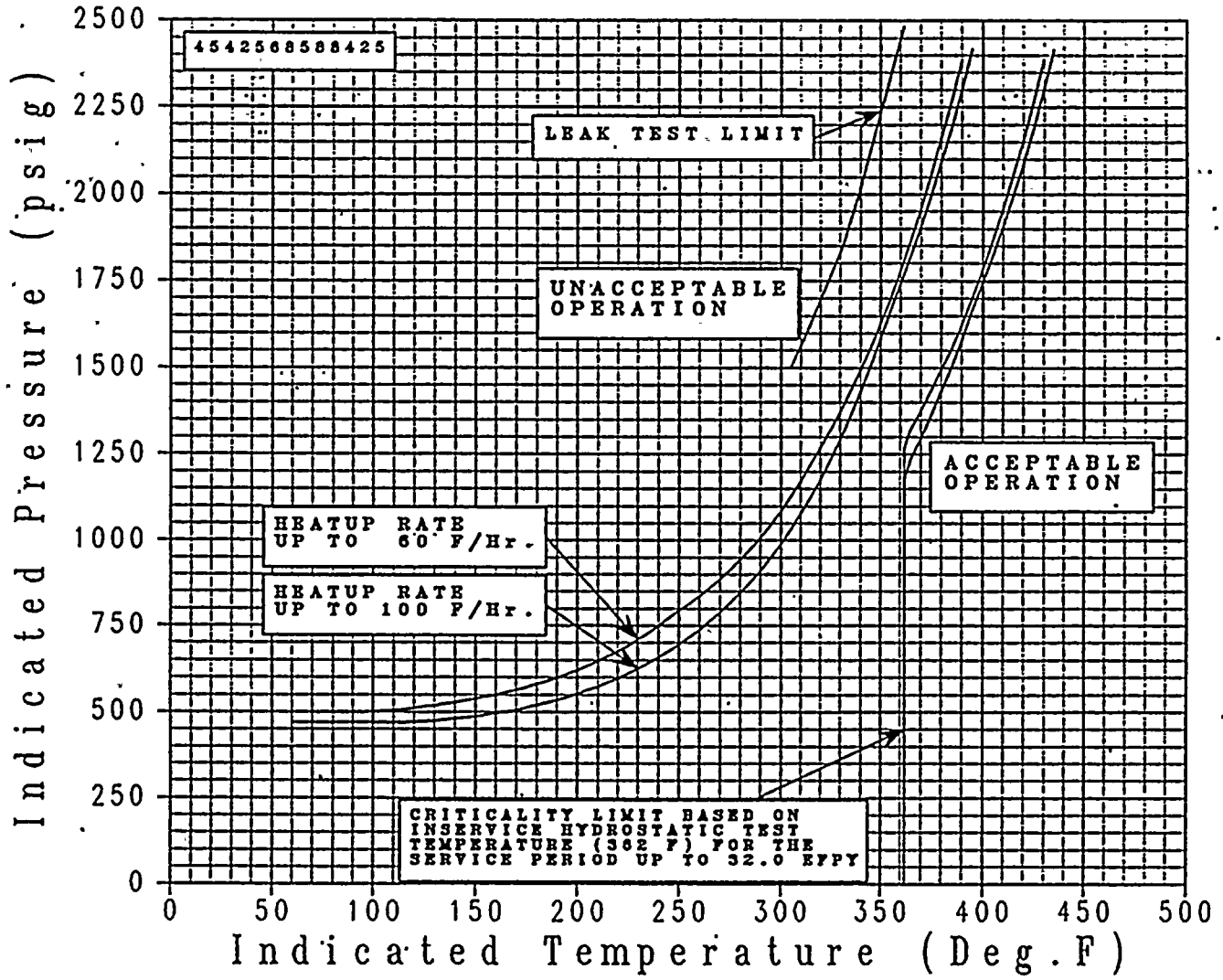

FIGURE 6-5 R. E. Ginna Reactor Coolant System Heatup Limitations (Heatup Rates of 60 and 100°F) Applicable to 32 EFPY (Without Margins for Instrumentation Errors)

MATERIAL PROPERTY BASIS

LIMITING MATERIAL: CIRCUMFERENTIAL WELD SA-847
LIMITING ART VALUES AT 32 EFPY: 1/4T, 241°F
3/4T, 207°F

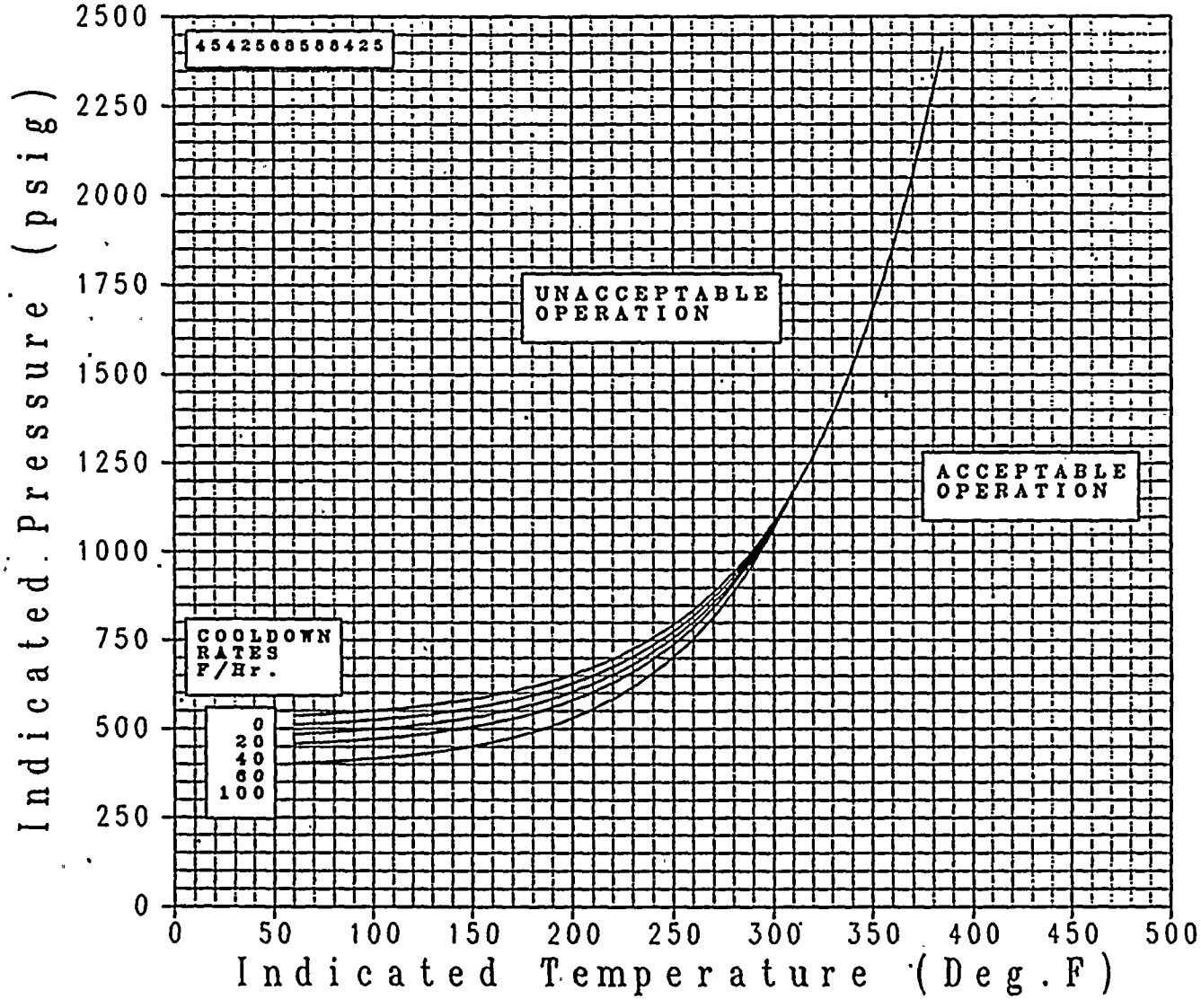

FIGURE 6-6 R. E. Ginna Reactor Coolant System Cooldown Limitations (Cooldown Rates of 0, 20 40 60 and 100°F/hr) Applicable to 32 EFPY (Without Margins for Instrumentation Errors)

MATERIAL PROPERTY BASIS

LIMITING MATERIAL: CIRCUMFERENTIAL WELD SA-847
LIMITING ART VALUES AT 40 EFPY: 1/4T, 249°F
3/4T, 217°F

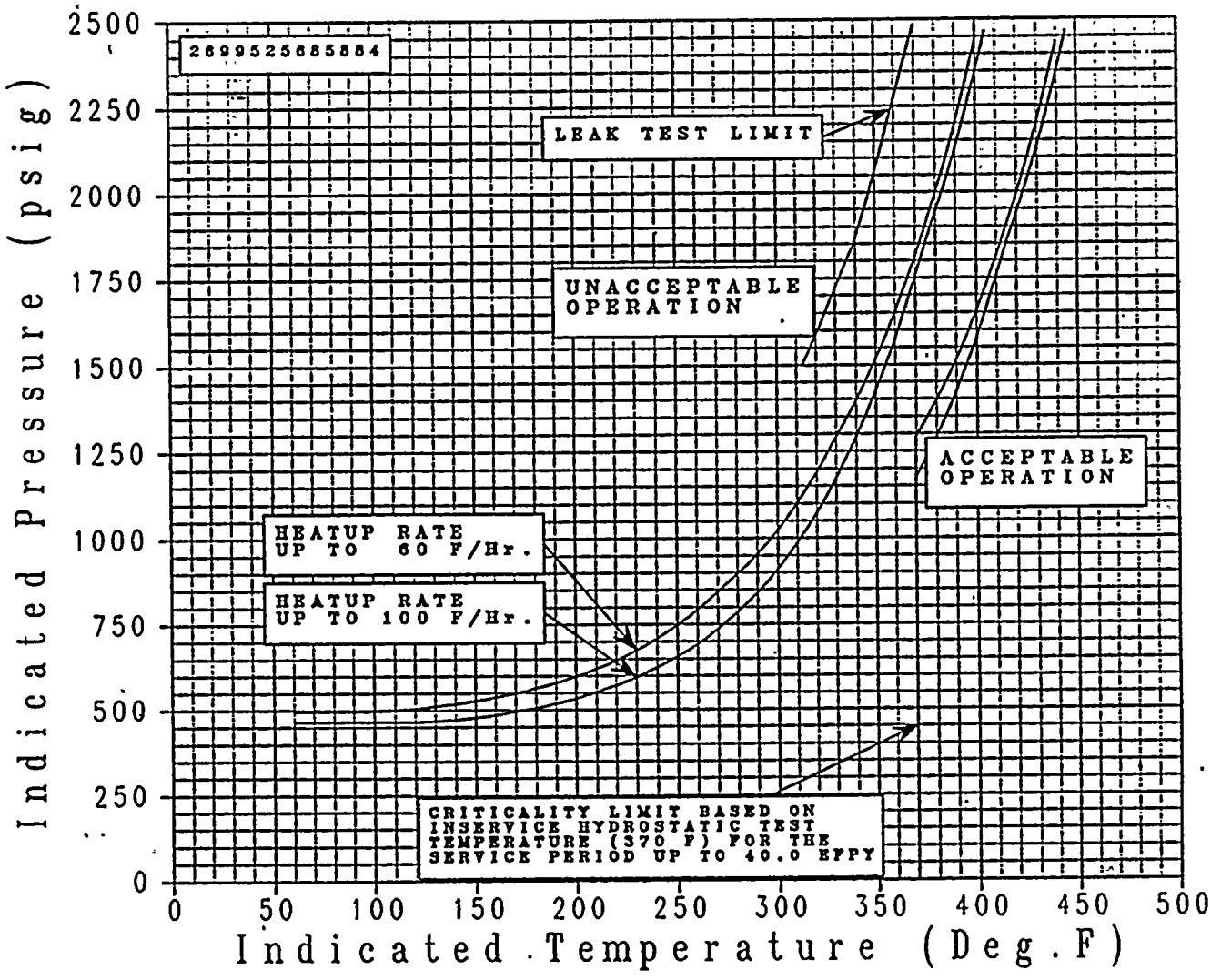

FIGURE 6-7 R. E. Ginna Reactor Coolant System Heatup Limitations (Heatup Rates of 60 and 100°F) Applicable to 40 EFPY (Without Margins for Instrumentation Errors)

MATERIAL PROPERTY BASIS

LIMITING MATERIAL: CIRCUMFERENTIAL WELD SA-847
LIMITING ART VALUES AT 40 EFPY: 1/4T, 249°F
3/4T, 217°F

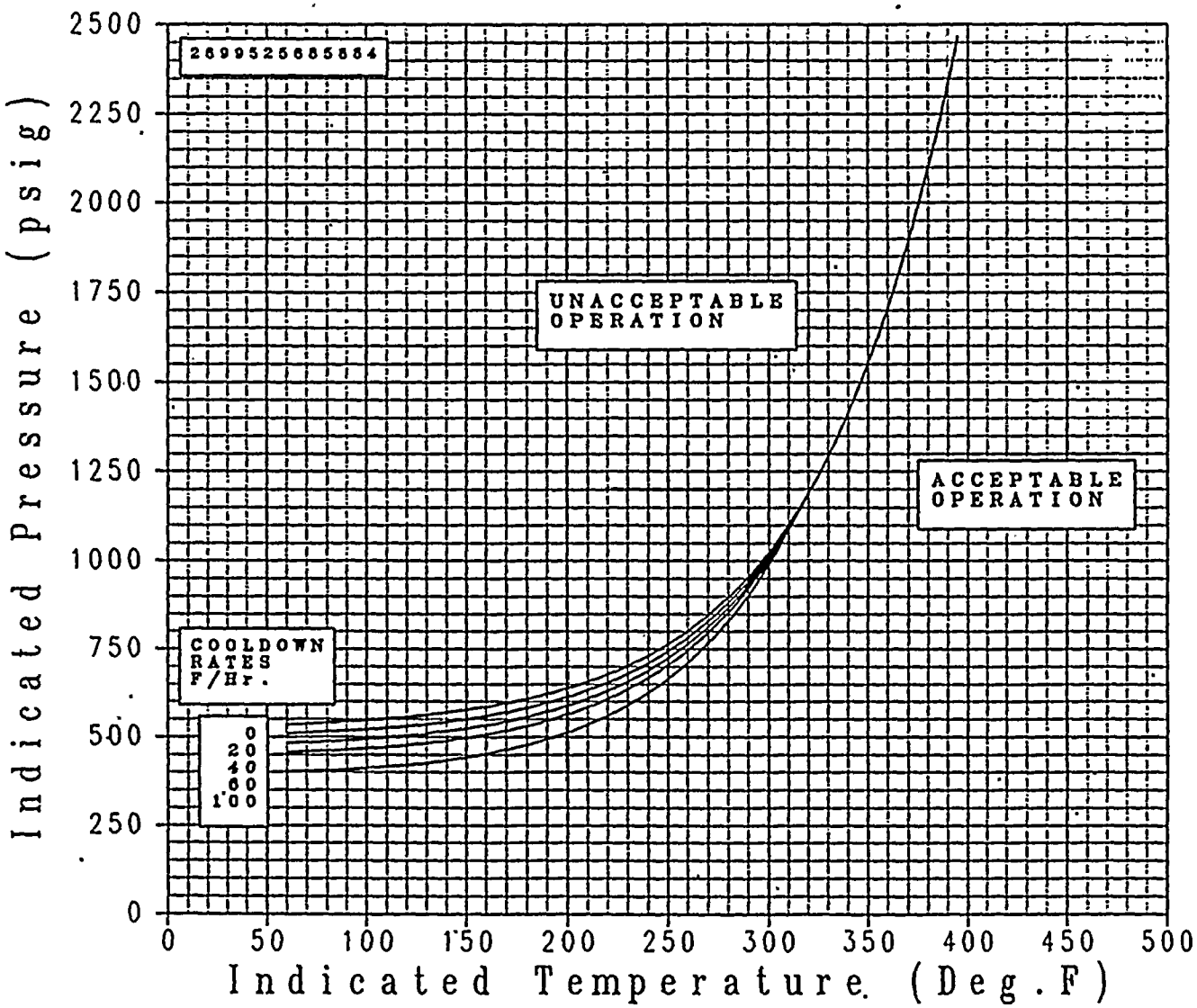

FIGURE 6-8 R. E. Ginna Reactor Coolant System Cooldown Limitations (Cooldown Rates of 0, 20 40 60 and 100°F/hr) Applicable to 40 EFPY (Without Margins for Instrumentation Errors)

TABLE 6-1
R. E. Ginna 24 EFPY Heatup Curve Data Points

Heatup Curves 60F		Critical. Limit		100F		Critical. Limit		Leak Test Limit	
T	P	T	P	T	P	T	P	T	P
60	507	353	0	60	478	353	0	296	1500
65	507	353	525	65	478	353	524	304	1600
70	507	353	516	70	478	353	511	315	1750
75	507	353	511	75	478	353	501	322	1850
80	507	353	508	80	478	353	493	330	2000
85	507	353	507	85	478	353	487	353	2485
90	507	353	507	90	478	353	483		
95	508	353	508	95	478	353	480		
100	509	353	509	100	478	353	478		
105	512	353	512	105	478	353	478		
110	515	353	515	110	478	353	478		
115	518	353	518	115	478	353	478		
120	522	353	522	120	480	353	480		
125	526	353	526	125	482	353	482		
130	530	353	530	130	485	353	485		
135	535	353	535	135	488	353	488		
140	541	353	541	140	491	353	491		
145	547	353	547	145	495	353	495		
150	553	353	553	150	500	353	500		
155	560	353	560	155	505	353	505		
160	567	353	567	160	511	353	511		
165	575	353	575	165	517	353	517		
170	584	353	584	170	524	353	524		
175	593	353	593	175	531	353	531		
180	603	353	603	180	539	353	539		
185	614	353	614	185	548	353	548		
190	625	353	625	190	557	353	557		
195	638	353	638	195	567	353	567		
200	651	353	651	200	578	353	578		
205	665	353	665	205	590	353	590		
210	681	353	681	210	603	353	603		
215	697	353	697	215	616	353	616		
220	715	353	715	220	631	353	631		
225	734	353	734	225	647	353	647		
230	754	353	754	230	664	353	664		
235	772	353	772	235	682	353	682		
240	791	353	791	240	702	353	702		
245	811	353	811	245	723	353	723		
250	833	353	833	250	746	353	746		
255	856	353	856	255	770	353	770		
260	881	353	881	260	796	353	796		
265	908	353	908	265	825	353	825		
270	937	353	937	270	855	353	855		
275	968	353	968	275	887	353	887		
280	1002	353	1002	280	922	353	922		
285	1038	353	1038	285	960	353	960		
290	1077	353	1077	290	1000	353	1000		
295	1118	353	1118	295	1044	353	1044		
300	1163	353	1163	300	1090	353	1090		
305	1211	353	1211	305	1140	353	1140		
310	1262	353	1262	310	1193	353	1193		
315	1312	355	1312	315	1250	355	1250		
320	1364	360	1364	320	1312	360	1312		
325	1420	365	1420	325	1378	365	1378		
330	1479	370	1479	330	1448	370	1448		
335	1543	375	1543	335	1524	375	1524		
340	1612	380	1612	340	1590	380	1590		
345	1685	385	1685	345	1657	385	1657		
350	1764	390	1764	350	1729	390	1729		
355	1848	395	1848	355	1807	395	1807		
360	1938	400	1938	360	1889	400	1889		
365	2035	405	2035	365	1977	405	1977		
370	2138	410	2138	370	2072	410	2072		
375	2248	415	2248	375	2173	415	2173		
380	2365	420	2365	380	2280	420	2280		
				385	2395	425	2395		

TABLE 6-2
R. E. Ginna 24 EFPY Cooldown Curve Data Points

Cooldown Curves Steady State		20F		40F		60F		100F	
T	P	T	P	T	P	T	P	T	P
60	540	60	515	60	489	60	462	60	408
65	542	65	516	65	490	65	463	65	409
70	544	70	518	70	492	70	465	70	410
75	545	75	519	75	493	75	466	75	412
80	547	80	521	80	495	80	468	80	414
85	549	85	523	85	497	85	470	85	415
90	551	90	525	90	499	90	472	90	418
95	554	95	528	95	501	95	474	95	420
100	556	100	530	100	504	100	477	100	422
105	559	105	533	105	506	105	480	105	425
110	562	110	536	110	509	110	483	110	428
115	565	115	539	115	512	115	486	115	431
120	568	120	542	120	516	120	489	120	435
125	572	125	546	125	519	125	493	125	438
130	576	130	550	130	523	130	497	130	442
135	580	135	554	135	528	135	501	135	447
140	584	140	558	140	532	140	506	140	452
145	589	145	563	145	537	145	511	145	457
150	594	150	568	150	542	150	516	150	463
155	599	155	574	155	548	155	522	155	469
160	605	160	580	160	554	160	529	160	476
165	612	165	587	165	561	165	536	165	483
170	619	170	594	170	568	170	543	170	491
175	626	175	601	175	576	175	551	175	500
180	634	180	609	180	585	180	560	180	509
185	642	185	618	185	594	185	569	185	519
190	652	190	628	190	603	190	579	190	530
195	661	195	638	195	614	195	590	195	542
200	672	200	649	200	625	200	602	200	554
205	683	205	661	205	637	205	615	205	568
210	696	210	673	210	651	210	628	210	583
215	709	215	687	215	665	215	643	215	599
220	723	220	701	220	680	220	659	220	616
225	738	225	717	225	696	225	676	225	634
230	754	230	734	230	714	230	694	230	654
235	772	235	752	235	733	235	714	235	676
240	791	240	772	240	753	240	735	240	699
245	811	245	793	245	775	245	758	245	724
250	833	250	816	250	799	250	783	250	751
255	856	255	840	255	825	255	809	255	780
260	881	260	866	260	852	260	838	260	811
265	908	265	895	265	881	265	869	265	845
270	937	270	925	270	913	270	902	270	881
275	968	275	957	275	947	275	937	275	920
280	1002	280	993	280	983	280	975	280	962
285	1038	285	1030	285	1023	285	1016	285	1007
290	1077	290	1070	290	1065	290	1061	290	1056
295	1118	295	1114	295	1110	295	1108	295	1108
300	1163	300	1160	300	1159	300	1159		
305	1211	305	1211						
310	1262								
315	1318								
320	1377								
325	1440								
330	1509								
335	1581								
340	1660								
345	1744								
350	1834								
355	1931								
360	2034								
365	2144								
370	2262								
375	2388								

TABLE 6-3
R. E. Ginna 28 EFPY Heatup Curve Data Points

Heatup Curves 60F	Critical. Limit		100F	Critical. Limit		Leak Test Limit		
T	P	T P	T	P	T	P	T	P
60	502	357 0	60	472	357	0	300	1500
65	502	357 521	65	472	357	521	308	1600
70	502	357 513	70	472	357	508	319	1750
75	502	357 507	75	472	357	497	326	1850
80	502	357 504	80	472	357	489	334	2000
85	502	357 502	85	472	357	483	357	2485
90	502	357 502	90	472	357	479		
95	503	357 503	95	472	357	476		
100	504	357 504	100	472	357	474		
105	506	357 506	105	472	357	473		
110	509	357 509	110	472	357	472		
115	511	357 511	115	473	357	473		
120	515	357 515	120	474	357	474		
125	518	357 518	125	476	357	476		
130	522	357 522	130	478	357	478		
135	527	357 527	135	480	357	480		
140	532	357 532	140	483	357	483		
145	537	357 537	145	487	357	487		
150	542	357 542	150	491	357	491		
155	548	357 548	155	496	357	496		
160	555	357 555	160	500	357	500		
165	562	357 562	165	506	357	506		
170	570	357 570	170	512	357	512		
175	578	357 578	175	518	357	518		
180	587	357 587	180	526	357	526		
185	596	357 596	185	533	357	533		
190	607	357 607	190	541	357	541		
195	618	357 618	195	550	357	550		
200	629	357 629	200	560	357	560		
205	642	357 642	205	570	357	570		
210	656	357 656	210	582	357	582		
215	671	357 671	215	594	357	594		
220	686	357 686	220	607	357	607		
225	703	357 703	225	621	357	621		
230	722	357 722	230	636	357	636		
235	741	357 741	235	652	357	652		
240	763	357 763	240	670	357	670		
245	785	357 785	245	688	357	688		
250	810	357 810	250	709	357	709		
255	836	357 836	255	730	357	730		
260	861	357 861	260	754	357	754		
265	887	357 887	265	779	357	779		
270	914	357 914	270	806	357	806		
275	944	357 944	275	835	357	835		
280	975	357 975	280	866	357	866		
285	1009	357 1009	285	899	357	899		
290	1046	357 1046	290	935	357	935		
295	1085	357 1085	295	974	357	974		
300	1127	357 1127	300	1015	357	1015		
305	1172	357 1172	305	1059	357	1059		
310	1221	357 1221	310	1107	357	1107		
315	1273	357 1273	315	1158	357	1158		
320	1322	360 1322	320	1213	360	1213		
325	1375	365 1375	325	1272	365	1272		
330	1431	370 1431	330	1335	370	1335		
335	1492	375 1492	335	1402	375	1402		
340	1557	380 1557	340	1475	380	1475		
345	1626	385 1626	345	1552	385	1552		
350	1701	390 1701	350	1635	390	1635		
355	1780	395 1780	355	1724	395	1724		
360	1865	400 1865	360	1819	400	1819		
365	1957	405 1957	365	1906	405	1906		
370	2054	410 2054	370	1996	410	1996		
375	2159	415 2159	375	2091	415	2091		
380	2270	420 2270	380	2193	420	2193		
385	2389	425 2389	385	2302	425	2302		
			390	2419	430	2419		

TABLE 6-4
R. E. Ginna 28 EFPY Cooldown Curve Data Points

Cooldown Curves Steady State		20F		40F		60F		100F	
T	P	T	P	T	P	T	P	T	P
60	539	60	513	60	487	60	461	60	406
65	541	65	515	65	489	65	462	65	408
70	542	70	516	70	490	70	463	70	409
75	544	75	518	75	492	75	465	75	410
80	546	80	520	80	493	80	467	80	412
85	547	85	522	85	495	85	468	85	414
90	550	90	524	90	497	90	470	90	415
95	552	95	526	95	499	95	472	95	417
100	554	100	528	100	501	100	475	100	420
105	557	105	531	105	504	105	477	105	422
110	559	110	533	110	507	110	480	110	425
115	562	115	536	115	510	115	483	115	428
120	565	120	539	120	513	120	486	120	431
125	569	125	543	125	516	125	490	125	435
130	572	130	546	130	520	130	493	130	439
135	576	135	550	135	524	135	497	135	443
140	581	140	555	140	528	140	502	140	447
145	585	145	559	145	533	145	506	145	453
150	590	150	564	150	538	150	512	150	458
155	595	155	569	155	543	155	517	155	464
160	601	160	575	160	549	160	523	160	470
165	607	165	581	165	556	165	530	165	477
170	613	170	588	170	562	170	537	170	485
175	620	175	595	175	570	175	544	175	493
180	628	180	603	180	578	180	552	180	501
185	635	185	611	185	586	185	561	185	511
190	644	190	620	190	595	190	571	190	521
195	653	195	630	195	605	195	581	195	532
200	664	200	640	200	616	200	592	200	544
205	674	205	651	205	628	205	604	205	557
210	686	210	663	210	640	210	617	210	571
215	698	215	676	215	653	215	631	215	586
220	712	220	690	220	668	220	646	220	602
225	726	225	704	225	683	225	662	225	619
230	741	230	720	230	700	230	679	230	638
235	758	235	738	235	718	235	698	235	658
240	776	240	756	240	737	240	718	240	680
245	795	245	776	245	758	245	739	245	704
250	815	250	797	250	780	250	763	250	729
255	837	255	820	255	804	255	788	255	756
260	861	260	845	260	830	260	815	260	786
265	887	265	872	265	858	265	844	265	818
270	914	270	900	270	887	270	875	270	852
275	944	275	931	275	919	275	908	275	888
280	975	280	964	280	954	280	944	280	928
285	1009	285	1000	285	991	285	983	285	971
290	1046	290	1038	290	1031	290	1025	290	1016
295	1085	295	1079	295	1074	295	1070	295	1066
300	1127	300	1123	300	1120	300	1118	300	1119
305	1172	305	1170	305	1170	305	1170		
310	1221								
315	1273								
320	1329								
325	1389								
330	1454								
335	1523								
340	1597								
345	1676								
350	1762								
355	1853								
360	1951								
365	2055								
370	2167								
375	2286								
380	2414								

TABLE 6-5
R. E. Ginna 32 EFPY Heatup Curve Data Points

Heatup Curves 60F		Critical. Limit		100F		Critical. Limit		Leak Test Limit	
T	P	T	P	T	P	T	P	T	P
60	501	362	0	60	471	362	0	305	1500
65	501	362	520	65	471	362	520	313	1600
70	501	362	512	70	471	362	507	324	1750
75	501	362	506	75	471	362	496	331	1850
80	501	362	503	80	471	362	488	339	2000
85	501	362	501	85	471	362	482	362	2485
90	501	362	501	90	471	362	477		
95	501	362	501	95	471	362	474		
100	502	362	502	100	471	362	472		
105	504	362	504	105	471	362	471		
110	507	362	507	110	471	362	471		
115	509	362	509	115	471	362	471		
120	512	362	512	120	472	362	472		
125	516	362	516	125	473	362	473		
130	520	362	520	130	475	362	475		
135	524	362	524	135	478	362	478		
140	529	362	529	140	481	362	481		
145	533	362	533	145	484	362	484		
150	539	362	539	150	488	362	488		
155	545	362	545	155	492	362	492		
160	551	362	551	160	497	362	497		
165	558	362	558	165	502	362	502		
170	565	362	565	170	508	362	508		
175	573	362	573	175	514	362	514		
180	581	362	581	180	521	362	521		
185	590	362	590	185	528	362	528		
190	600	362	600	190	536	362	536		
195	611	362	611	195	544	362	544		
200	622	362	622	200	554	362	554		
205	634	362	634	205	564	362	564		
210	647	362	647	210	574	362	574		
215	661	362	661	215	586	362	586		
220	677	362	677	220	598	362	598		
225	693	362	693	225	612	362	612		
230	710	362	710	230	626	362	626		
235	729	362	729	235	642	362	642		
240	749	362	749	240	659	362	659		
245	771	362	771	245	677	362	677		
250	795	362	795	250	696	362	696		
255	815	362	815	255	717	362	717		
260	837	362	837	260	739	362	739		
265	861	362	861	265	763	362	763		
270	887	362	887	270	789	362	789		
275	914	362	914	275	817	362	817		
280	944	362	944	280	846	362	846		
285	975	362	975	285	878	362	878		
290	1009	362	1009	290	913	362	913		
295	1046	362	1046	295	950	362	950		
300	1085	362	1085	300	989	362	989		
305	1127	362	1127	305	1032	362	1032		
310	1172	362	1172	310	1077	362	1077		
315	1221	362	1221	315	1126	362	1126		
320	1273	362	1273	320	1179	362	1179		
325	1322	365	1322	325	1235	365	1235		
330	1375	370	1375	330	1295	370	1295		
335	1431	375	1431	335	1360	375	1360		
340	1492	380	1492	340	1430	380	1430		
345	1557	385	1557	345	1504	385	1504		
350	1626	390	1626	350	1583	390	1583		
355	1701	395	1701	355	1669	395	1669		
360	1780	400	1780	360	1744	400	1744		
365	1865	405	1865	365	1822	405	1822		
370	1956	410	1956	370	1906	410	1906		
375	2054	415	2054	375	1995	415	1995		
380	2159	420	2159	380	2091	420	2091		
385	2270	425	2270	385	2193	425	2193		
390	2389	430	2389	390	2302	430	2302		
				395	2418	435	2418		

TABLE 6-6
R. E. Ginna 32 EFPY Cooldown Curve Data Points

Cooldown Curves Steady State		20F		40F		60F		100F	
T	P	T	P	T	P	T	P	T	P
60	538	60	512	60	486	60	459	60	405
65	539	65	513	65	487	65	460	65	406
70	541	70	515	70	488	70	462	70	407
75	542	75	516	75	490	75	463	75	408
80	544	80	518	80	491	80	465	80	410
85	546	85	520	85	493	85	466	85	411
90	547	90	521	90	495	90	468	90	413
95	550	95	523	95	497	95	470	95	415
100	552	100	526	100	499	100	472	100	417
105	554	105	528	105	501	105	474	105	419
110	557	110	530	110	504	110	477	110	422
115	559	115	533	115	506	115	480	115	424
120	562	120	536	120	509	120	483	120	427
125	565	125	539	125	513	125	486	125	431
130	569	130	543	130	516	130	489	130	434
135	572	135	546	135	520	135	493	135	438
140	576	140	550	140	524	140	497	140	442
145	581	145	554	145	528	145	501	145	447
150	585	150	559	150	533	150	506	150	452
155	590	155	564	155	538	155	511	155	457
160	595	160	569	160	543	160	517	160	463
165	601	165	575	165	549	165	523	165	470
170	607	170	581	170	555	170	529	170	476
175	613	175	588	175	562	175	536	175	484
180	620	180	595	180	570	180	544	180	492
185	628	185	603	185	578	185	552	185	501
190	635	190	611	190	586	190	561	190	510
195	644	195	620	195	595	195	571	195	520
200	653	200	629	200	605	200	581	200	531
205	664	205	640	205	616	205	592	205	543
210	674	210	651	210	627	210	604	210	556
215	686	215	663	215	640	215	617	215	570
220	698	220	676	220	653	220	630	220	585
225	712	225	689	225	667	225	645	225	601
230	726	230	704	230	683	230	661	230	619
235	741	235	720	235	699	235	679	235	637
240	758	240	737	240	717	240	697	240	658
245	776	245	756	245	737	245	718	245	680
250	795	250	776	250	757	250	739	250	703
255	815	255	797	255	780	255	762	255	729
260	837	260	820	260	804	260	787	260	756
265	861	265	845	265	829	265	814	265	785
270	887	270	872	270	857	270	843	270	817
275	914	275	900	275	887	275	875	275	851
280	944	280	931	280	919	280	908	280	888
285	975	285	964	285	954	285	944	285	928
290	1009	290	1000	290	991	290	983	290	970
295	1046	295	1038	295	1031	295	1025	295	1016
300	1085	300	1079	300	1074	300	1070	300	1066
305	1127	305	1123	305	1120	305	1118	305	1119
310	1172	310	1170	310	1169	310	1170		
315	1221								
320	1273								
325	1329								
330	1389								
335	1454								
340	1523								
345	1597								
350	1676								
355	1762								
360	1853								
365	1951								
370	2055								
375	2167								
380	2286								
385	2414								

TABLE 6-7
R. E. Ginna 40 EFPY Heatup Curve Data Points

Heatup Curves 60F		Critical. Limit		100F		Critical. Limit		Leak Test Limit	
T	P	T	P	T	P	T	P	T	P
60	496	370	0	60	465	370	0	313	1500
65	496	370	516	65	465	370	516	321	1600
70	496	370	508	70	465	370	503	332	1750
75	496	370	502	75	465	370	492	339	1850
80	496	370	498	80	465	370	484	347	2000
85	496	370	496	85	465	370	478	370	2485
90	496	370	496	90	465	370	473		
95	496	370	496	95	465	370	470		
100	497	370	497	100	465	370	467		
105	498	370	498	105	465	370	466		
110	500	370	500	110	465	370	465		
115	503	370	503	115	465	370	465		
120	505	370	505	120	466	370	466		
125	508	370	508	125	467	370	467		
130	511	370	511	130	468	370	468		
135	515	370	515	135	470	370	470		
140	519	370	519	140	472	370	472		
145	523	370	523	145	475	370	475		
150	528	370	528	150	478	370	478		
155	533	370	533	155	482	370	482		
160	538	370	538	160	486	370	486		
165	544	370	544	165	490	370	490		
170	550	370	550	170	495	370	495		
175	557	370	557	175	500	370	500		
180	564	370	564	180	506	370	506		
185	572	370	572	185	512	370	512		
190	580	370	580	190	519	370	519		
195	589	370	589	195	527	370	527		
200	599	370	599	200	535	370	535		
205	610	370	610	205	543	370	543		
210	621	370	621	210	552	370	552		
215	633	370	633	215	562	370	562		
220	646	370	646	220	573	370	573		
225	660	370	660	225	585	370	585		
230	676	370	676	230	597	370	597		
235	692	370	692	235	610	370	610		
240	709	370	709	240	625	370	625		
245	728	370	728	245	640	370	640		
250	748	370	748	250	657	370	657		
255	770	370	770	255	675	370	675		
260	793	370	793	260	694	370	694		
265	819	370	819	265	715	370	715		
270	845	370	845	270	737	370	737		
275	871	370	871	275	761	370	761		
280	897	370	897	280	787	370	787		
285	925	370	925	285	814	370	814		
290	956	370	956	290	844	370	844		
295	988	370	988	295	876	370	876		
300	1023	370	1023	300	910	370	910		
305	1061	370	1061	305	947	370	947		
310	1101	370	1101	310	987	370	987		
315	1145	370	1145	315	1029	370	1029		
320	1191	370	1191	320	1074	370	1074		
325	1241	370	1241	325	1123	370	1123		
330	1293	370	1293	330	1176	370	1176		
335	1343	375	1343	335	1232	375	1232		
340	1397	380	1397	340	1292	380	1292		
345	1455	385	1455	345	1356	385	1356		
350	1517	390	1517	350	1426	390	1426		
355	1584	395	1584	355	1500	395	1500		
360	1655	400	1655	360	1579	400	1579		
365	1732	405	1732	365	1664	405	1664		
370	1813	410	1813	370	1755	410	1755		
375	1901	415	1901	375	1852	415	1852		
380	1995	420	1995	380	1940	420	1940		
385	2095	425	2095	385	2032	425	2032		
390	2202	430	2202	390	2130	430	2130		
395	2316	435	2316	395	2235	435	2235		
400	2438	440	2438	400	2346	440	2346		
				405	2466	445	2466		

TABLE 6-8
R. E. Ginna 40 EFPY Cooldown Curve Data Points

Cooldown Curves Steady State		20F		40F		60F		100F	
T	P	T	P	T	P	T	P	T	P
60	536	60	510	60	484	60	457	60	403
65	537	65	511	65	485	65	458	65	403
70	538	70	512	70	486	70	459	70	404
75	540	75	514	75	487	75	460	75	405
80	541	80	515	80	489	80	462	80	406
85	543	85	517	85	490	85	463	85	408
90	545	90	518	90	492	90	465	90	409
95	546	95	520	95	493	95	466	95	411
100	548	100	522	100	495	100	468	100	413
105	550	105	524	105	497	105	470	105	415
110	553	110	526	110	499	110	472	110	417
115	555	115	529	115	502	115	475	115	419
120	558	120	531	120	504	120	477	120	422
125	560	125	534	125	507	125	480	125	425
130	563	130	537	130	510	130	483	130	428
135	567	135	540	135	514	135	487	135	431
140	570	140	544	140	517	140	490	140	435
145	574	145	548	145	521	145	494	145	439
150	578	150	552	150	525	150	498	150	443
155	582	155	556	155	530	155	503	155	448
160	587	160	561	160	534	160	508	160	453
165	592	165	566	165	540	165	513	165	459
170	597	170	571	170	545	170	519	170	465
175	603	175	577	175	551	175	525	175	471
180	609	180	584	180	558	180	532	180	478
185	616	185	590	185	565	185	539	185	486
190	623	190	598	190	572	190	547	190	494
195	631	195	606	195	581	195	555	195	504
200	639	200	614	200	589	200	564	200	513
205	648	205	623	205	599	205	574	205	524
210	657	210	633	210	609	210	585	210	535
215	668	215	644	215	620	215	596	215	547
220	679	220	655	220	632	220	608	220	561
225	691	225	668	225	645	225	622	225	575
230	703	230	681	230	658	230	636	230	591
235	717	235	695	235	673	235	651	235	607
240	732	240	710	240	689	240	668	240	625
245	748	245	727	245	706	245	686	245	645
250	765	250	745	250	725	250	705	250	666
255	783	255	764	255	744	255	726	255	688
260	803	260	784	260	766	260	748	260	713
265	824	265	806	265	789	265	772	265	739
270	847	270	830	270	814	270	798	270	767
275	871	275	855	275	840	275	825	275	797
280	897	280	883	280	869	280	855	280	830
285	925	285	912	285	900	285	887	285	865
290	956	290	944	290	933	290	922	290	903
295	988	295	978	295	968	295	959	295	944
300	1023	300	1015	300	1006	300	999	300	988
305	1061	305	1054	305	1048	305	1042	305	1035
310	1101	310	1096	310	1092	310	1089	310	1086
315	1145	315	1141	315	1139	315	1138	315	1141
320	1191	320	1190	320	1190				
325	1241								
330	1295								
335	1352								
340	1414								
345	1481								
350	1552								
355	1628								
360	1710								
365	1797								
370	1891								
375	1992								
380	2099								
385	2214								
390	2336								
395	2467								

7 REFERENCES

1 Regulatory Guide 1.99, Revision 2, "Radiation Embrittlement of Reactor Vessel Materials", U.S. Nuclear Regulatory Commission, May, 1988.

2 WCAP-14040-NP-A, Revision 2, "Methodology used to Develop Cold Overpressure Mitigating System Setpoints and RCS Heatup and Cooldown Limit Curves", J. D. Andrachek, et al., January 1996.

3 10 CFR Part 50, Appendix G, "Fracture Toughness Requirements", Federal Register, Volume 60, No. 243, dated December 19, 1995.

4 RSIC Computer Code Collection CCC-543, "TORT-DORT Two- and Three-Dimensional Discrete Ordinates Transport, Version 2.7.3", May 1993.

5 RSIC Data Library Collection DLC-175, "BUGLE-93, Production and Testing of the VITAMIN-B6 Fine Group and the BUGLE-93 Broad Group Neutron/Photon Cross-Section Libraries Derived from ENDF/B-VI Nuclear Data", April 1994.

6 R. E. Maerker, et al, "Accounting for Changing Source Distributions in Light Water Reactor Surveillance Dosimetry Analysis", Nuclear Science and Engineering, Volume 94, Pages 291-308, 1986.

7 R. E. Radcliffe, et. al., "The Core Physics Characteristics of the R. E. Ginna Nuclear Plant - Cycle 1", WCAP-7352, September 1969. [Westinghouse Proprietary Class 2]

8 W. L. Baldewicz, et. al., "The Nuclear Design and Core Management of the R. E. Ginna Nuclear Reactor - Cycle 1B", WCAP-7658, January 1971. [Westinghouse Proprietary Class 2]

9 W. L. Baldewicz, et. al., "The Nuclear Design and Core Management of the R. E. Ginna Nuclear Reactor - Cycle 1B", Addendum to WCAP-7658, April 1971. [Westinghouse Proprietary Class 2]

10 W. L. Baldewicz, et. al., "The Nuclear Design and Core Management of the R. E. Ginna Nuclear Reactor - Cycle 2", WCAP-7871 Rev 1, July 1972. [Westinghouse Proprietary Class 2]

11 W. L. Baldewicz, "The Nuclear Design and Core Management of the R. E. Ginna Nuclear Reactor - Cycle 3", WCAP-8066, March 1973. [Westinghouse Proprietary Class 2]

12 J. C. Vanderstraeten, "The Nuclear Design and Core Management of the R. E. Ginna Nuclear Reactor - Cycle 4", WCAP-8316, May 1974. [Westinghouse Proprietary Class 2]

13 M. A. Mann, "The Nuclear Design and Core Management of the R. E. Ginna Nuclear Reactor - Cycle 5", WCAP-8514, March 1975. [Westinghouse Proprietary Class 2]

14 S. A. Schellin, et. al., "The Nuclear Design and Core Management of the R. E. Ginna Nuclear Reactor - Cycle 6", WCAP-8680 January 1976. [Westinghouse Proprietary Class 2]

15 C. Watarumi, et. al., "The Nuclear Design and Core Management of the R. E. Ginna Nuclear Reactor - Cycle 7", WCAP-8943, February 1977. [Westinghouse Proprietary Class 2]

16 J. Walden,, fax transmittal of R. E. Ginna Cycle 8 to 13 core loading, April 12, 1996. [RG&E Proprietary]

17 P. W. Robertson, et. al., "The Nuclear Design and Core Management of the R. E. Ginna Nuclear Reactor - Cycle 14", WCAP-10505, March 1984. [Westinghouse Proprietary Class 2]

18 Y. A. Chao, et. al., "The Nuclear Design and Core Management of the R. E. Ginna Nuclear Reactor - Cycle 15", WCAP-10794, March 1985. [Westinghouse Proprietary Class 2]

19 N. D. Jones, et. al., "The Nuclear Design and Core Management of the R. E. Ginna Nuclear Reactor - Cycle 16", WCAP-11069, March 1986. [Westinghouse Proprietary Class 2]

20 N. D. Jones, et. al., "The Nuclear Design and Core Management of the R. E. Ginna Nuclear Reactor - Cycle 17", WCAP-11404, February 1987. [Westinghouse Proprietary Class 2]

21 S. Srinilta, et. al., "The Nuclear Design and Core Management of the R. E. Ginna Nuclear Reactor - Cycle 18", WCAP-11713, February 1988. [Westinghouse Proprietary Class 2]

22 S. Srinilta, et. al., "The Nuclear Design and Core Management of the R. E. Ginna Nuclear Reactor - Cycle 19", WCAP-12210, April 1989. [Westinghouse Proprietary Class 2]

23 D. J. Krieg, et. al., "The Nuclear Design and Core Management of the R. E. Ginna Nuclear Reactor - Cycle 20", WCAP-12525 Rev 1, March 1990. [Westinghouse Proprietary Class 2]

24 S. Srinilta, et. al., "The Nuclear Design and Core Management of the R. E. Ginna Nuclear Reactor - Cycle 21", WCAP-12859, April 1991. [Westinghouse Proprietary Class 2]

25 S. Srinilta, et. al., "The Nuclear Design and Core Management of the R. E. Ginna Nuclear Reactor - Cycle 22", WCAP-13225, April 1992. [Westinghouse Proprietary Class 2]

26 S. Srinilta, et. al., "The Nuclear Design and Core Management of the R. E. Ginna Nuclear Reactor - Cycle 23", WCAP-13609, April 1993. [Westinghouse Proprietary Class 2]

27 S. Srinilta, et. al., "The Nuclear Design and Core Management of the R. E. Ginna Nuclear Reactor - Cycle 24", WCAP-13965, March 1994. [Westinghouse Proprietary Class 2]

28 S. Srinilta, et. al., "The Nuclear Design and Core Management of the R. E. Ginna Nuclear Reactor - Cycle 25", WCAP-14290, April 1995. [Westinghouse Proprietary Class 2]

29 Preliminary Nuclear Design and Core Management of the R. E. Ginna Nuclear Reactor - Cycle 26, file rge26anc.33 of the Westinghouse On-line Document Management System, April 12, 1996. [Westinghouse Proprietary Class 2]

30 ASTM Designation E482-89, "Standard Guide for Application of Neutron Transport Methods for Reactor Vessel Surveillance", in ASTM Standards, Section 12, American Society for Testing and Materials, Philadelphia, PA, 1993.

31 ASTM Designation E560-84, "Standard Recommended Practice for Extrapolating Reactor Vessel Surveillance Dosimetry Results", in ASTM Standards, Section 12, American Society for Testing and Materials, Philadelphia, PA, 1993.

32 ASTM Designation E693-79, "Standard Practice for Characterizing Neutron Exposures in Ferritic Steels in Terms of Displacements per Atom (dpa)", in ASTM Standards, Section 12, American Society for Testing and Materials, Philadelphia, PA, 1993.

33 ASTM Designation E706-87, "Standard Master Matrix for Light-Water Reactor Pressure Vessel Surveillance Standard", in ASTM Standards, Section 12, American Society for Testing and Materials, Philadelphia, PA, 1993.

34 ASTM Designation E853-87, "Standard Practice for Analysis and Interpretation of Light-Water Reactor Surveillance Results", in ASTM Standards, Section 12, American Society for Testing and Materials, Philadelphia, PA, 1993.

35 ASTM Designation E261-90, "Standard Practice for Determining Neutron Fluence Rate, Fluence, and Spectra by Radioactivation Techniques", in ASTM Standards, Section 12, American Society for Testing and Materials, Philadelphia, PA, 1993.

36 ASTM Designation E262-86, "Standard Method for Determining Thermal Neutron Reaction and Fluence Rates by Radioactivation Techniques", in ASTM Standards, Section 12, American Society for Testing and Materials, Philadelphia, PA, 1993.

37 ASTM Designation E263-88, "Standard Method for Measuring Fast-Neutron Reaction Rates by Radioactivation of Iron", in ASTM Standards, Section 12, American Society for Testing and Materials, Philadelphia, PA, 1993.

38 ASTM Designation E264-92, "Standard Method for Measuring Fast-Neutron Reaction Rates by Radioactivation of Nickel", in ASTM Standards, Section 12, American Society for Testing and Materials, Philadelphia, PA, 1993.

39 ASTM Designation E481-92, "Standard Method for Measuring Neutron-Fluence Rate by Radioactivation of Cobalt and Silver", in ASTM Standards, Section 12, American Society for Testing and Materials, Philadelphia, PA, 1993.

40 ASTM Designation E523-87, "Standard Test Method for Measuring Fast-Neutron Reaction Rates by Radioactivation of Copper", in ASTM Standards, Section 12, American Society for Testing and Materials, Philadelphia, PA, 1993.

41 ASTM Designation E704-90, "Standard Test Method for Measuring Reaction Rates by Radioactivation of Uranium-238", in ASTM Standards, Section 12, American Society for Testing and Materials, Philadelphia, PA, 1993.

42 ASTM Designation E705-90, "Standard Test Method for Measuring Reaction Rates by Radioactivation of Neptunium-237", in ASTM Standards, Section 12, American Society for Testing and Materials, Philadelphia, PA, 1993.

43 ASTM Designation E1005-84, "Standard Test Method for Application and Analysis of Radiometric Monitors for Reactor Vessel Surveillance", in ASTM Standards, Section 12, American Society for Testing and Materials, Philadelphia, PA, 1993.

44 F. A. Schmittroth, "FERRET Data Analysis Core", HEDL-TME 79-40, Hanford Engineering Development Laboratory, Richland, WA, September 1979.

45 W. N. McElroy, S. Berg and T. Crocket, "A Computer-Automated Iterative Method of Neutron Flux Spectra Determined by Foil Activation", AFWL-TR-7-41, Vol. I-IV, Air Force Weapons Laboratory, Kirkland AFB, NM, July 1967.

46 RSIC Data Library Collection DLC-178, "SNLRML Recommended Dosimetry Cross-Section Compendium", July 1994.

47 EPRI-NP-2188, "Development and Demonstration of an Advanced Methodology for LWR Dosimetry Applications", R. E. Maerker, et al., 1981.

48 1989 ASME Boiler and Pressure Vessel (B&PV) Code, Section XI, Appendix G, "Fracture Toughness Criteria for Protection Against Failure".

49 MSE-REME-0280, "R. E. Ginna Heatup/Cooldown Curves at 20 EFPY for Normal Operation", Letter from P. A. Grendys (W) to Mr George Wrobel (RGE), Dated April 26, 1996.

50 1989 Section III, Division 1 of the ASME Boiler and Pressure Vessel Code, Paragraph NB-2331, "Material for Vessels".

51 WCAP-13902, "Analysis of Capsule S from the Rochester Gas and Electric Corporation R. E. Ginna Reactor Vessel Radiation Surveillance Program", Dated December 1993.

52 "R. E. Ginna Nuclear Power Plant RCS Pressure and Temperature Limits Report", Revision 1, Fax from Mr. Ron Jaquin (RGE) to Mr E. Terek (W), Dated April 17, 1996

53 WCAP-7924-A, "Basis for Heatup and Cooldown Limit Curves", W. S. Hazelton, et al., April 1975.

54 RGE-96-503, "Your P.O. # CP-64647-C-RD, Chemical Analysis of Eight Weld Metal Samples", from Mr. S. M. Sconce (W) to Mr Ron Jaquin (RGE),Dated February 27, 1996.

Attachment IX

Response to NRC Questions Concerning Previous LTOP Analysis

(Revised from that provided in Enclosure 3 to June 3, 1997 letter to NRC)

1. **Provide a discussion of the dynamic and static head effects and how these were accounted for in the analyses for the mass addition and heat addition cases. For the dynamic head effect, consider the effect of all RCPs and RHR pumps that are allowed to operate. If you are limiting operation of such pumps in the LTOP region, provide a discussion of such controls.**

The RELAP model used for the analysis automatically accounts for dynamic and static head effects. The pressure sensors for the LTOPs actuation are taken from the RCP suction leg volumes, consistent with their location in the plant. For Appendix G pressure limits the pressure is taken at the lowest downcomer node in the reactor vessel. This results in the highest pressure in the reactor vessel and is therefore conservative. For RHR pressure, the highest pressure in the RHR system is used (pump discharge).

Cases chosen for the LTOPs analysis utilize running pumps consistent with the operating conditions, and conservatisms as described below.

Mass Addition Cases

For the mass addition cases, two conditions bound all operating conditions:

1. SI Pump injecting with a 1.1 in^2 vent on the RCS, no RCPs running.

2. 3 Charging Pumps injecting with both RCPs running.

In all three mass addition cases, the RHR system is considered isolated. Isolation of the RHR system is conservative in that the RHR relief valve (designed to handle the full flowrate of 3 charging pumps) is isolated, and isolating the RHR system provides a smaller volume for the injected mass to expand into, thus resulting in a higher RCS pressure. Case 1 is run at 60°F and 212°F, bounding the conditions for which a vent can be established in the RCS. RCPs cannot be run when the RCS is vented. Case 2 is run for RCS temperatures above 60°F, for cases when protection is provided by the pressurizer PORVs. Results of these cases are attached.

Heat Addition

For the heat addition cases, several scenarios were evaluated in order to determine the limiting cases, allowing adequate conservatism but not being unreasonably conservative which could result in unnecessary operation restrictions, as discussed below.

From an Appendix G standpoint not attaching the RHR system results in the most limiting pressure transient, since the RHR system would remove some of the heat being added from the start of an RCP. It was, however, necessary to model the RHR system in order to demonstrate adequate protection of the RHR system from overpressurization (assuming shutoff head for the RHR pumps for all cases while conservative would result in undesirable operating constraints). In order to ensure bounding conservatism for Appendix G, the heat exchangers were modeled as being inactive.

In order to determine the number of running RHR pumps, several sensitivities were run to determine minimum and maximum flowrates within the constraints of cooldown limits, considering both minimum and maximum decay heat removal requirements. The results indicate that for RCS temperatures below 280°F two RHR pumps may be in operation, above 280°F one pump would be in operation. Therefore the analyses assumes two pumps running for cases below 280°F, and one pump running above 280°F. The impact of these conditions on the transient is not significant since the pump curves for the RHR pumps is relatively flat.

Additionally, it should be noted that the heat addition case was not considered in the original design basis for overpressurization protection of the RHR system. Inadvertent start of an RCP takes several distinct actions by the operator which were not considered credible. Therefore, consideration of this transient for RHR overpressure protection is in and of itself added conservatism.

2. **Justify the use of 85°F as the limiting low temperature for LTOP analyses (both heat and mass addition), in light of your curves extending to 60°F; or provide analyses at the lower value.**

Transients were run at 85°F due to the fact that until recently curves were only available down to 85°F. Additional cases have been run at 60°F. For the heat addition cases utilizing a higher temperature for the initiating temperature results in a higher peak pressure. This is due to the fact that the change in density of water per degree fahrenheit increases as the temperature increases. For the mass addition case a lower temperature is more limiting, due to the higher density of the RCS liquid. Again, the change in density is less that 0.5% and will have a negligible impact. Results of these cases are attached.

3. **Justify the use of 430 psig for PORV lift setpoint in the analysis. List the parameters that may affect this setpoint (e.g., Instrument uncertainty and others) and show that the proposed limit of 411 psig is sufficient to protect the Appendix G curves.**

The analysis assumes a setpoint of 430 psig. It demonstrates, with this assumed setpoint, that all limits are met (with margin). The instrument uncertainty for the actuation channels has been calculated to be 16.95 psig. When added to the proposed 411 psig limit, an acceptable analytical value of $\geq$ 427.95 psig is arrived at. The analyzed 430 psig setpoint is therefore conservative.

4. **The submittal indicates that instrument uncertainty need not be accounted for in Appendix G analyses. This in incorrect. Revise methodology to correct this statement.**

The methodology document states that instrument uncertainty is accounted for (page 3.3 item q). The initial analysis done utilizing the methodology did account for instrument uncertainty, however a statement in the calculation was made that it did not need to be accounted for for Appendix G cases. This was consistent with the previously approved methodology. The current methodology requires instrument uncertainty to be accounted for and therefore all future analyses will account for it. No revision to the methodology is required.

5. **Justify the use of the RHR system for cooling in the heat addition analysis. Discuss the effect of this configuration on the analysis in terms of differences in peak pressures that would be obtained had the RHR system been assumed not operating.**

See response to question 1. No credit is taken for cooling from the RHR system.

6. **You assumed no RCS flow in the mass addition analysis. You must account for dynamic head effects for this analyses from both the RCPs and RHR pumps that may be operating. Did you account for the dynamic head effect separately?**

See discussion in response to question 1.

7. **In Section 6.2 you state that in the future you can credit the instrument uncertainty if needed. Instrument uncertainty must be accounted for. Therefore, this statement is incorrect. Correct this statement in your methodology.**

See discussion under question 4. Instrument uncertainty is included in the methodology and must be accounted for in all future analysis.

8. **TS 3.5.3, "ECCS-MODE 4," requires that one train of ECCS be operable in Mode 4. This appears to be in conflict with the LTOP TS 3.4.12 which required that all SI pumps be incapable of injecting into the RCS. Explain how Ginna meets these two TSs when in the LTOP region and in Mode 4.**

See last paragraph of LCO bases for LCO 3.5.3 (page B3.5-26). Our ECCS requirements specify the capability of injection within 10 minutes which specifically addresses the need to place the SI pumps in pull-stop for LTOP.

9. **TS 3.4.12, "Low Temperature Overpressure Protection (LTOP) System," allows an SI pump to be capable of injecting into the RCS if the RCS is depressurized and an RCS vent of 1.1 square inches is established. Provide the analysis for this configuration with the new P/T curves.**

Calculation of the pressure limit for the limiting mass addition cases when protection is provided by a 1.1 in^2 vent are provided in the updated LTOP analysis and results are attached.

10. **Justify the use of Table 3 for RCP start profile and 1 second opening time for the PORV.**

Acceleration times for the RCPs are dependent upon pump loading, electrical system impedance, and voltage levels. For the LTOP heat addition cases a faster accelerating time results in more limiting transients since the heat addition occurs over a shorter time period.

A computer model (ETAP) was developed and benchmarked based on vendor pump performance curves and actual current, voltage, and power measurements taken during RCP starts during the 1991 and 1994 outages. Conservatisms employed in the model include:

<u>Pump Loading</u>

1. The density of RCS fluid is taken at 350°F (lowest density) for all cases. This minimizes load and therefore results in a faster acceleration.

2. Flowrates were maximized in the RCS. Again, this decreases load and results in a faster acceleration.

<u>System Impedance</u>

1. The offsite power impedance varies with changes in transmission system configuration. For the analysis, the configuration with the least impedance was used. A conservatively low impedance for this configuration was used.

System Voltage

With Ginna Station off-line, the voltage level on the 4160V busses is reduced. A conservatively high voltage above measured voltages was chosen (4300V).

Utilizing the above conservatisms computer runs were made for all RCPs (A, B, Spare) with acceleration times ranging from 17.4 to 18.6 seconds. For the LTOPs analysis the fastest acceleration, 17.4 seconds was chosen.

For the PORV, a stroke time of 1 second is chosen in the analysis. The acceptance criteria in periodic test procedure PT-2.6.5-SD specifies a maximum stroke time of 0.62 seconds. Actual stroke times recorded during the test have been consistently on the order of 0.5 seconds or less. Therefore, the analytical stroke time is conservative.

Attachment 1
LTOP Cases
Summary of Results

Type/Case	RCS Temp, °F	# of RCPs running	Limit*, psia	RV Peak, psia	RHR limit, psia	RHR Peak, psia
Mass Addition						
SI pump	60	0	608.7	413.5	674.7	542.3
SI pump	212	0	780.3	396.7	674.7	525.9
3 Charging	60	2	608.7	587.4	674.7	664.0
Heat Addition						
RCP Start	60	1 start	608.7	551.3	674.7	650.0
RCP Start	280	1 start	1116.9	569.3	674.7	663.7
RCP Start	320	1 start	1529.4	563.8	674.7	655.7

* 110% of Appendix G limit per code case N-514.

FIGURE 7

CASE 2 MASS ADDITION CASE PRIMARY TEMPERATURE 60°F
PRIMARY PRESSURE 329.7 PSIA
1 CHARGING PUMP ONE RC PUMP RUNNING
3 GPM SEAL LEAKAGE

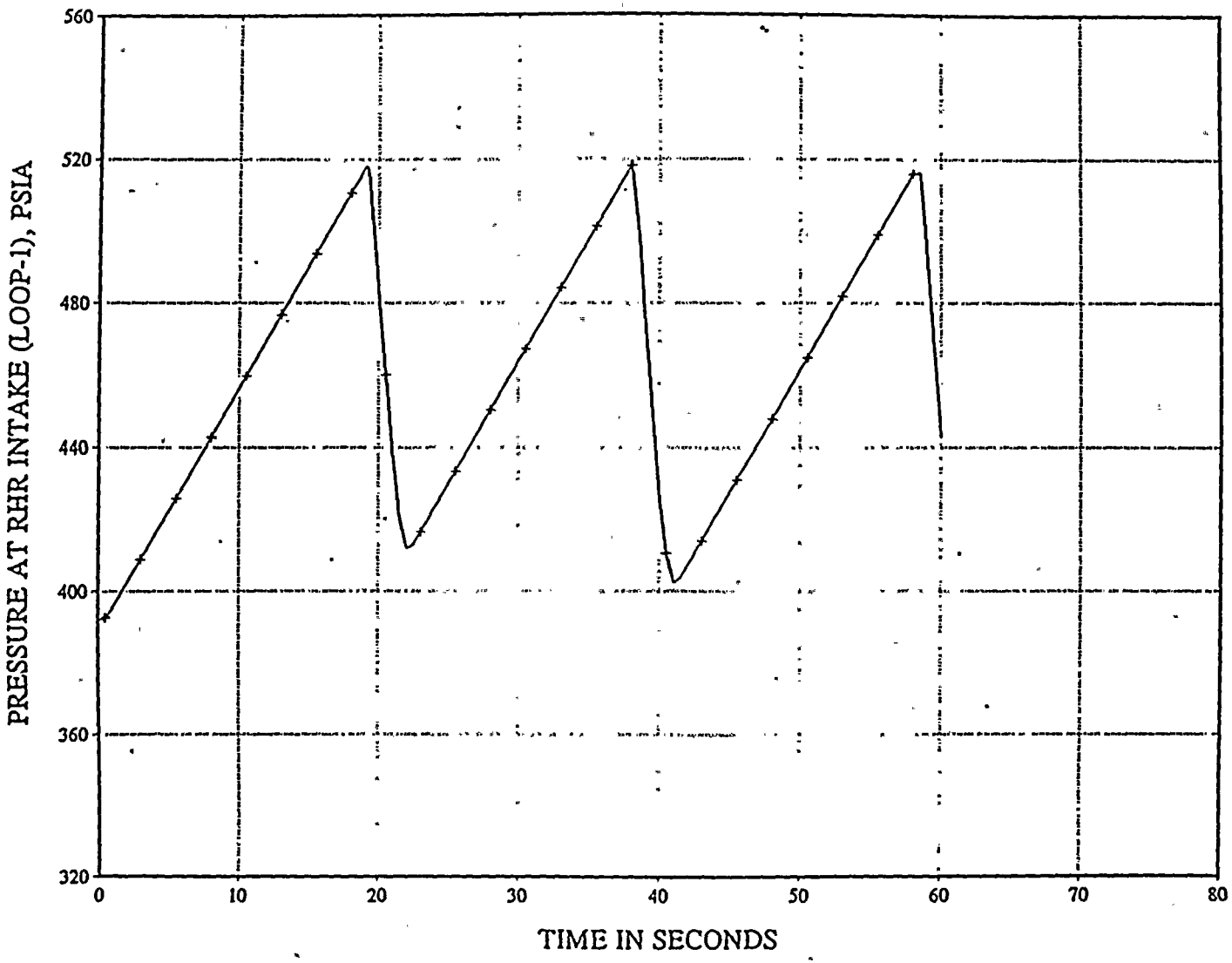

FIGURE 8

CASE 3 MASS ADDITION CASE PRIMARY TEMPERATURE 60°F
PRIMARY PRESSURE 14.7 PSIA
1 SI PUMP STARTED NO RC PUMP RUNNING
1.1 SQ.INCH VENT NO SEAL LEAKAGE

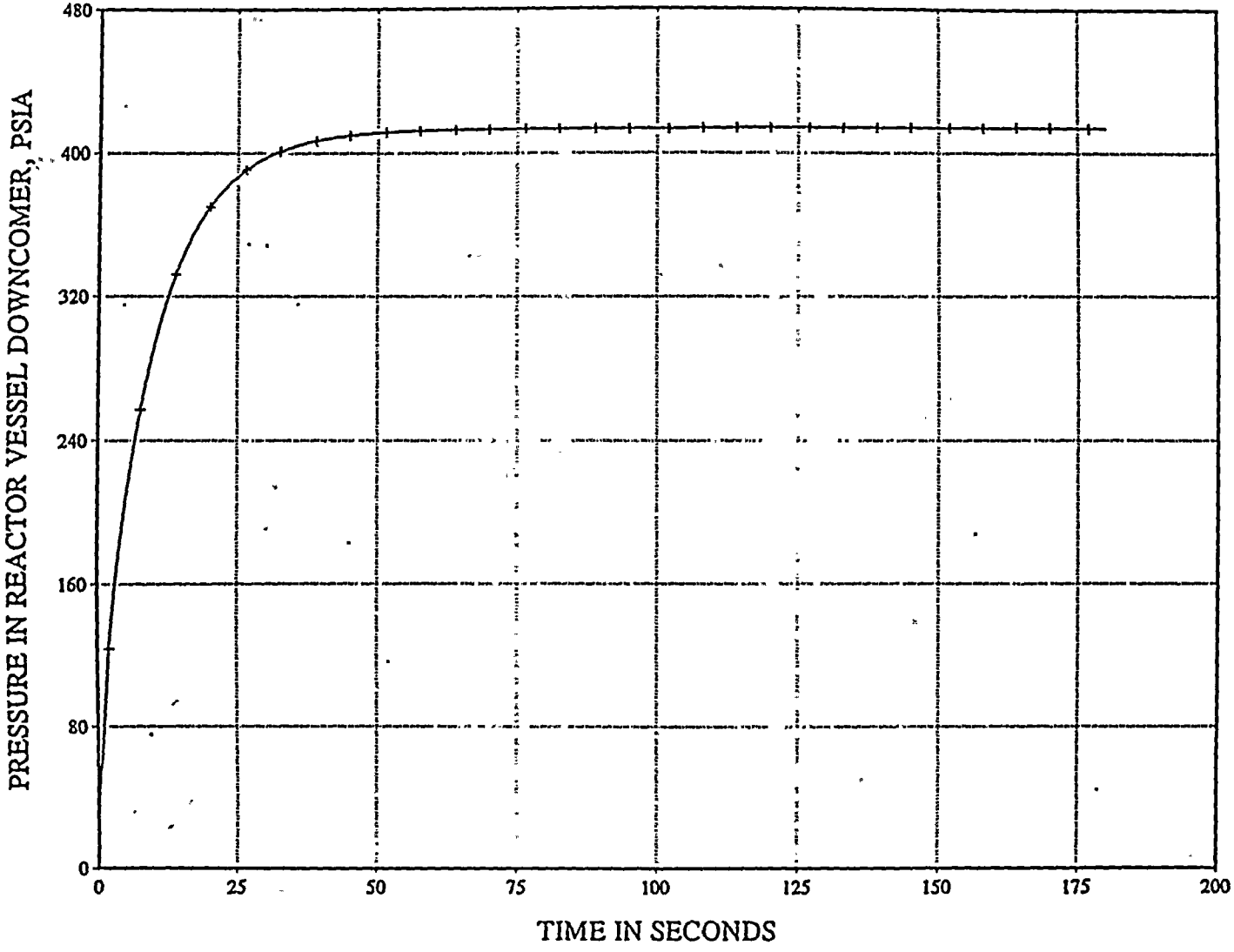

FIGURE 9

CASE 3 MASS ADDITION CASE PRIMARY TEMPERATURE 60°F
PRIMARY PRESSURE 14.7 PSIA
1 SI PUMP STARTED NO RC PUMP RUNNING
1.1 SQ.INCH VENT NO SEAL LEAKAGE

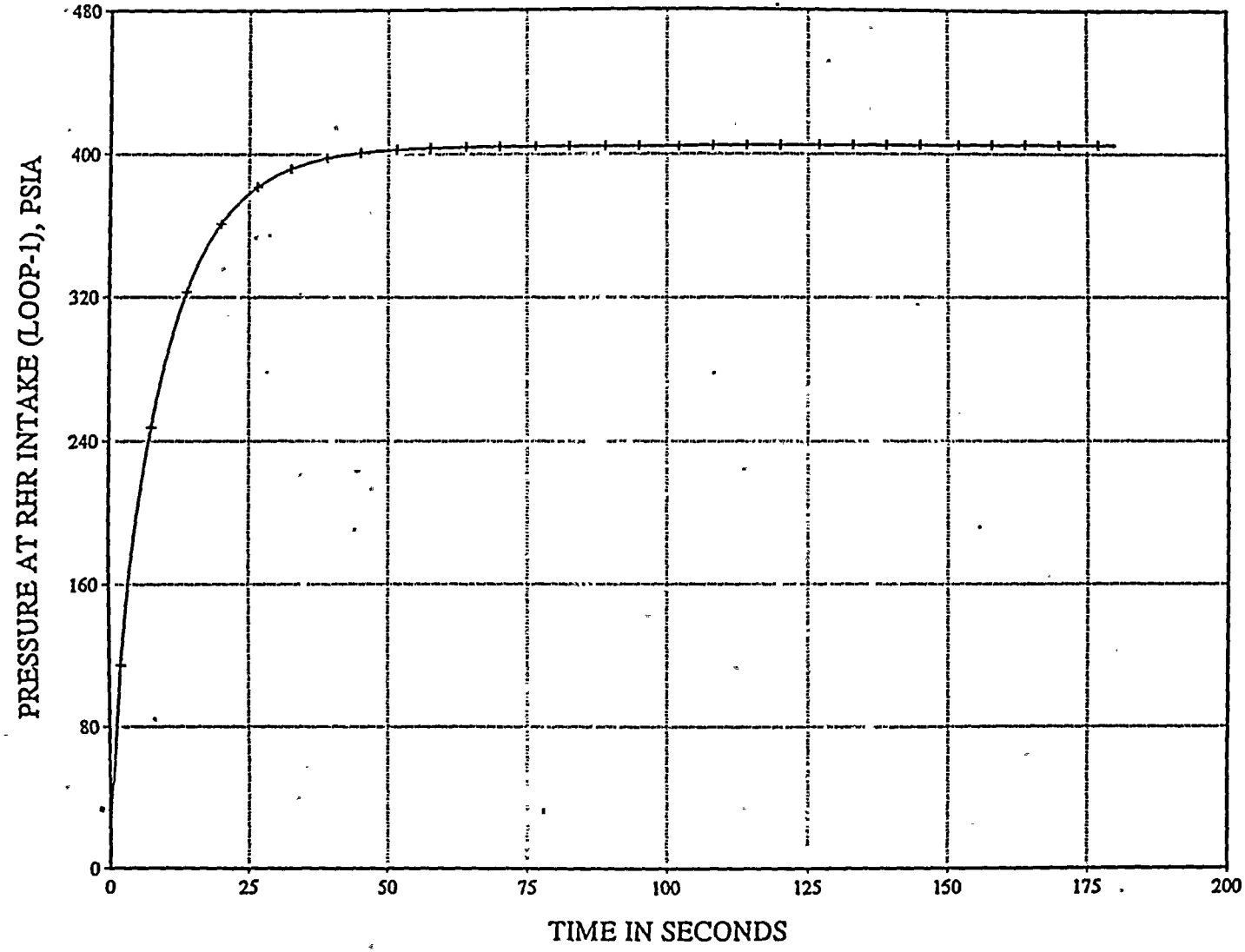

FIGURE 10

CASE 4 MASS ADDITION CASE PRIMARY TEMPERATURE 212°F
PRIMARY PRESSURE 14.7 PSIA
1 SI PUMP STARTED NO RC PUMP RUNNING
1.1 SQ.INCH VENT NO SEAL LEAKAGE

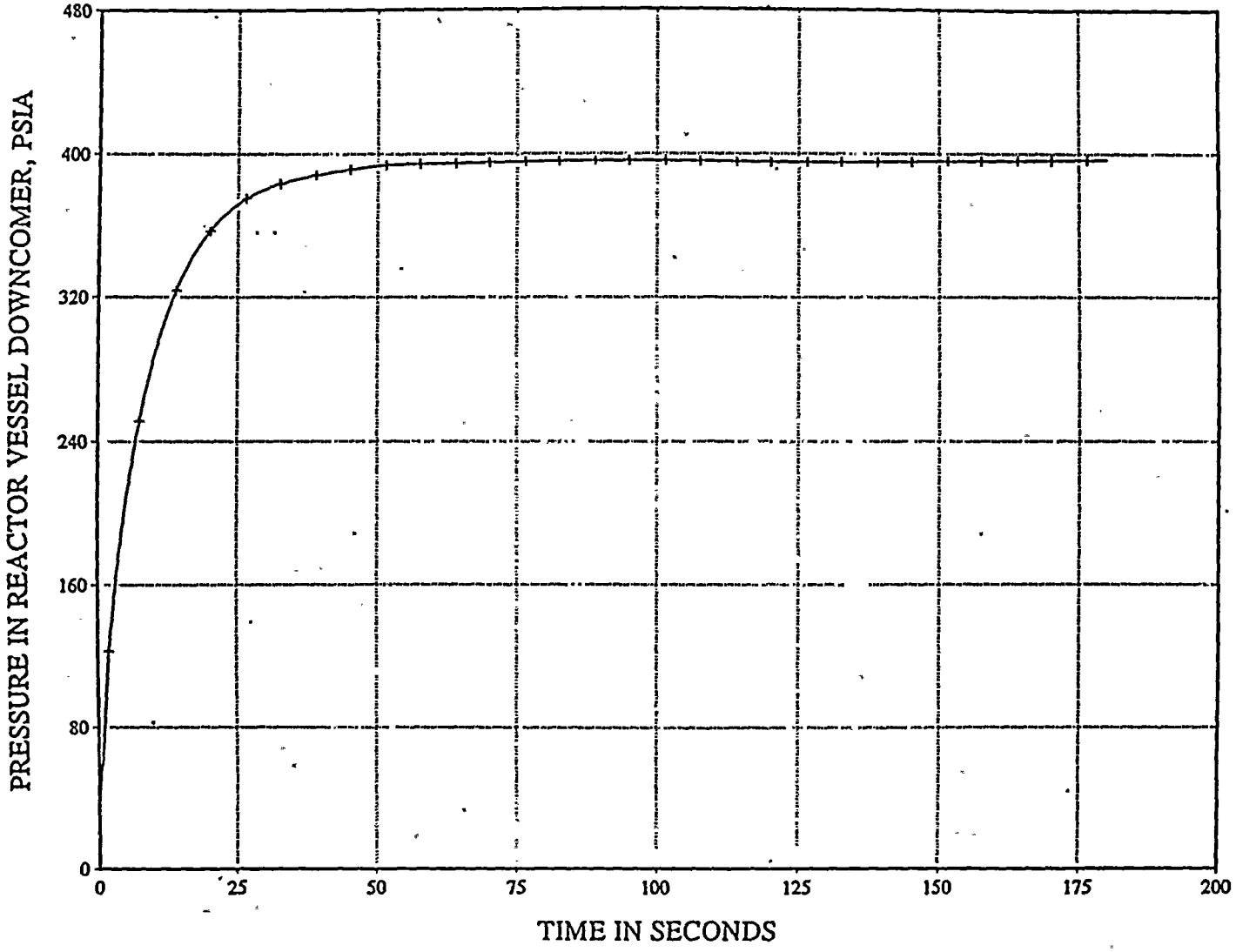

FIGURE 11

CASE 4 MASS ADDITION CASE PRIMARY TEMPERATURE 212°F
PRIMARY PRESSURE 14.7 PSIA
1 SI PUMP STARTED NO RC PUMP RUNNING
1.1 SQ.INCH VENT NO SEAL LEAKAGE

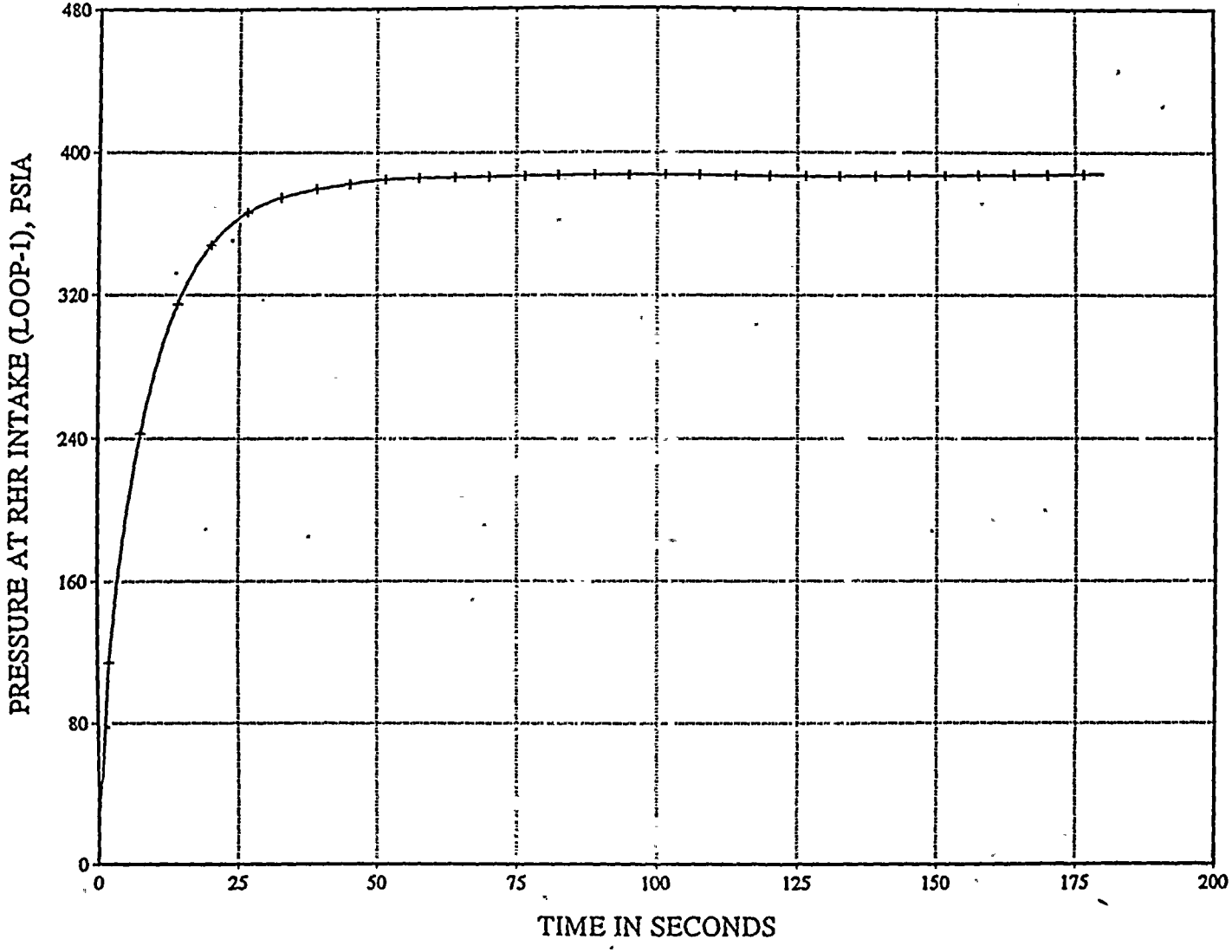

FIGURE
CASE 5 HEAT ADDITION CASE PRIMARY TEMPERATURE 60°F
PRIMARY PRESSURE 329.7 PSIA
NO VENT, NO SI, NO CHARGING PUMP
ONE RC PUMP STARTED
2000 GPM RHR

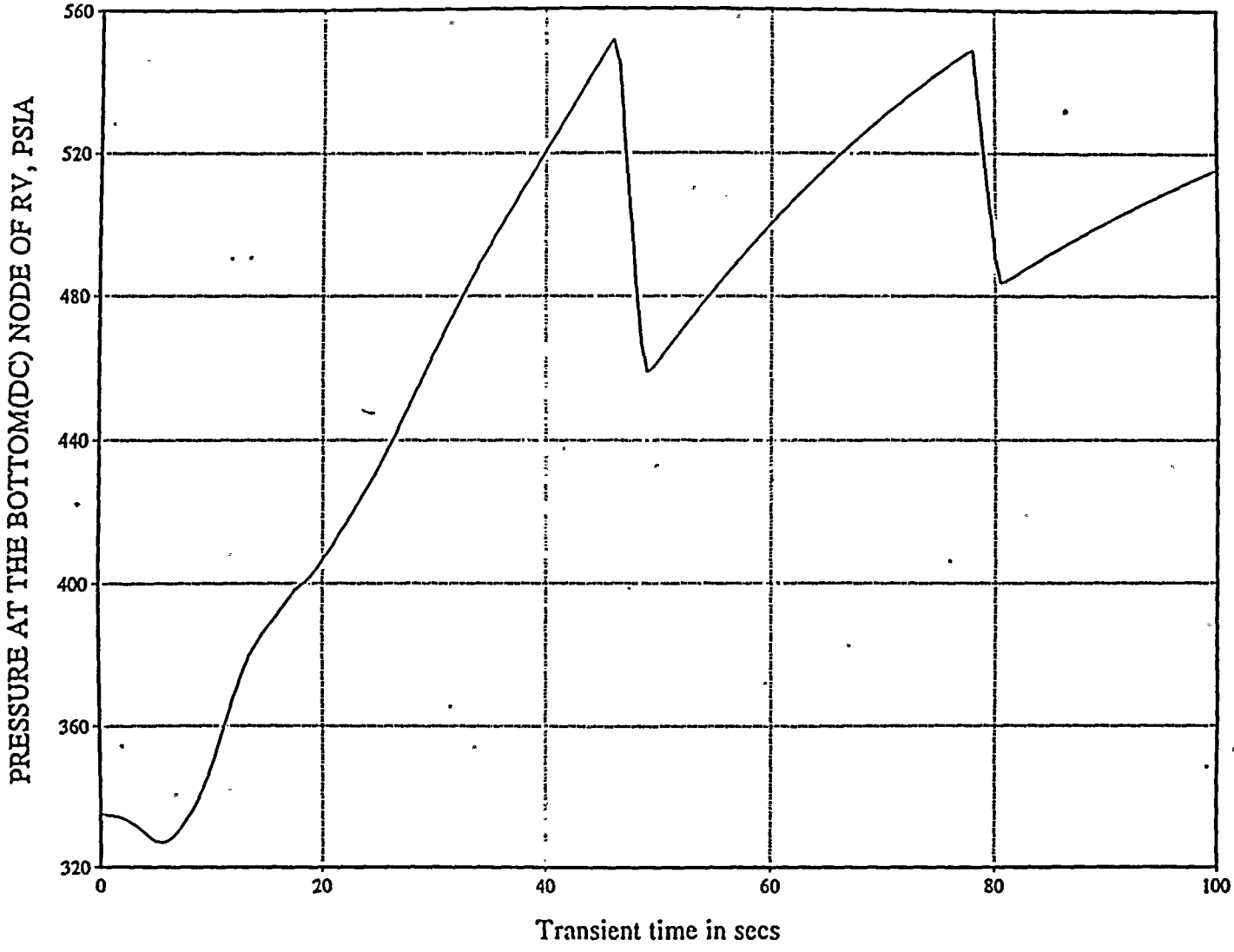

FIGURE 13
CASE 5 HEAT ADDITION CASE PRIMARY TEMPERATURE 60°F
PRIMARY PRESSURE 329.7 PSIA
NO VENT, NO SI, NO CHARGING PUMP
ONE RC PUMP STARTED
2000 GPM RHR

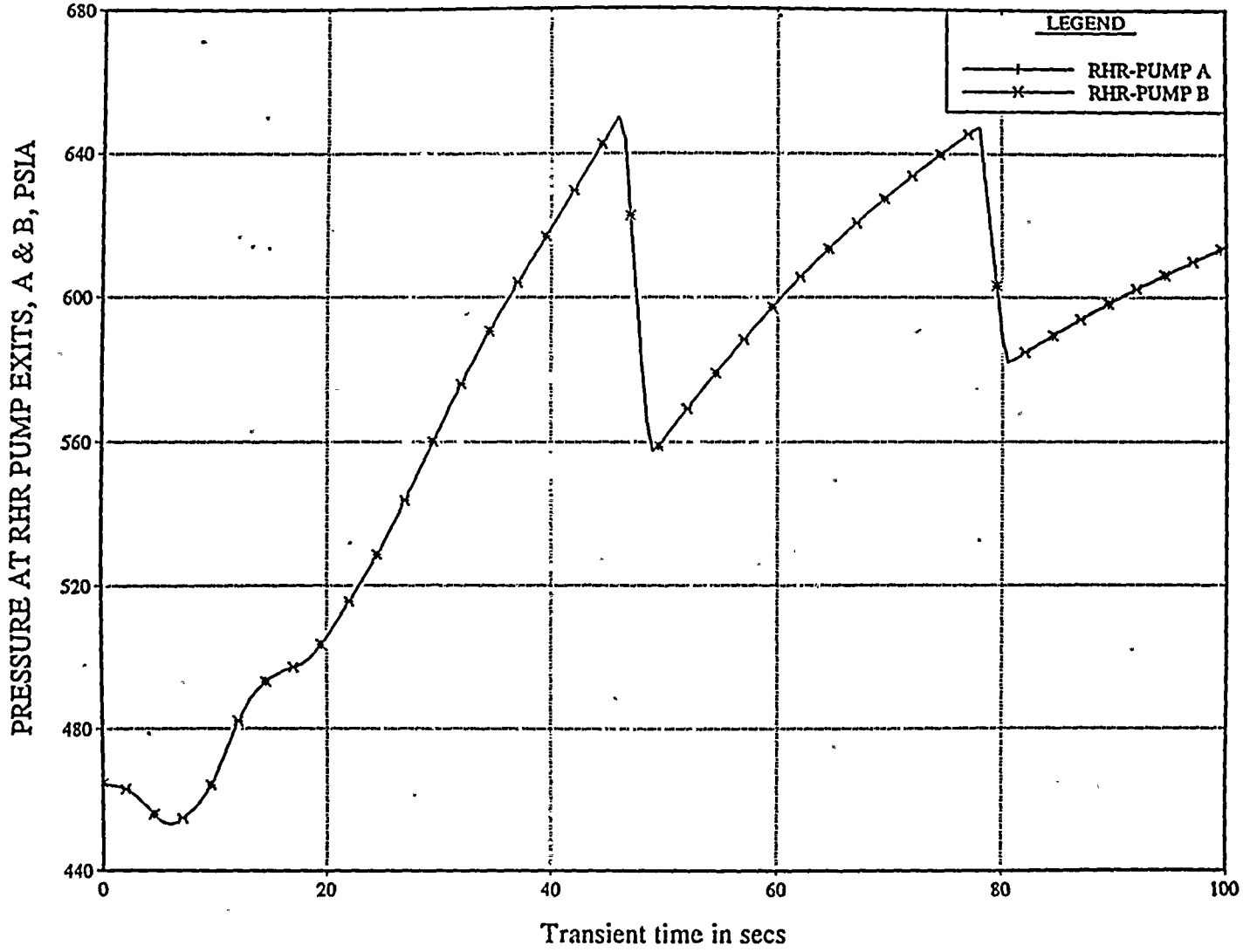

FIGURE 14

CASE 5 HEAT ADDITION CASE PRIMARY TEMPERATURE 60°F
PRIMARY PRESSURE 329.7 PSIA
NO VENT, NO SI, NO CHARGING PUMP
ONE RC PUMP STARTED
2000 GPM RHR

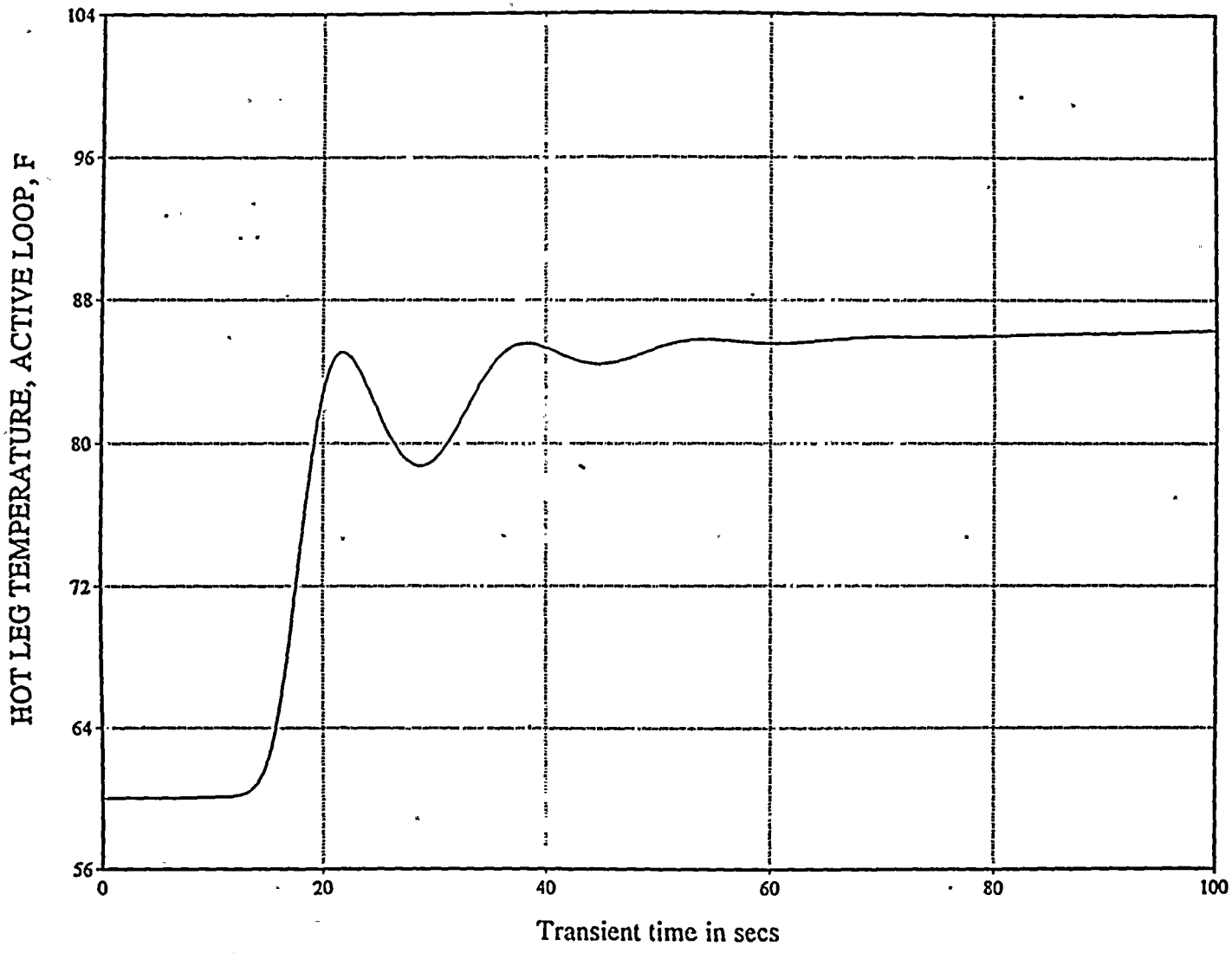

FIGURE 15

CASE 5 HEAT ADDITION CASE PRIMARY TEMPERATURE 60°F
PRIMARY PRESSURE 329.7 PSIA
NO VENT, NO SI, NO CHARGING PUMP
ONE RC PUMP STARTED
2000 GPM RHR

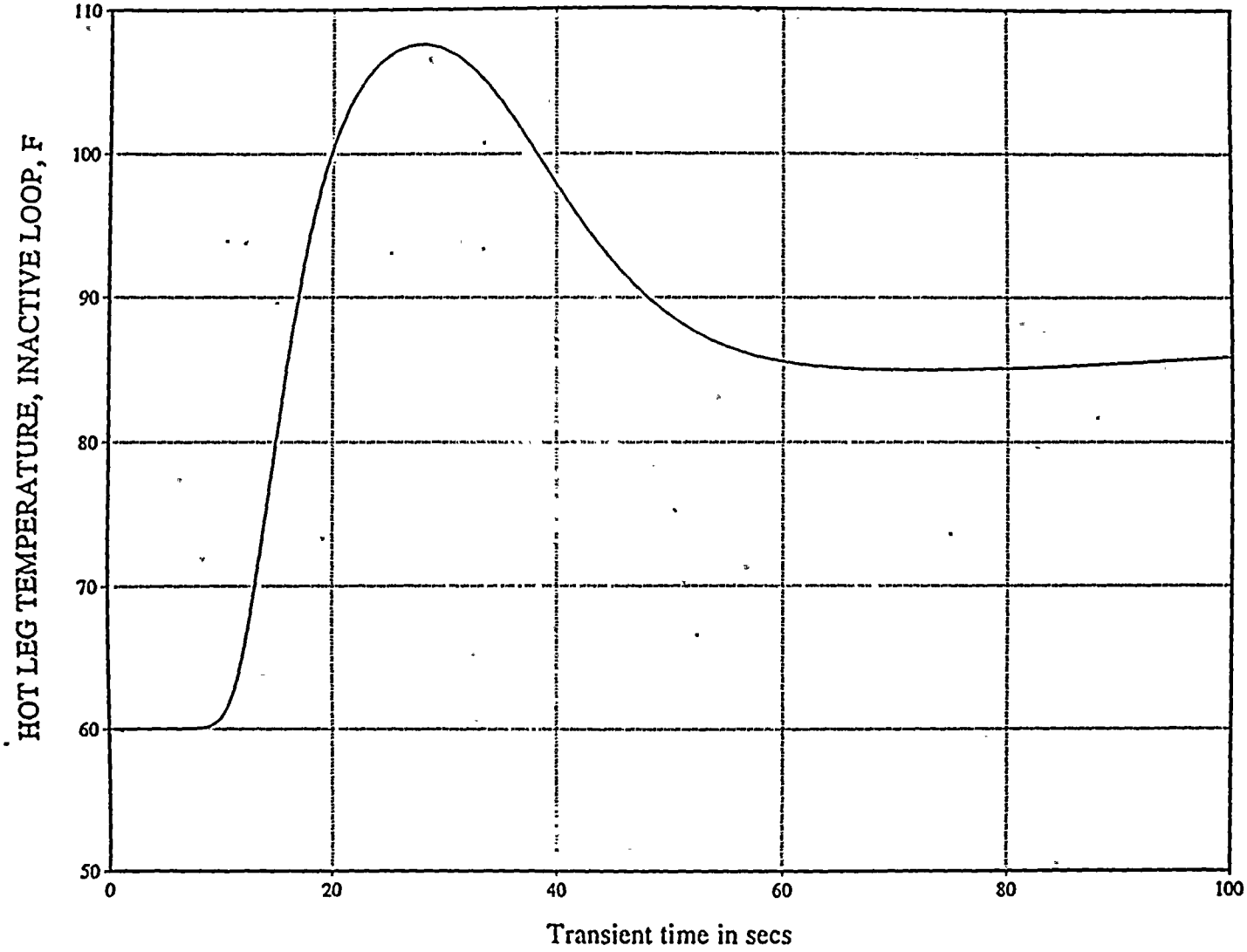

FIGURE

CASE 5 HEAT ADDITION CASE PRIMARY TEMPERATURE 60°F
PRIMARY PRESSURE 329.7 PSIA
NO VENT, NO SI, NO CHARGING PUMP
ONE RC PUMP STARTED
2000 GPM RHR

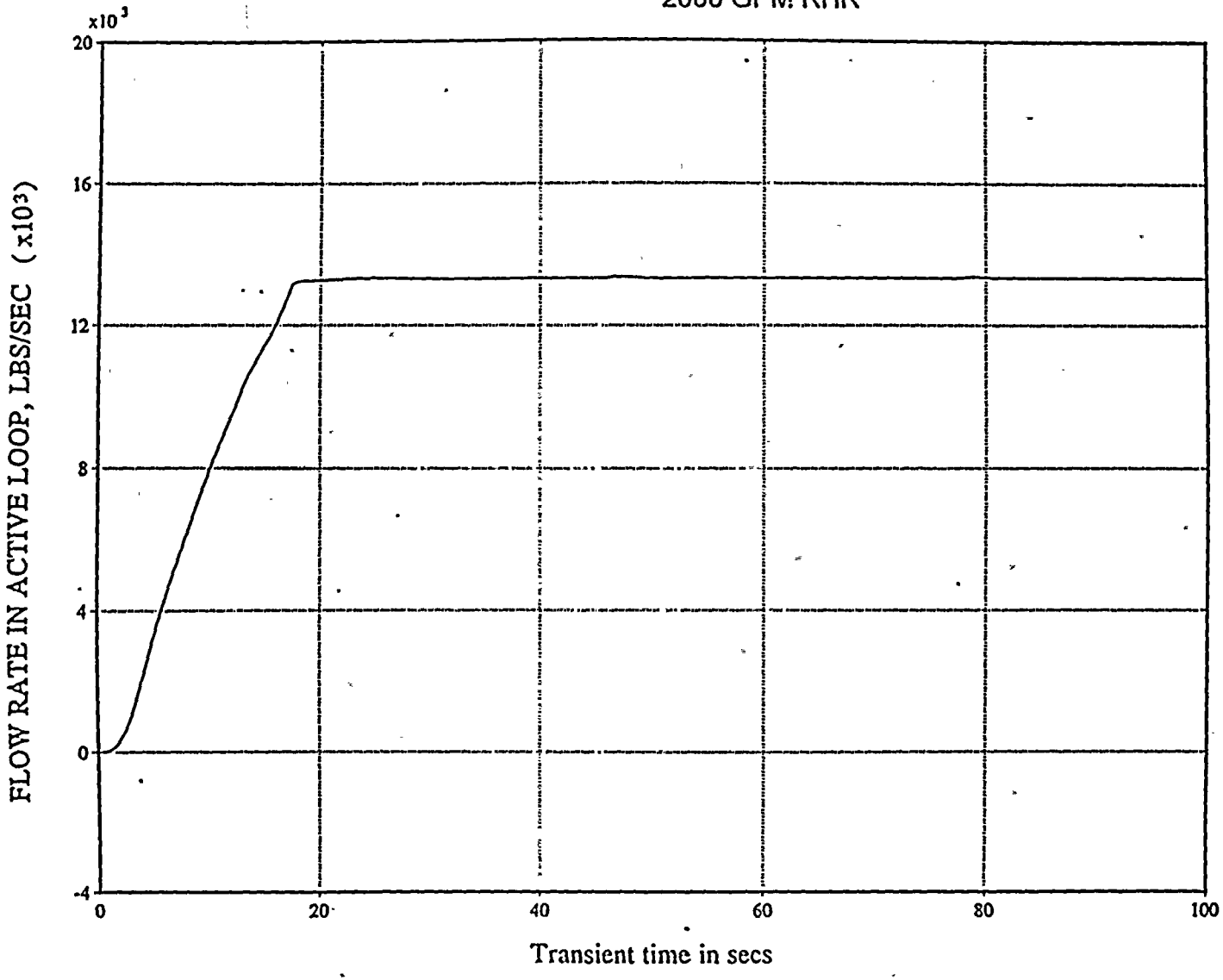

FIGURE
CASE 5 HEAT ADDITION CASE PRIMARY TEMPERATURE 60°F
PRIMARY PRESSURE 329.7 PSIA
NO VENT, NO SI, NO CHARGING PUMP
ONE RC PUMP STARTED
2000 GPM RHR

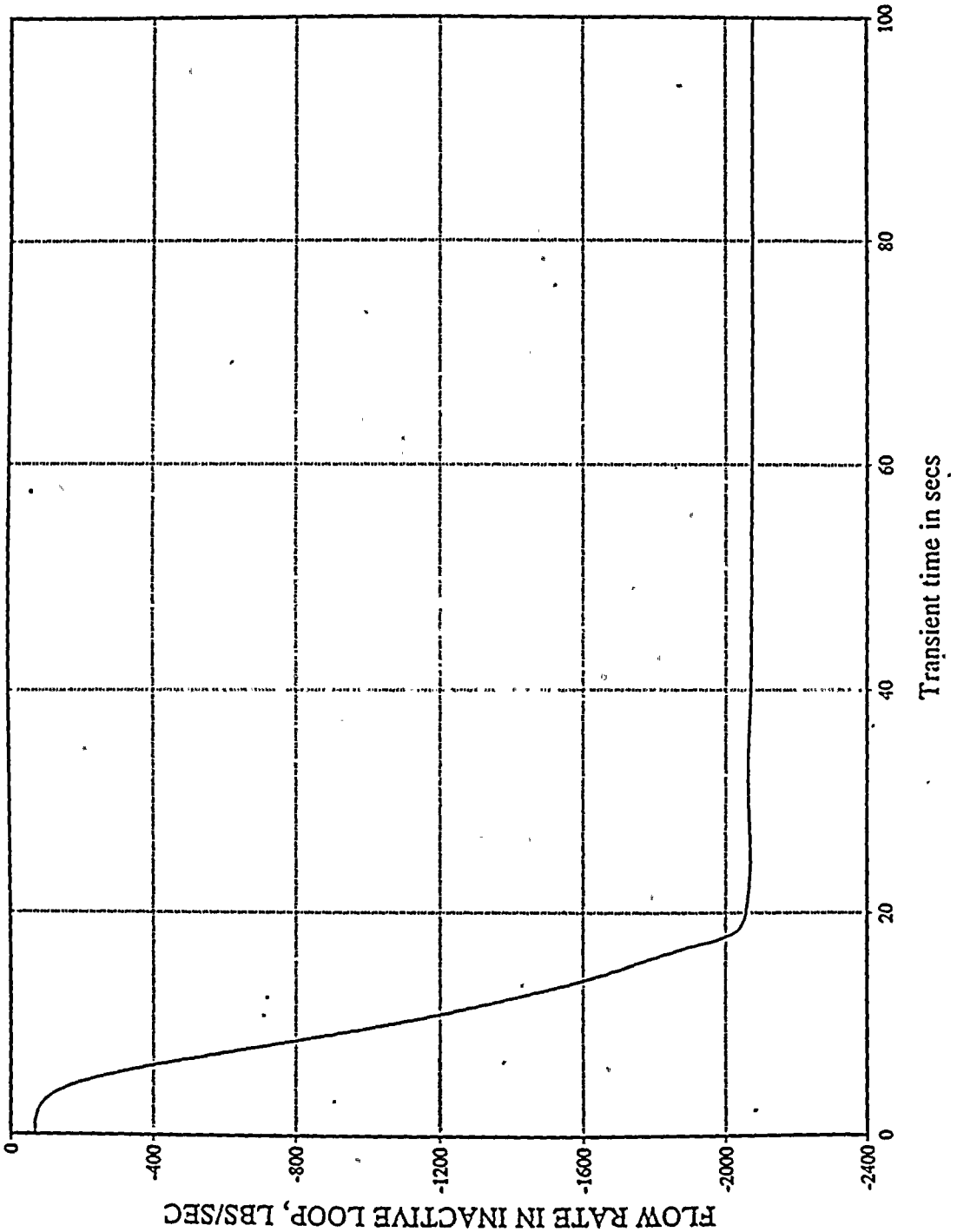

FIGURE
CASE 5 HEAT ADDITION CASE PRIMARY TEMPERATURE 60°F
PRIMARY PRESSURE 329.7 PSIA
NO VENT, NO SI, NO CHARGING PUMP
ONE RC PUMP STARTED
2000 GPM RHR

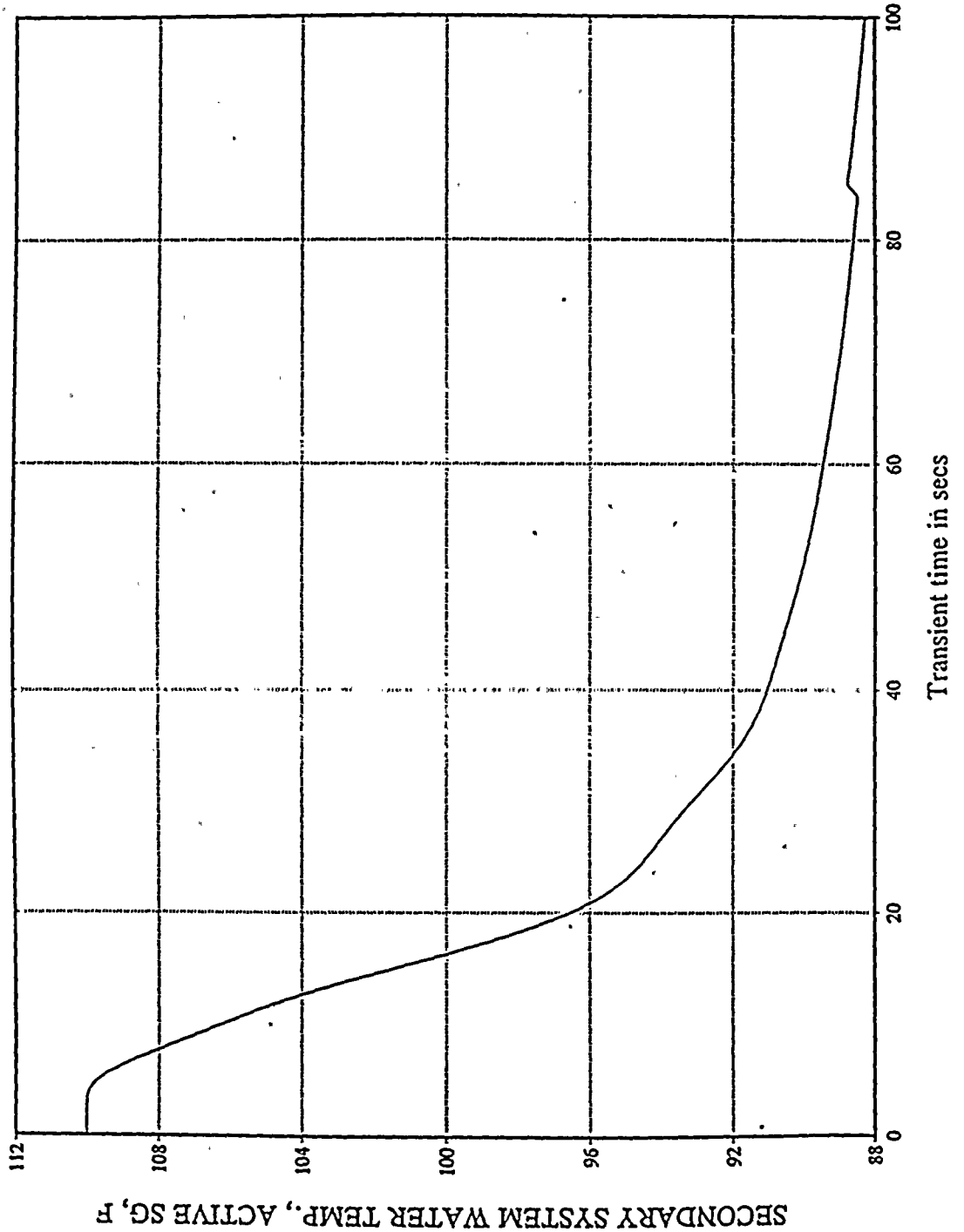

FIGURE 19
CASE 5 HEAT ADDITION CASE PRIMARY TEMPERATURE 60°F
PRIMARY PRESSURE 329.7 PSIA
NO VENT, NO SI, NO CHARGING PUMP
ONE RC PUMP STARTED
2000 GPM RHR

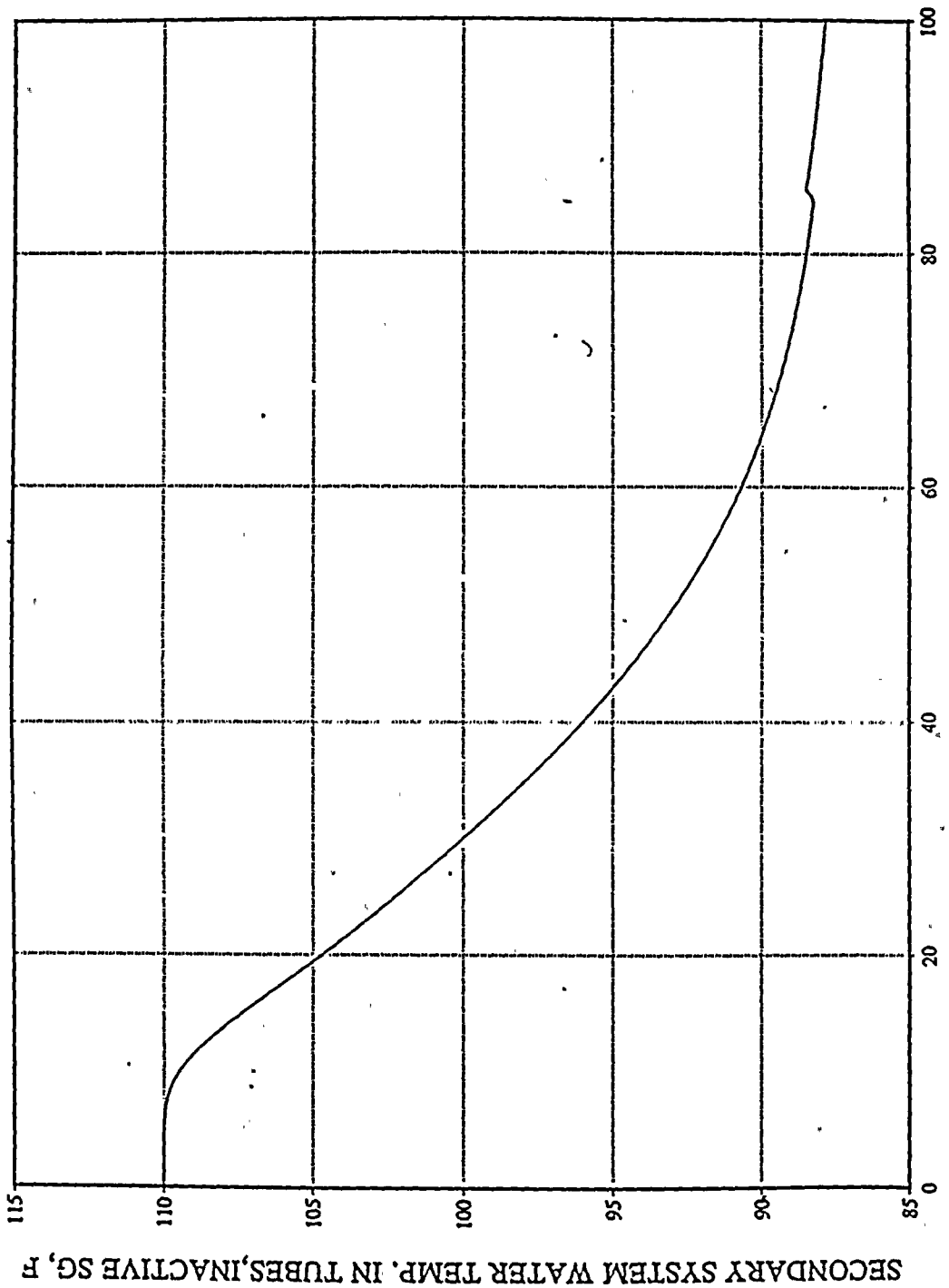

FIGURE 20

CASE 5 HEAT ADDITION CASE PRIMARY TEMPERATURE 60°F
PRIMARY PRESSURE 329.7 PSIA
NO VENT, NO SI, NO CHARGING PUMP
ONE RC PUMP STARTED
2000 GPM RHR

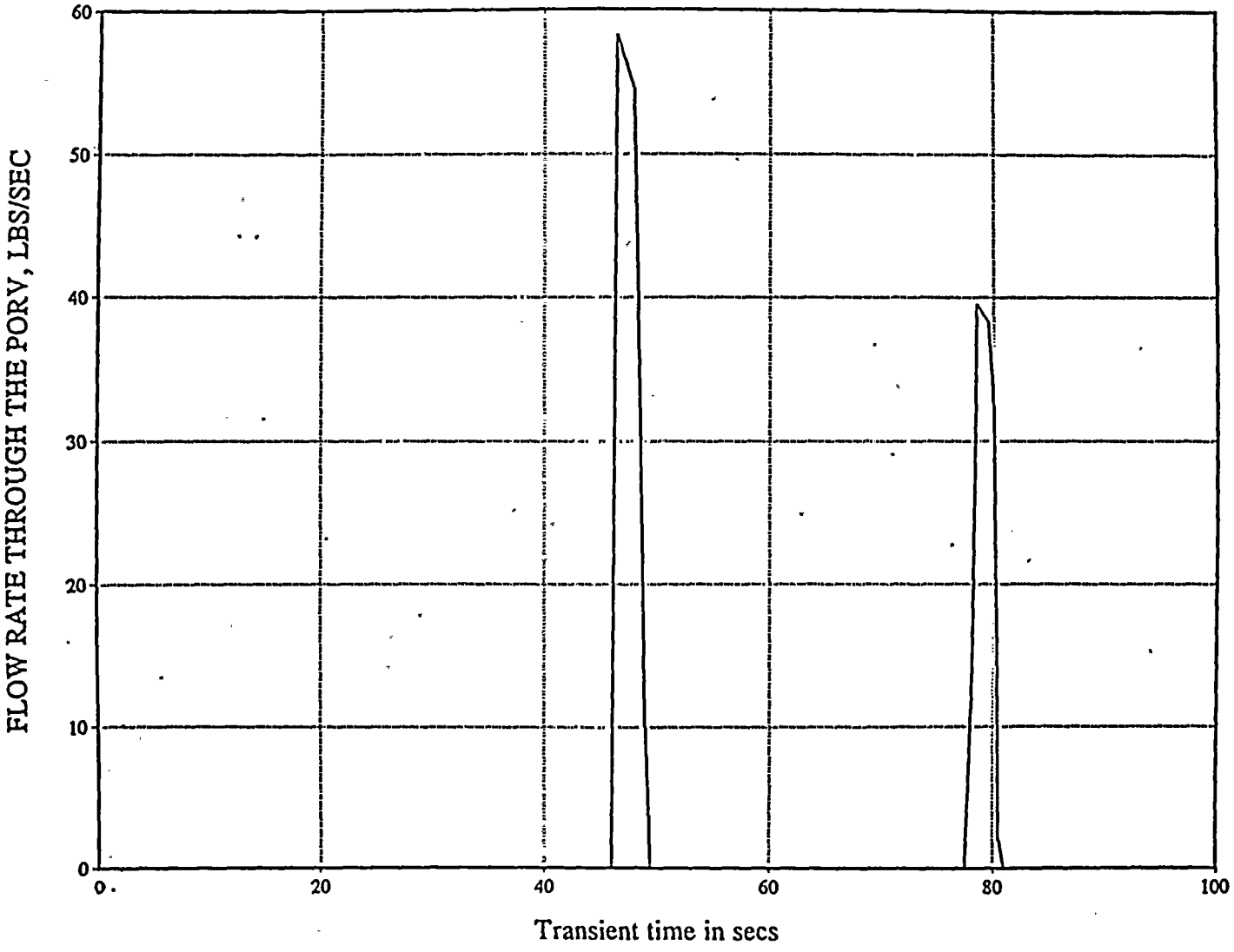

FIGURE 2

CASE 6 HEAT ADDITION CASE PRIMARY TEMPERATURE 85°F
PRIMARY PRESSURE 329.7 PSIA
NO VENT, NO SI, NO CHARGING PUMP
ONE RC PUMP STARTED
2000 GPM RHR

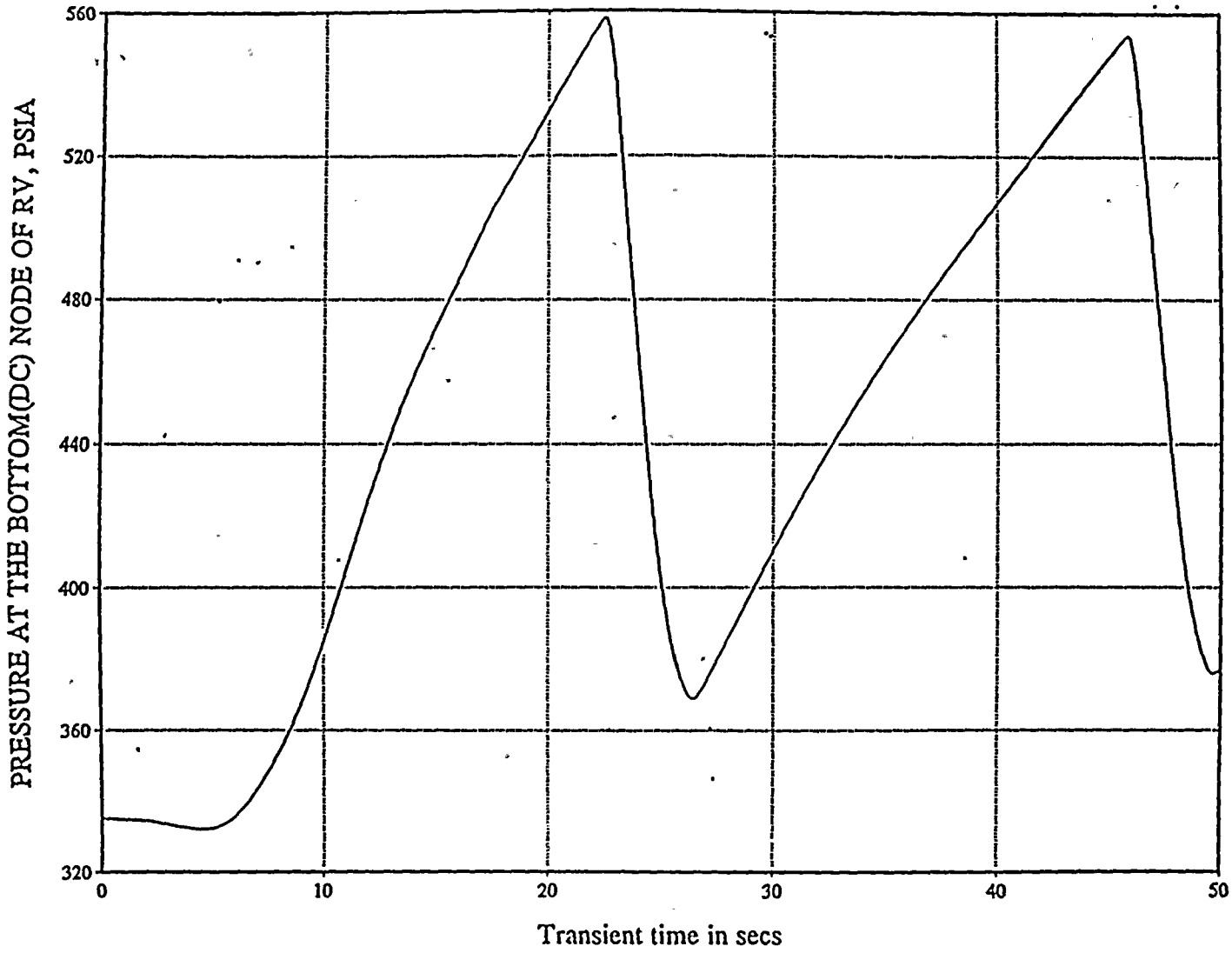

FIGURE
CASE 6 HEAT ADDITION CASE . PRIMARY TEMPERATURE 85°F
PRIMARY PRESSURE 329.7 PSIA
NO VENT, NO SI, NO CHARGING PUMP
ONE RC PUMP STARTED
2000 GPM RHR

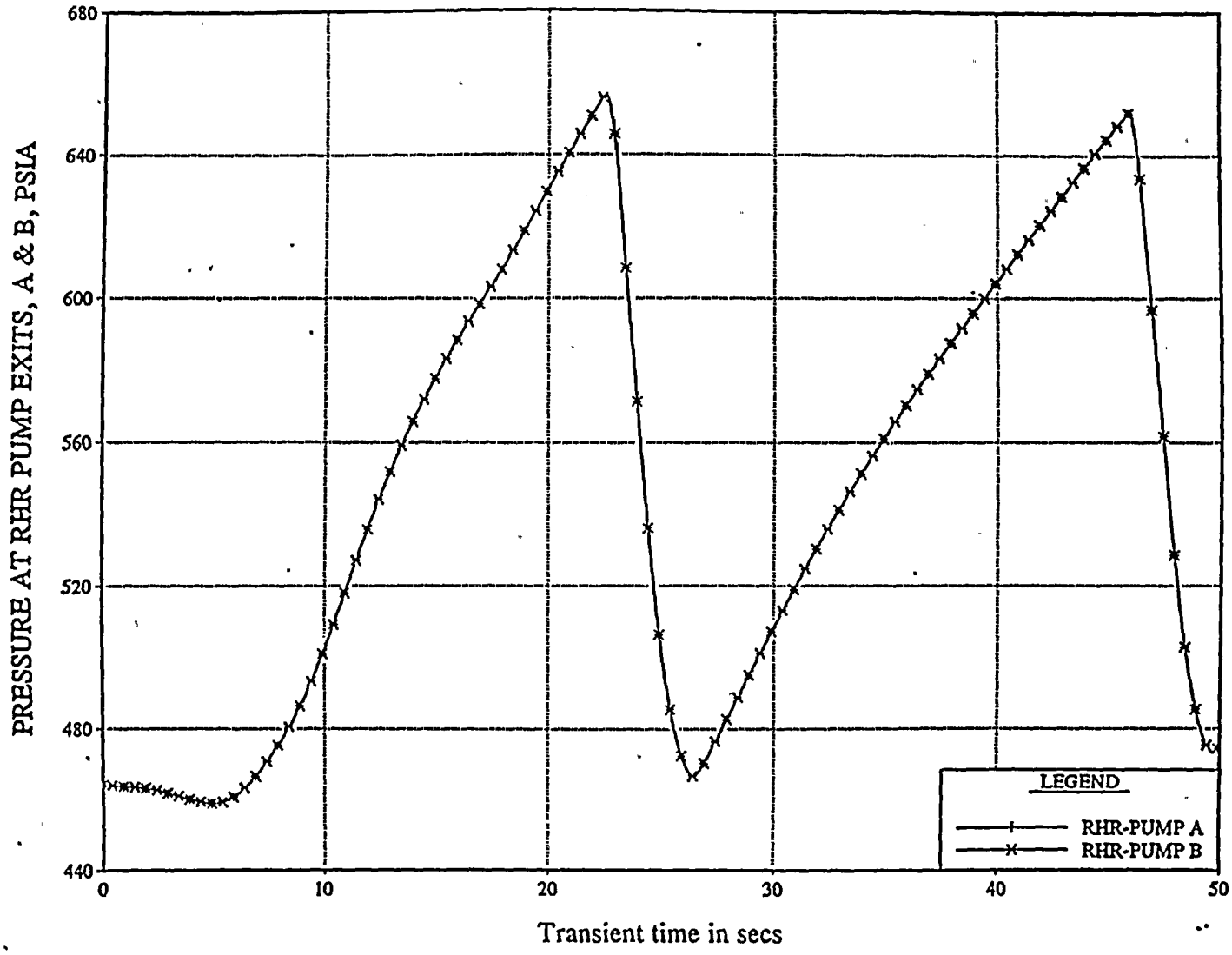

FIGURE
CASE 6 HEAT ADDITION CA

PRIMARY TEMPERATURE 85°F
PRIMARY PRESSURE 329.7 PSIA
NO VENT, NO SI, NO CHARGING PUMP
ONE RC PUMP STARTED
2000 GPM RHR

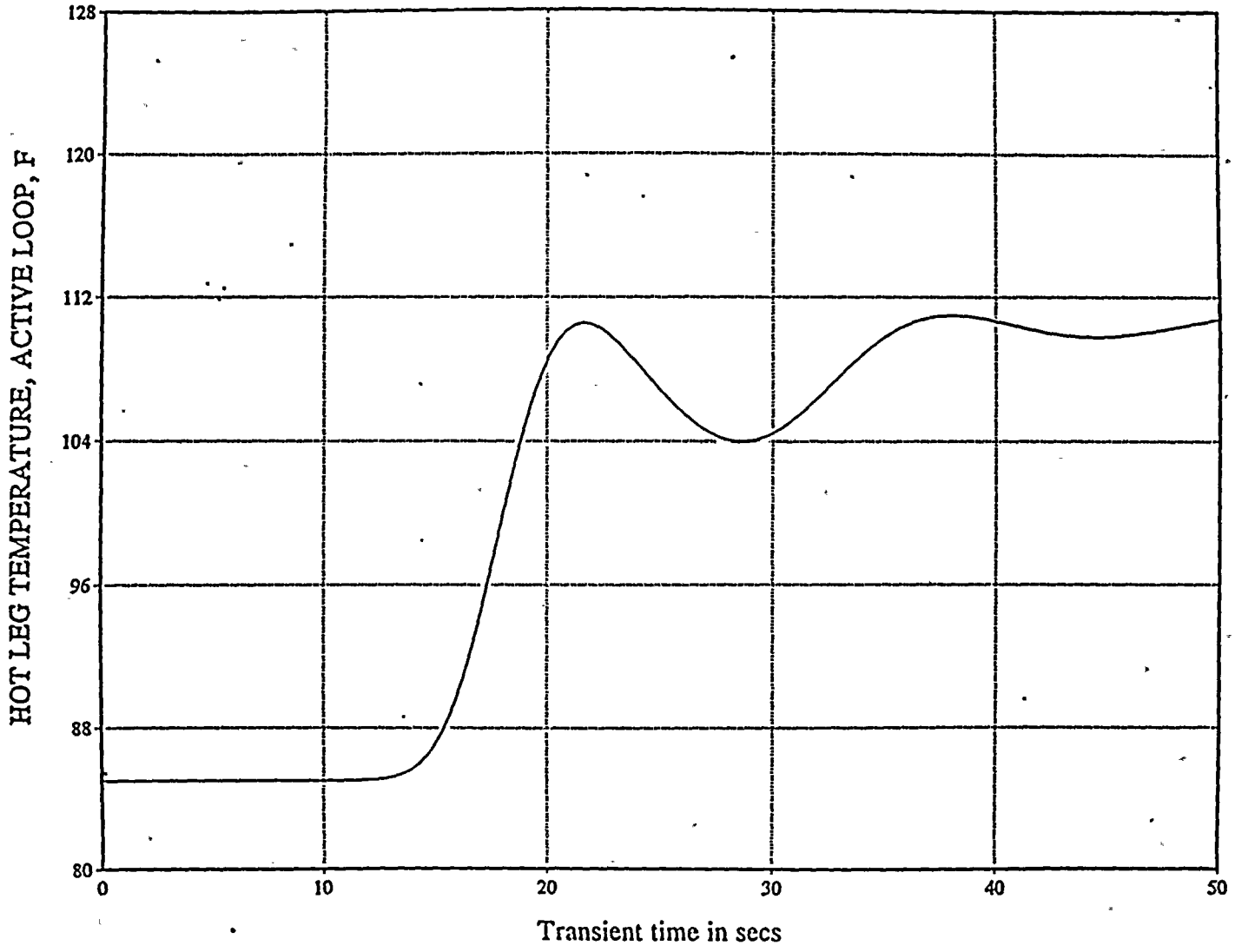

FIGURE

CASE 6 HEAT ADDITION CASE PRIMARY TEMPERATURE 85°F
PRIMARY PRESSURE 329.7 PSIA
NO VENT, NO SI, NO CHARGING PUMP
ONE RC PUMP STARTED
2000 GPM RHR

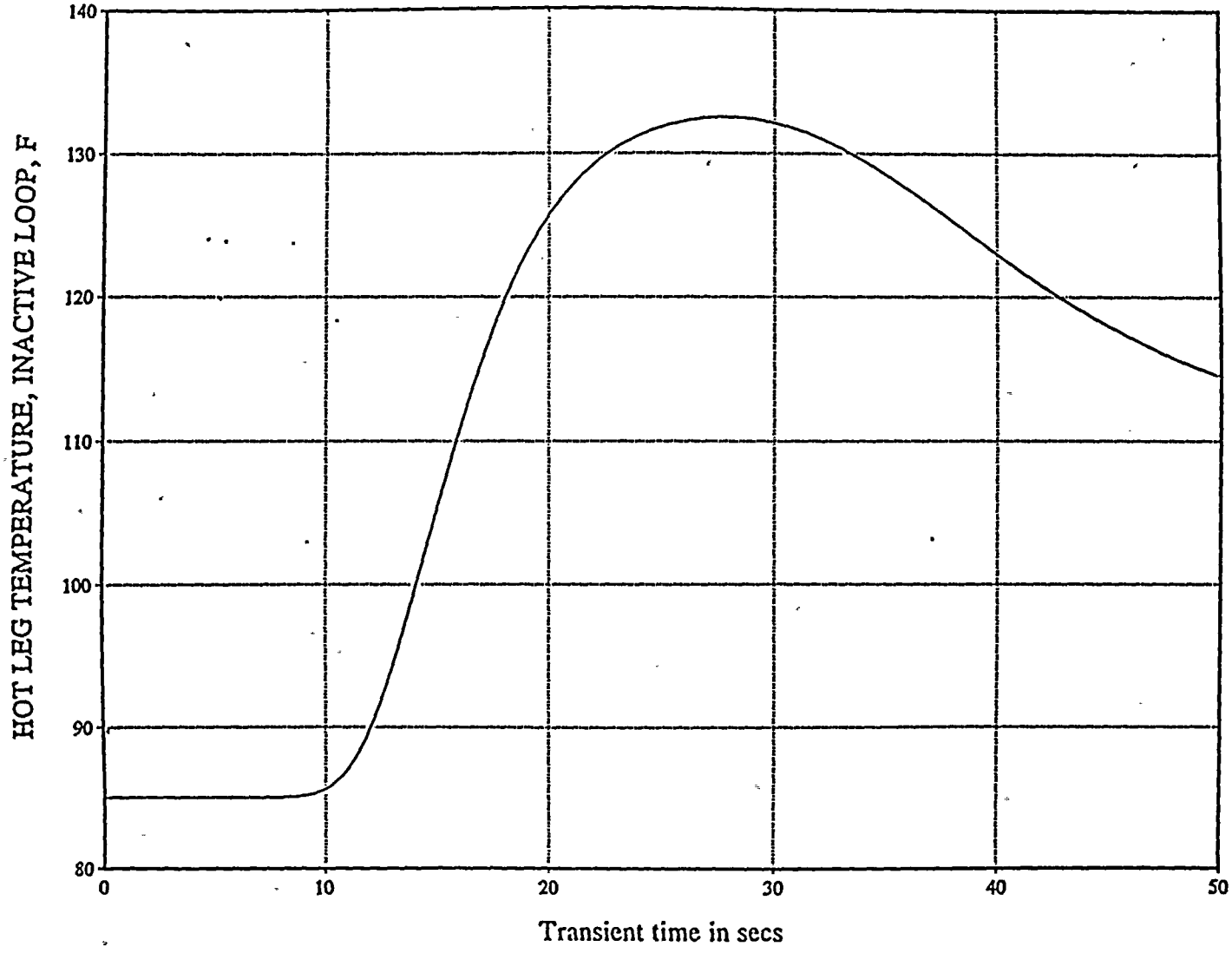

FIGURE 25

CASE 6 HEAT ADDITION CASE PRIMARY TEMPERATURE 85°F
PRIMARY PRESSURE 329.7 PSIA
NO VENT, NO SI, NO CHARGING PUMP
ONE RC PUMP STARTED
2000 GPM RHR

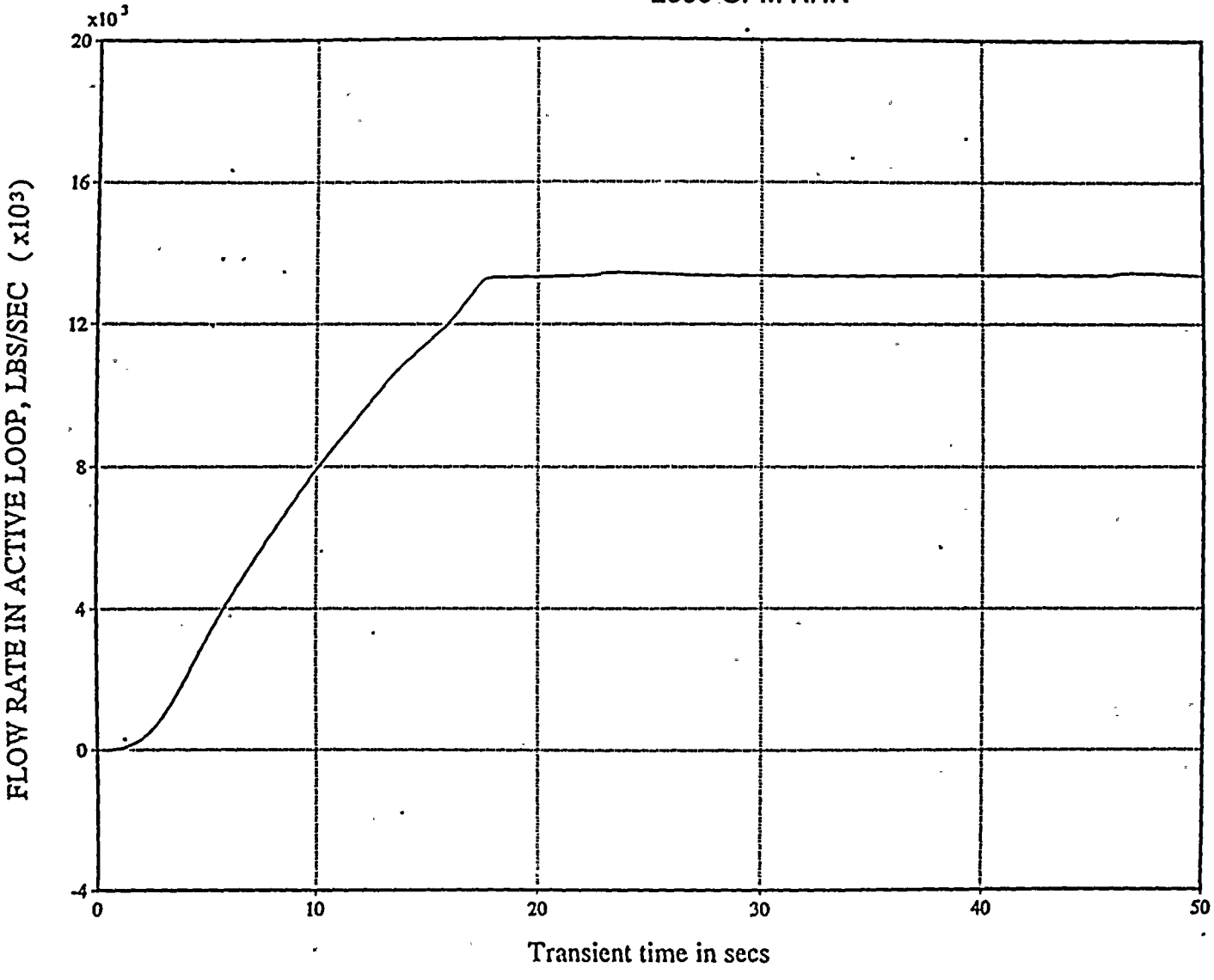

FIGURE 26

CASE 6 HEAT ADDITION CASE PRIMARY TEMPERATURE 85°F
PRIMARY PRESSURE 329.7 PSIA
NO VENT, NO SI, NO CHARGING PUMP
ONE RC PUMP STARTED
2000 GPM RHR

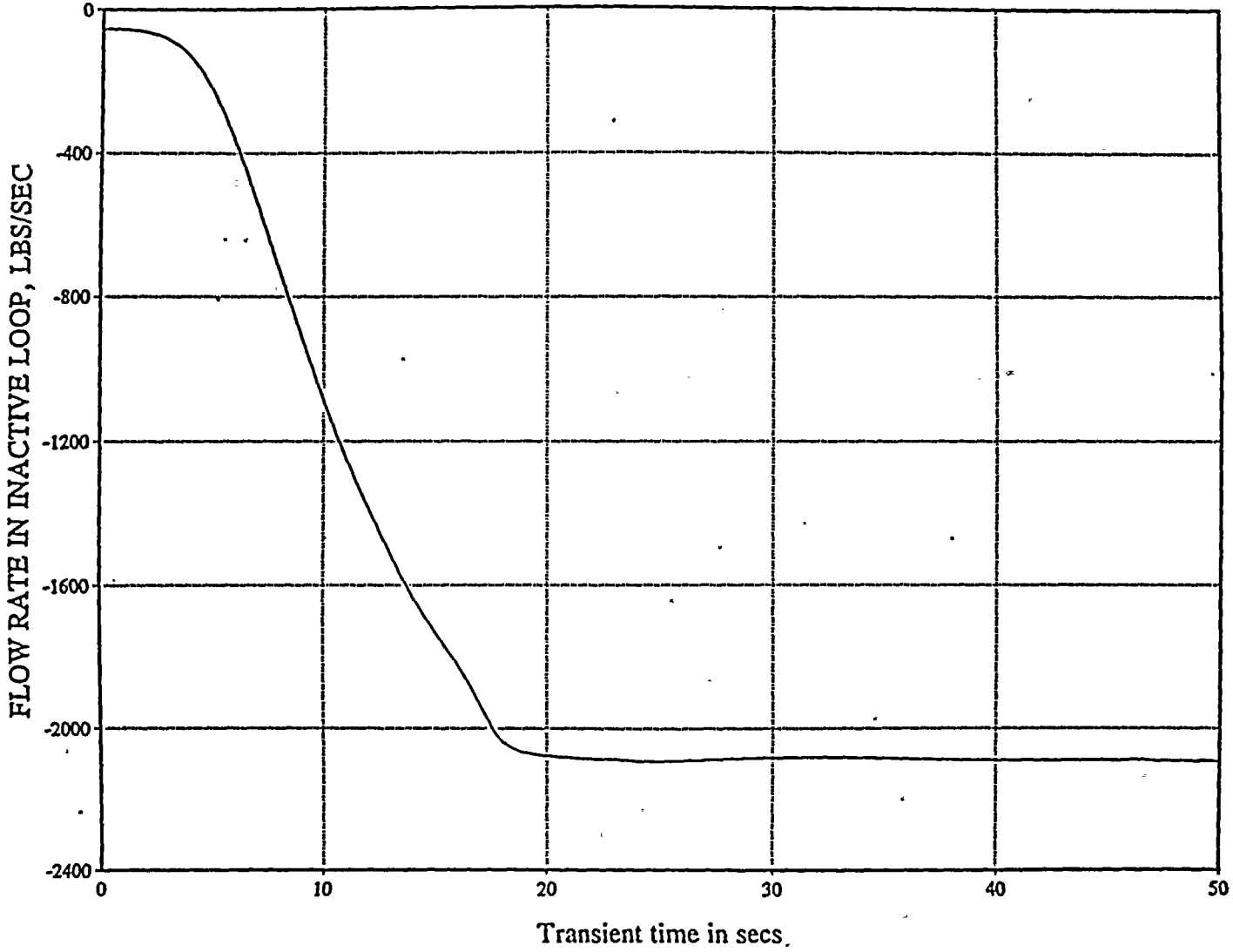

FIGURE 2

CASE 6 HEAT ADDITION CASE PRIMARY TEMPERATURE 85°F
PRIMARY PRESSURE 329.7 PSIA
NO VENT, NO SI, NO CHARGING PUMP
ONE RC PUMP STARTED
2000 GPM RHR

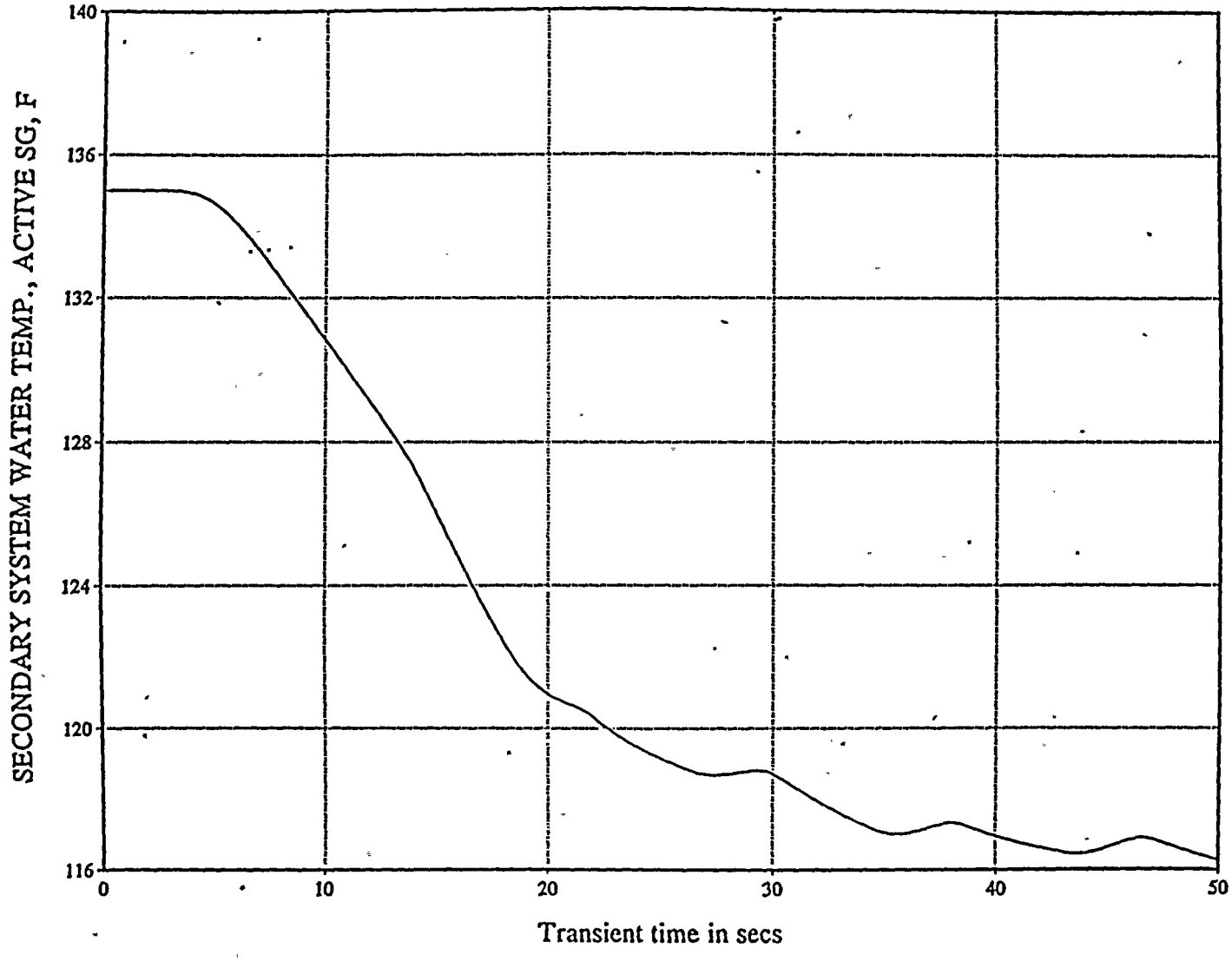

FIGURE
CASE 6 HEAT ADDITION CASE

PRIMARY TEMPERATURE 85°F
PRIMARY PRESSURE 329.7 PSIA
NO VENT, NO SI, NO CHARGING PUMP
ONE RC PUMP STARTED
2000 GPM RHR

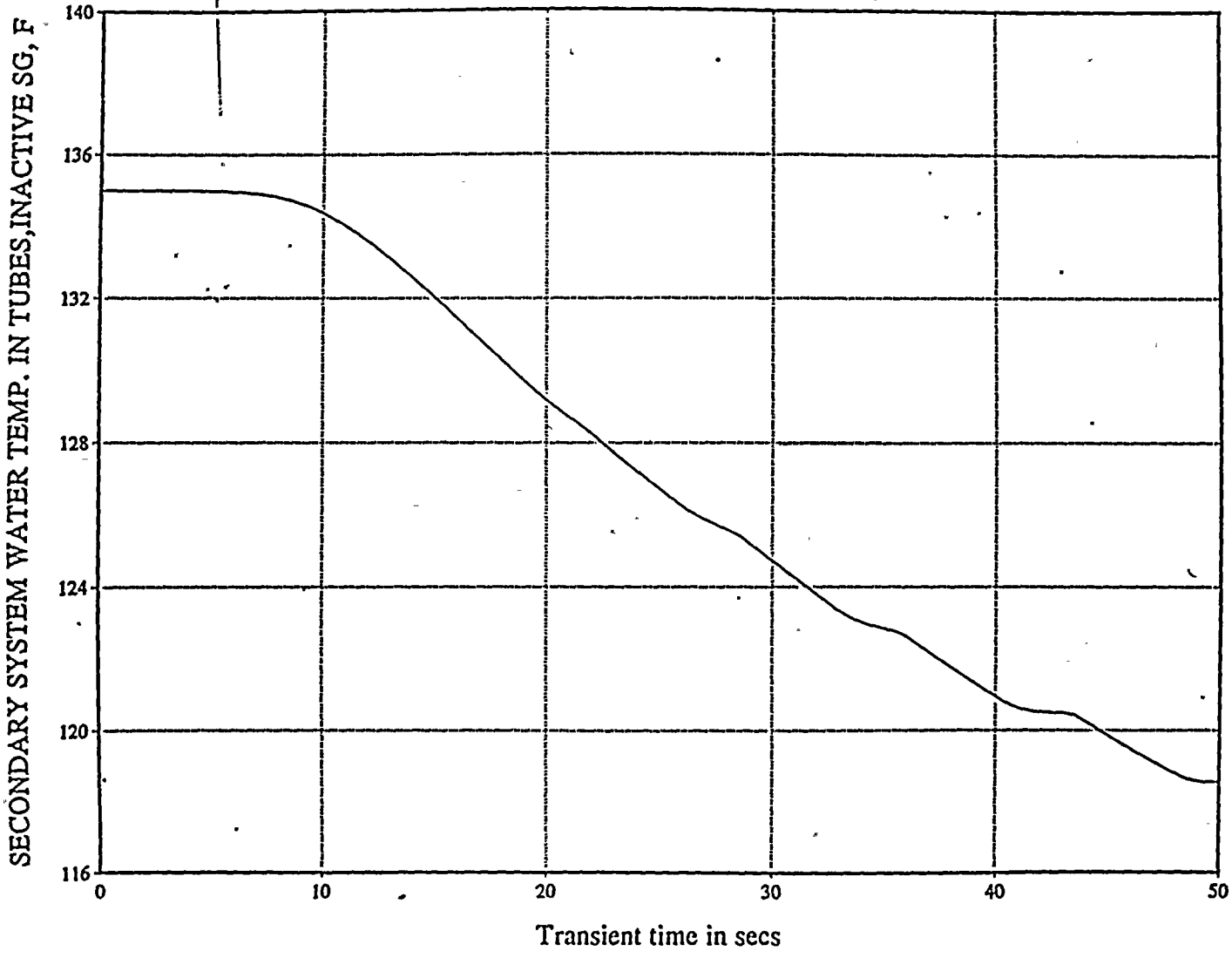

FIGURE 29

CASE 6 HEAT ADDITION CASE PRIMARY TEMPERATURE 85°F
PRIMARY PRESSURE 329.7 PSIA
NO VENT, NO SI, NO CHARGING PUMP
ONE RC PUMP STARTED
2000 GPM RHR

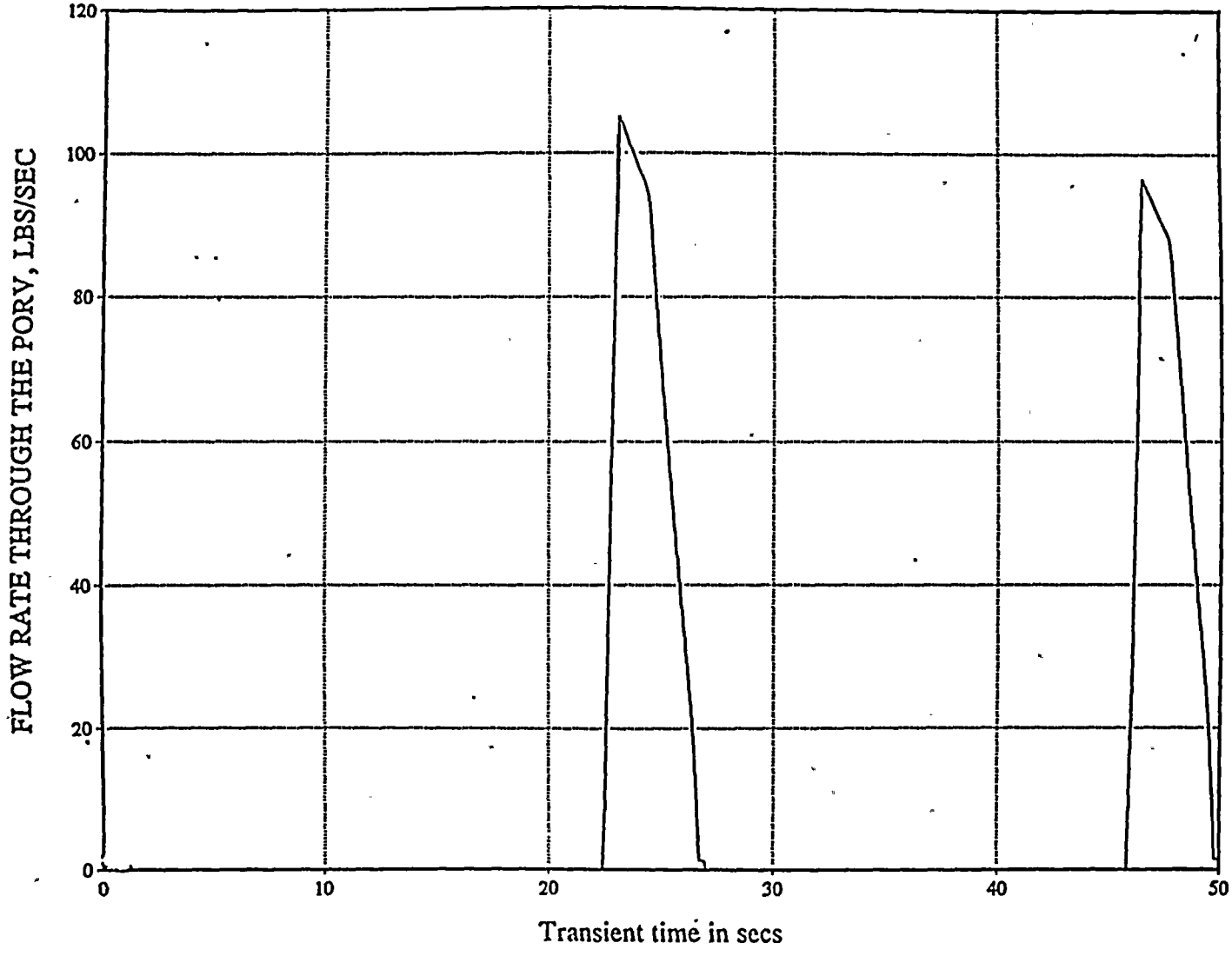

FIGURE 30
CASE 7 HEAT ADDITION CASE PRIMARY TEMPERATURE 280°F
PRIMARY PRESSURE 329.7 PSIA
NO VENT, NO SI, NO CHARGING PUMP
ONE RC PUMP STARTED
2000 GPM RHR

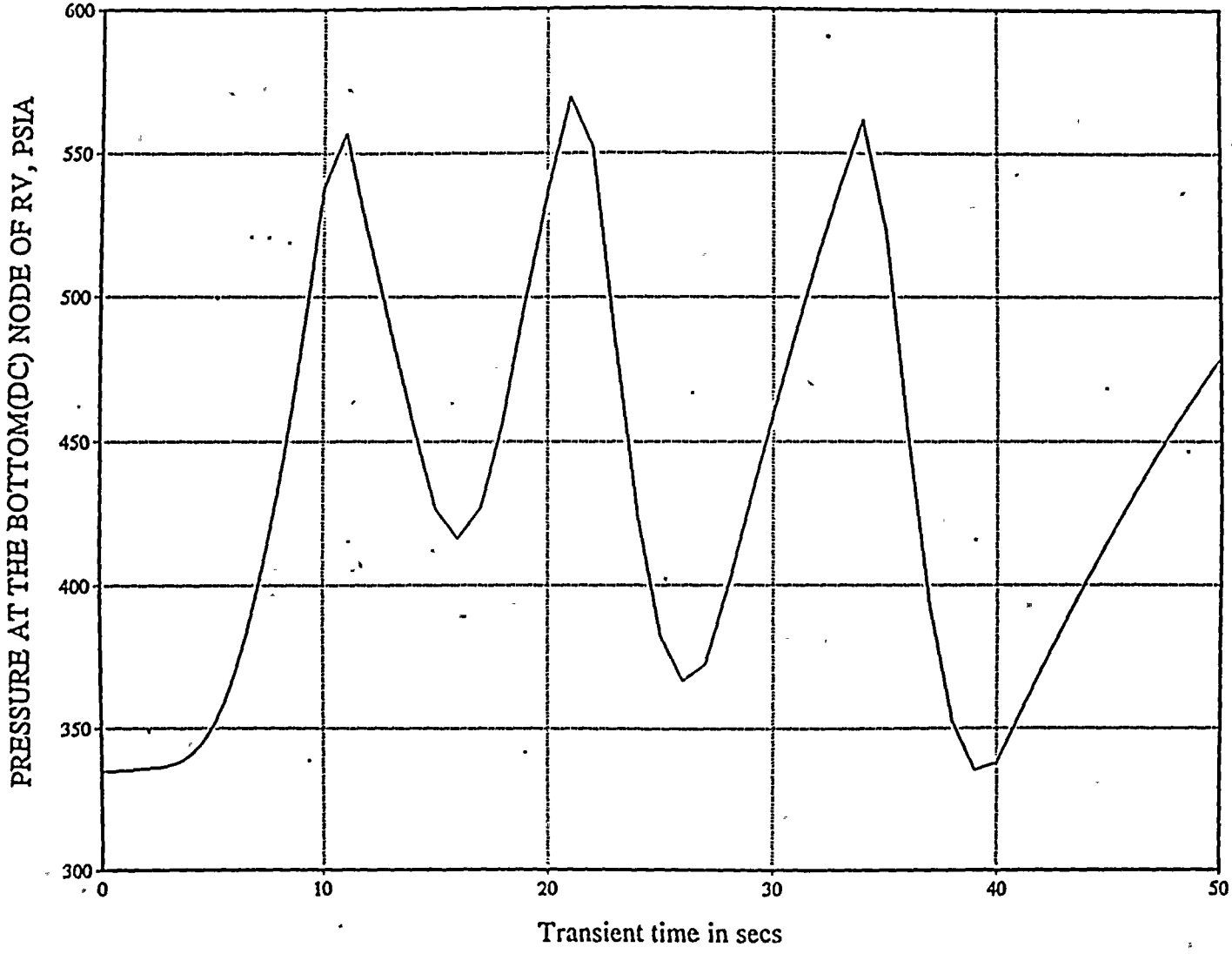

FIGURE 31

CASE 7 HEAT ADDITION CASE PRIMARY TEMPERATURE 280°F
PRIMARY PRESSURE 329.7 PSIA
NO VENT, NO SI, NO CHARGING PUMP
ONE RC PUMP STARTED
2000 GPM RHR

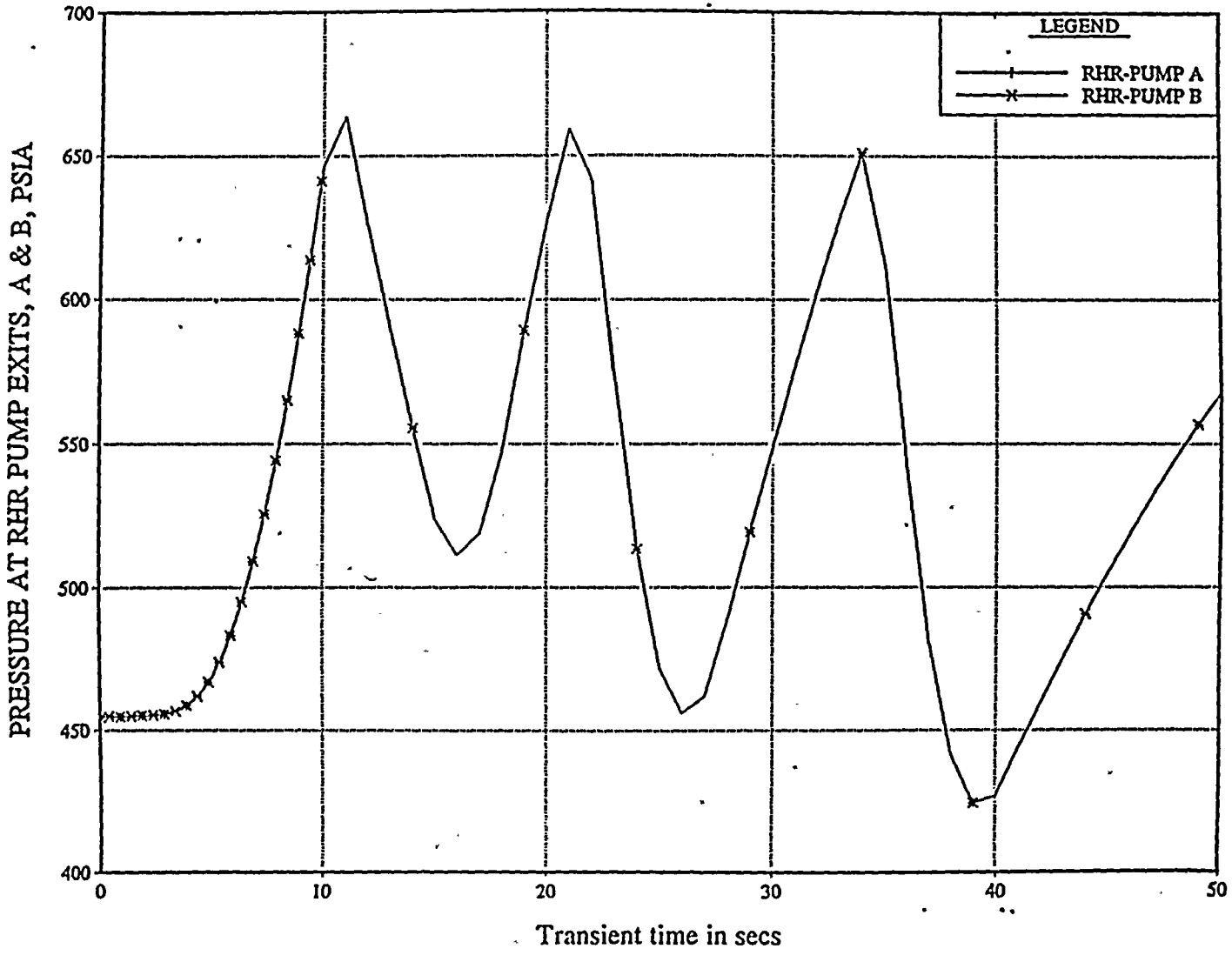

FIGURE 2

CASE 7 HEAT ADDITION CASE PRIMARY TEMPERATURE 280°F
PRIMARY PRESSURE 329.7 PSIA
NO VENT, NO SI, NO CHARGING PUMP
ONE RC PUMP STARTED
2000 GPM RHR

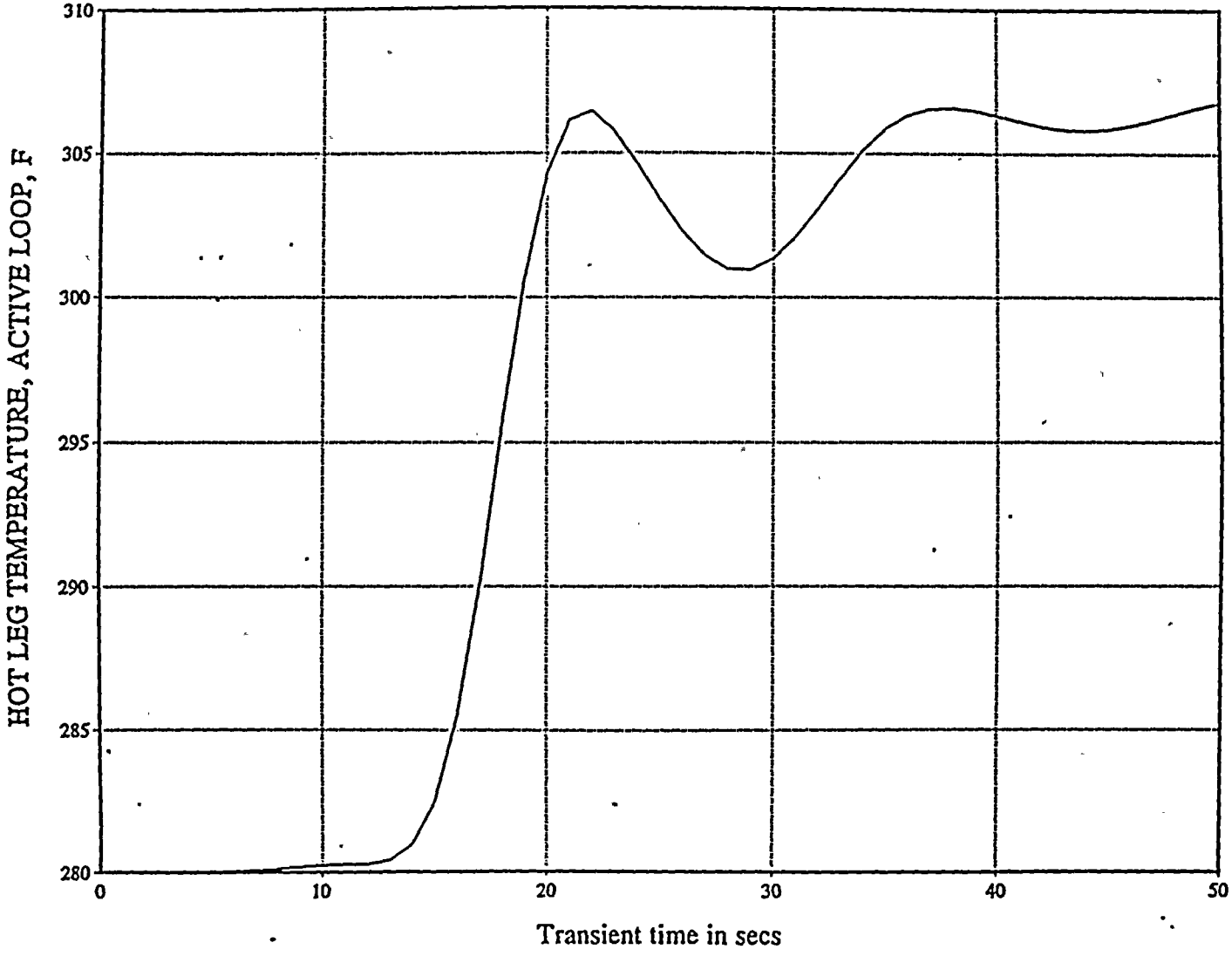

FIGURE 33

CASE 7 HEAT ADDITION CASE PRIMARY TEMPERATURE 280°F
PRIMARY PRESSURE 329.7 PSIA
NO VENT, NO SI, NO CHARGING PUMP
ONE RC PUMP STARTED
2000 GPM RHR

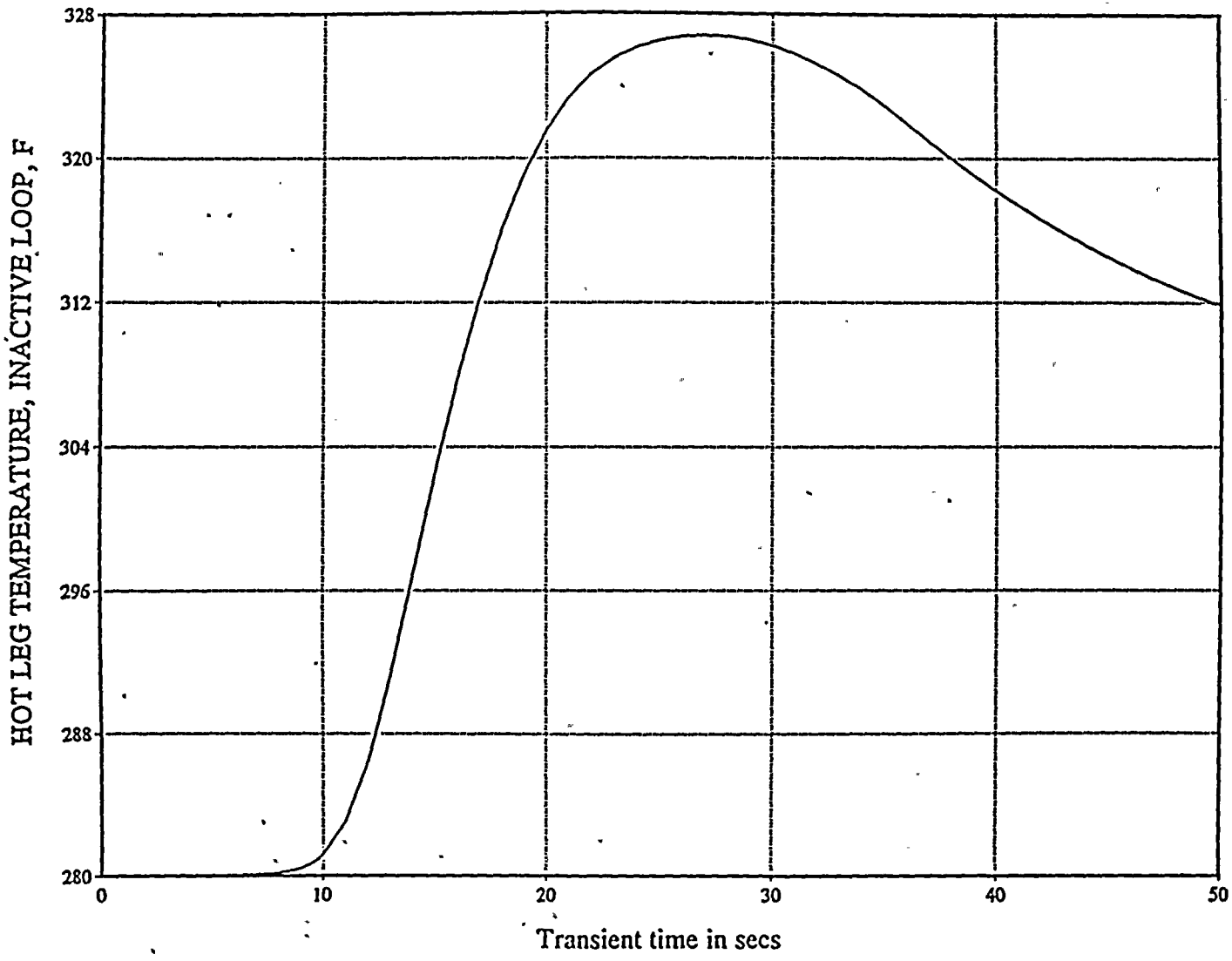

FIGURE 34

CASE 7 HEAT ADDITION CASE PRIMARY TEMPERATURE 280°F
PRIMARY PRESSURE 329.7 PSIA
NO VENT, NO SI, NO CHARGING PUMP
ONE RC PUMP STARTED
2000 GPM RHR

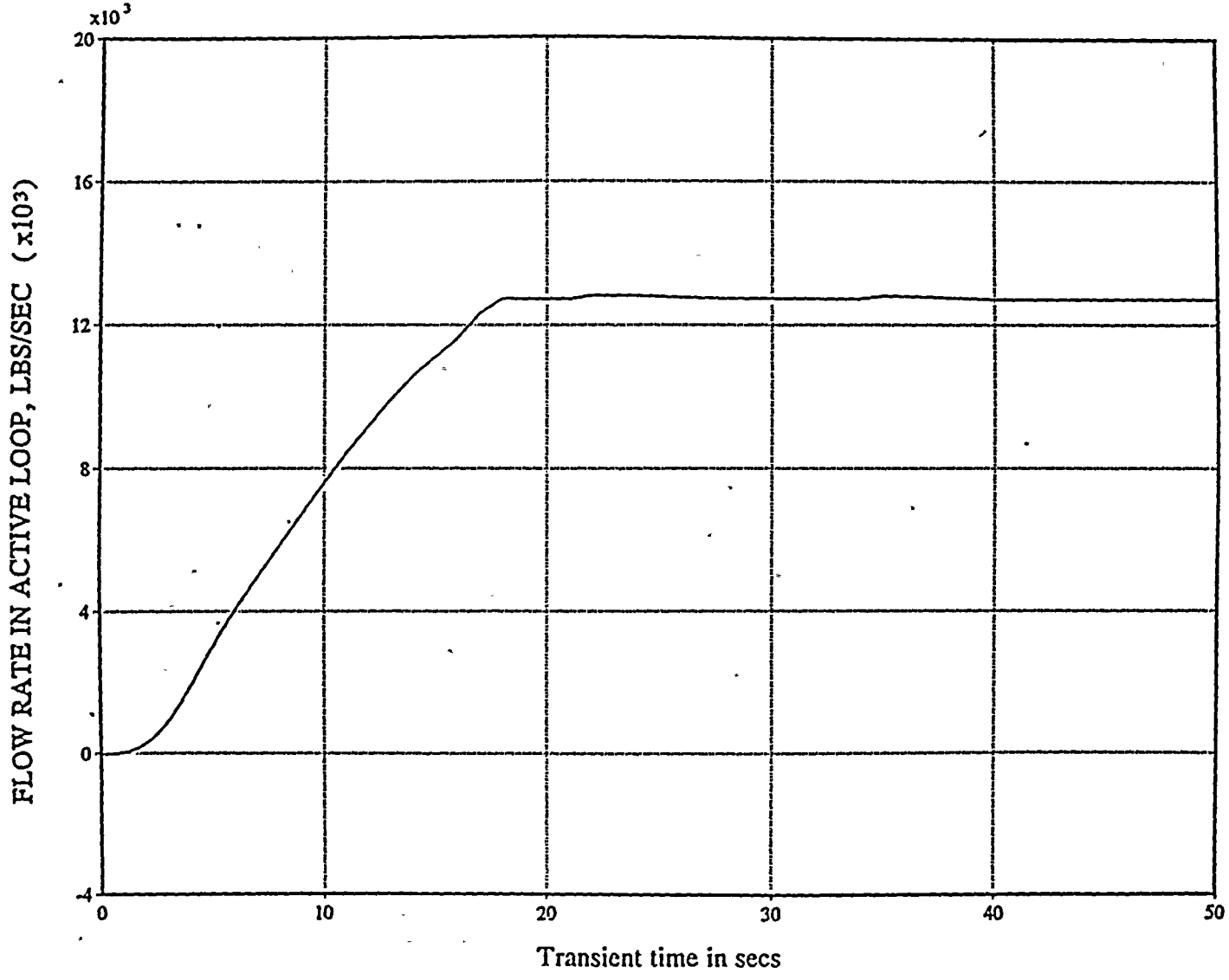

FIGURE 35

CASE 7 HEAT ADDITION CASE PRIMARY TEMPERATURE 280°F
PRIMARY PRESSURE 329.7 PSIA
NO VENT, NO SI, NO CHARGING PUMP
ONE RC PUMP STARTED
2000 GPM RHR